LIÈGE université
Gembloux
Agro-Bio Tech

Controlled release antimicrobial packaging films systembased on essential oils loaded Pickering emulsion for meat preservation

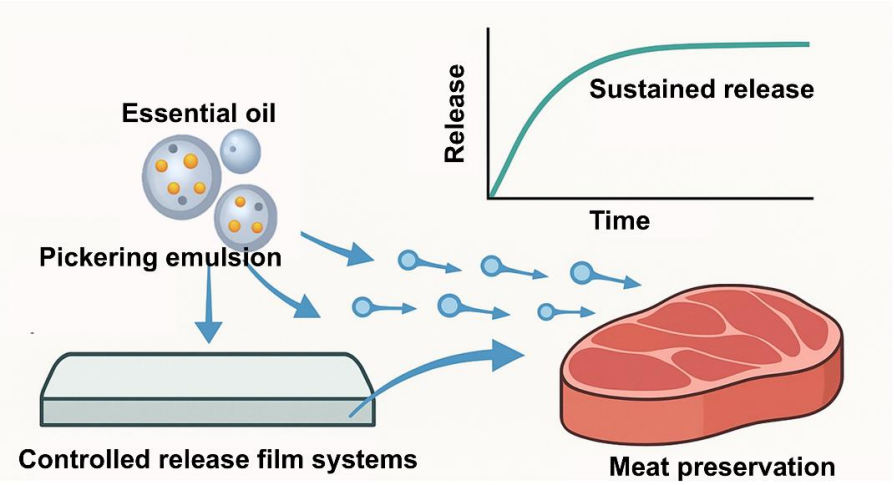

Author: Simin FAN

Supervisor: Prof. Aurore RICHEL

Prof. Marie-Laure FAUCONNIER

Prof. Dequan ZHANG

Year: 2025

COMMUNAUTÉ FRANÇAISE DE BELGIQUE
UNIVERSITÉ DE LIÈGE – GEMBLOUX AGRO-BIO TECH

Controlled release antimicrobial packaging films system based on essential oils loaded Pickering emulsion for meat preservation

Simin FAN

Dissertation originale présentée (ou essai présenté) en vue de l'obtention du grade de doctorat en sciences agronomiques et ingénierie biologique

Promoteur(s) : Aurore Richel, Marie-Laure Fauconnier and Dequan Zhang
Année civile (= année du dépôt) :06/2025

Abstract

Simin FAN (2025). "Controlled release antimicrobial packaging films system based on essential oils loaded Pickering emulsion for meat preservation" (PhD Dissertation in English)

Gembloux, Belgium, Gembloux Agro-Bio Tech, University of Liege.

In recent years, increasing concerns regarding food safety and waste have accelerated the development of antimicrobial active packaging materials. However, conventional antimicrobial packaging systems often suffer from issues such as burst release, poor stability of active compounds, and limited long-term efficacy. To address these challenges, this thesis proposes a novel packaging platform based on Pickering emulsions (PEs), in which essential oils (EOs) are stably encapsulated and released in a controlled system. This dissertation systematically investigated a EOs loaded PE delivery manner and two PEs-based film systems were designed and evaluated for their physicochemical properties, antimicrobial performance, release behavior and meat preservation.

Firstly, a EOs loaded PEs delivery was developed and optimized by loading cinnamon essential oil (CEO) in zein- tannic acid (ZT) complex particles stabilizer. The interfacial properties of the ZT particles were optimized by modulating the zein-tannic acid interactions through pH adjustment, thereby enhanced emulsion stability and improved CEO sustained-release behavior. The ZT5 complex (formed at pH 5) showed the most balanced interfacial properties, as evidenced by its lower interfacial tension (11.31 mN/m), stronger interfacial viscoelasticity, and stable anchoring at the oil-water interface, resulting in the smallest in Turbiscan Stability Index (TSI) and highest CEO encapsulation efficiency (86.83%) compared to other ZT complexes. ZTC5 showed excellent antimicrobial activity against critical meat spoilage species *P. paralactis* MN10 and *L. sakei* VMR17 with slow-release features.

Secondly, a biodegradable film with Janus structure was fabricated by incorporating the optimized CEO-loaded PEs into chitosan-based matrices, combined with a zein barrier layer, to regulate CEO release directionally, achieving unidirectional and prolonged CEO release. The good interfacial compatibility of CEO-loaded PEs/chitosan active layer and zein barrier layer was driven by non-covalent interactions, promoting interfacial adhesion and stability. The differential swelling behavior between the chitosan active layers (47.61% ~ 51.71%) and zein barrier layer (162.52%), played a crucial role in regulating the release kinetics of CEO. The films showed excellent antimicrobial activity against meat spoilage species and radical scavenging activity (2.5-fold enhancement). Moreover, the film loading layer showed predominantly controlled by a quasi-Fickian diffusion, and prolonged the shelf life of pork by 6 days under the unidirectional sustained release.

In parallel, CEO-loaded PEs were incorporated into chitosan/polyvinyl alcohol (CS/PVA) composites film, combined with quercetin nanocrystals (QNs) as functional fillers (named PCE@QNs), to improve the cross-linking density of the

polymer network and thereby further controlled release of CEO. The physical entanglement and hydrogen bonding interactions created a spatial barrier that restricted droplet migration or coalescence. This structural integrity contributes to enhanced mechanical properties in PCE@QNs, achieving a tensile strength of 39.09 ± 0.46 MPa. Moreover, PCE@QNs exhibited potent antimicrobial activity against food spoilage bacteria (achieving over 99.99% inhibition) and significantly improved antioxidant capacity (approximately 5-fold increase), along with superior UV-shielding, water sensitivity, volatile ammonia responsiveness, and biodegradability. CEO release from PCE@QNs followed Fickian diffusion. The multifunctional properties of PCE@QNs make it highly suitable for meat preservation, effectively extending shelf life of pork to 11 days at 4°C by reducing microbial diversity.

In conclusion, through systematic investigation, this research elucidated the structure-property-function relationships in PE-based packaging systems, providing theoretical insights into the role of interfacial engineering and microstructural modulation in regulating antimicrobial agents' release. The findings of this dissertation provided theoretical and practical guidance for future innovations in bio-based controlled-release systems and open new possibilities for the practical application of Pes-based technologies in the food packaging field.

Keywords: Antimicrobial packaging; Pickering emulsion; Controlled-release; Bio-based film; Cinnamon essential oil; Meat preservation.

Résumé

Simin FAN (2025). « Système de films d'emballage antimicrobiens à libération contrôlée basé sur une émulsion de Pickering chargée en huiles essentielles pour la conservation de la viande » (Thèse de doctorat rédigée en anglais).

Gembloux, Belgique, Gembloux Agro-Bio Tech, Université de Liège.

Ces dernières années, les préoccupations croissantes concernant la sécurité alimentaire et la conservation des aliments ont accéléré le développement de matériaux d'emballage actifs antimicrobiens. Cependant, les systèmes d'emballage antimicrobiens conventionnels présentent souvent des limitations telles qu'une libération explosive, une faible stabilité des composés actifs et une efficacité limitée à long terme. Pour relever ces défis, cette thèse propose une nouvelle plateforme d'emballage basée sur des émulsions de Pickering (PE), dans lesquelles les huiles essentielles (EOs) sont encapsulées de manière stable et libérées de façon contrôlée. Cette thèse a étudié de manière systématique un système de libération d'EOs basé sur des PE, et deux systèmes de films à base de PE ont été conçus et évalués pour leurs propriétés physico-chimiques, leurs performances antimicrobiennes, leur comportement de libération et leur capacité à conserver la viande.

Premièrement, un système de libération d'EOs à base de PE a été développé et optimisé en chargeant de l'huile essentielle de cannelle (CEO) dans des particules stabilisantes formées par le complexe zéine-acide tannique (ZT). Les propriétés interfaciales des particules ZT ont été optimisées en modulant les interactions zéine-acide tannique par ajustement du pH, améliorant ainsi la stabilité de l'émulsion et le comportement de libération prolongée de la CEO. Le complexe ZT5 (formé à pH 5) a présenté les propriétés interfaciales les plus équilibrées, comme en témoignent sa tension interfaciale réduite (11,31 mN/m), sa viscoélasticité interfaciale accrue, et son ancrage stable à l'interface huile-eau, aboutissant au plus faible indice de stabilité Turbiscan (TSI) et à la plus haute efficacité d'encapsulation de CEO (86,83 %) comparé aux autres complexes ZT. Le ZT5 a montré une excellente activité antimicrobienne contre des espèces clés responsables de l'altération de la viande, telles que P. paralactis MN10 et L. sakei VMR17, avec une libération prolongée.

Deuxièmement, des films de type Janus biodégradables ont été fabriqués en incorporant les PE optimisées contenant la CEO dans des matrices à base de chitosane, combinées à une couche barrière en zéine, afin de réguler la libération directionnelle de la CEO, obtenant ainsi une libération unidirectionnelle et prolongée. La bonne compatibilité interfaciale entre la couche active en chitosane contenant les PE chargées en CEO et la couche barrière en zéine a été favorisée par des interactions non covalentes, renforçant l'adhésion et la stabilité interfaciales. Le comportement différentiel de gonflement entre les couches actives au chitosane (47,61 % ~ 51,71 %) et la couche barrière en zéine (162,52 %) a joué un rôle clé dans la régulation de la

cinétique de libération de la CEO. Les films ont démontré une excellente activité antimicrobienne contre les bactéries d'altération de la viande et une activité de piégeage des radicaux libres (améliorée de 2,5 fois). De plus, la couche de chargement a suivi une diffusion quasi-Fickienne, prolongeant la durée de conservation du porc de 6 jours grâce à une libération unidirectionnelle soutenue.

En parallèle, les PE chargées en CEO ont été incorporées dans un film composite chitosane/alcool polyvinylique (CS/PVA), combinées à des nanocristaux de quercétine (QNs) en tant que charges fonctionnelles, afin d'augmenter la densité de réticulation du réseau polymère et ainsi contrôler davantage la libération de la CEO. L'enchevêtrement physique et les interactions par liaisons hydrogène ont formé une barrière spatiale limitant la migration ou la coalescence des gouttelettes. Cette intégrité structurale a contribué à l'amélioration des propriétés mécaniques du système PCE@QNs, atteignant une résistance à la traction de 39,09 ± 0,46 MPa. En outre, PCE@QNs a présenté une forte activité antimicrobienne contre les bactéries d'altération alimentaire (avec une inhibition supérieure à 99,99 %) et une capacité antioxydante significativement améliorée (augmentation d'environ cinq fois), ainsi qu'une protection UV, une sensibilité à l'humidité, une réactivité à l'ammoniac volatil et une biodégradabilité supérieures. La libération de CEO à partir de PCE@QNs a suivi une diffusion de type Fickien. Les propriétés multifonctionnelles de PCE@QNs le rendent particulièrement adapté à la conservation de la viande fraîche, prolongeant efficacement la durée de conservation jusqu'à 11 jours à 4 °C en réduisant la diversité microbienne.

En conclusion, à travers une investigation systématique, cette recherche a permis d'élucider les relations structure–propriétés–fonction dans les systèmes d'emballage à base de PE, apportant des connaissances théoriques sur le rôle de l'ingénierie interfaciale et de la modulation microstructurale dans la régulation de la libération des agents antimicrobiens. Les résultats de cette thèse offrent des bases théoriques et pratiques pour de futures innovations dans les systèmes bio-sourcés à libération contrôlée, et ouvrent de nouvelles perspectives d'application pratique des technologies d'émulsions de Pickering dans le domaine de l'emballage alimentaire.

Mots-clés : Emballage antimicrobien ; Émulsion de Pickering ; Libération contrôlée ; Film bio-sourcé ; Huile essentielle de cannelle ; Conservation de la vian

Acknowledgements

As I approach the culmination of my doctoral journey, I wish to reflect on the transformative years that have shaped both my academic and personal growth. To that determined young soul who insisted on pursuing this path against all cautions: your leap of faith has borne fruit beyond measure.

First and foremost, I wish to express my deepest gratitude to my primary supervisory mentors. Prof. Aurore Richel and Prof. Marie-Laure Fauconnier of Gembloux Agro-Bio Tech, University of Liège, offered invaluable insights and constructive feedback that greatly enhanced the quality of this thesis. Prof. Dequan Zhang (张德权) at the Chinese Academy of Agricultural Sciences provided unwavering guidance in defining the research topic and designing the experiments, which fundamentally shaped this work. Your collective wisdom and support transcended geographical boundaries, connecting Beijing and Gembloux. I am also sincerely grateful to Prof. Chengli Hou (侯成立), whose continuous mentorship throughout these four years has been the cornerstone of this doctoral journey. More than academic advisors, you have exemplified how principled mentorship fosters not only scientific excellence but also professional integrity.

Secondly, I am deeply grateful to the CAAS–ULiège Joint Doctoral Program for providing an outstanding academic platform that made this research possible. I am especially thankful to Professor Mingjun Zhang (张明军) of the Graduate School of the Chinese Academy of Agricultural Sciences for his invaluable support and constant encouragement throughout my doctoral journey. This research was generously supported by the National Key R&D Program of China (Grant No. 2021YFD2100802) and the China Scholarship Council (Grant No. 202303250065), whose contributions are gratefully acknowledged.

Additionally, I would like to extend my sincere thanks to all members of my thesis committee for their careful guidance and constructive feedback, which have been of immense help throughout my research. My heartfelt appreciation also goes to my colleagues from the Meat Science and Nutrition Engineering team and the Lab of Biomass and Green Technologies, whose collaboration and friendship have enriched both my research and daily life. A special thanks goes to the G4 colleagues, Qingfeng Yang (杨庆锋), Yuqian Xu (徐毓谦), Chaoqiao Zhu (祝朝巧), Ming Tian (田铭), Xiaoyu Chai (柴笑玉), Xiaotong Sun (孙晓彤) and Wenxin Wang (王文欣), for their constant support, laughter, and shared experiences. I am equally thankful to the many other colleagues whose names are not listed here, but whose kindness and companionship I will always remember with great warmth.

A special thank you goes out to all my fellow badminton enthusiasts. To everyone who shared the court with me, sweating it out together rally after rally, thank you for the fun, the challenge, and the escape. Those times were crucial for maintaining balance and perspective during the intense years of my doctoral studies. Beyond the court, I want to acknowledge and thank every single person who crossed my path

during my PhD journey. Your support, encouragement, or simple presence made a difference, and I am grateful to have shared this chapter of my life with all of you.

Most importantly, I owe my deepest gratitude to my parents. For thirty years, your unwavering love, endless support, and constant encouragement have been the foundation upon which I've built my life and pursued my dreams. Your sacrifices and belief in me, through every challenge and triumph, have been my greatest strength. This achievement would not have been possible without you. Thank you for everything.

Though the thesis may end with the acknowledgements, the journey of my life goes on.

Simin FAN
23/07/2025 in Gembloux, Belgium

Table of contents

List of figures

List of tables

List of acronyms

ABTS: 2,2'-azino-bis (3-ethylbenzothiazoline-6-sulfonic acid)

AIE: aggregation-induced emission

BCNs: bacterial cellulose nanofibers

CEO: cinnamon essential oil

CFU: Colony Forming Unit

CLSM: Confocal laser scanning microscopy

CRP: controlled release packaging

CS: chitosan

CS/PVA: chitosan/polyvinyl alcohol

DPPH: 2,2-diphenyl-1-picrylhydrazyl

E: interfacial dilatational modulus

EB: elongation at break

Ed: dilatational elasticity modulus

EE: Encapsulation efficiency

EOs: essential oils

Ev: dilatational viscosity modulus

FAO: Food and Agriculture Organization

FTIR: Fourier transform infrared spectroscopy

GEL: gelatin

KGM: konjac glucomannan

LB: Luria Broth

MIC: Minimum inhibitory concentration

O/W: oil-in-water

OP: oxygen permeability

PBS: phosphate buffer saline

PC@QNs: quercetin nanocrystal-enhanced chitosan/polyvinyl alcohol films

PCE@QNs: quercetin nanocrystal-enhanced chitosan/polyvinyl alcohol/CEO-loaded Pickering emulsion composite films

PE: Pickering emulsion

PVA: Polyvinyl alcohol

QNs: quercetin nanocrystals

SEM: scanning electron microscope

SR: swelling rate

TA: Tannic acid

TEM: Transmission electron microscopy

TG: Thermogravimetric analysis

TS: tensile strength

TSI: turbiscan stability index

TVB-N: total volatile basic nitrogen

TVC: total viable count

W/O: water-in-oil

WC: water content

WCA: water contact angle

WS: water solubility

WVP: water vapor permeability

XRD: X-ray diffraction

ZCPE: zein/chitosan films with Janus structure

ZT: zein and tannic acid hybrid particles

ZTC: Pickering emulsions co-loaded with tannic acid and cinnamon essential oil

Chapter 1

General introduction

Short overview

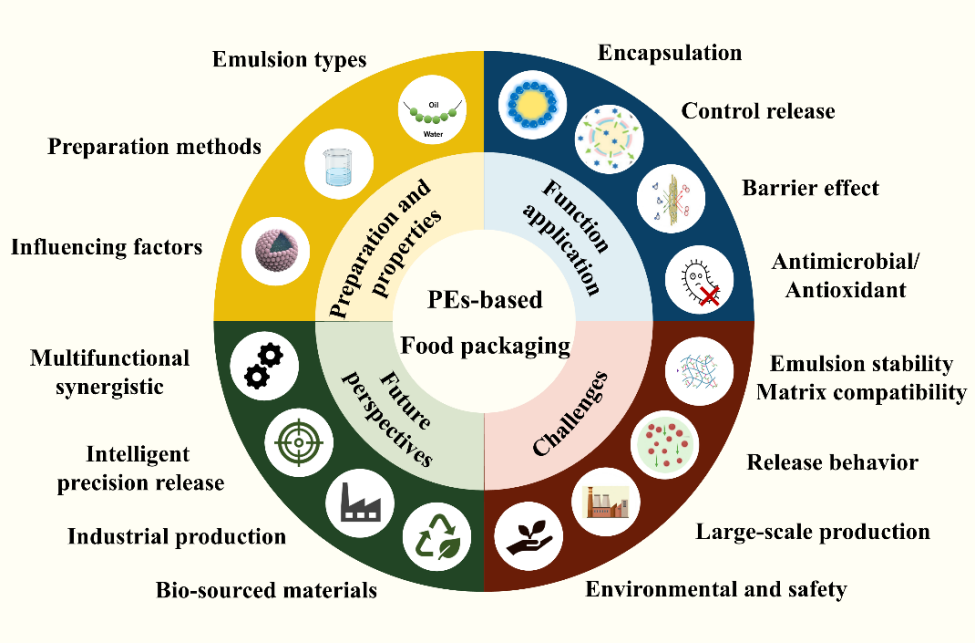

Graphical abstract: Pickering emulsions for enhancing the performance of food active packaging: Current research, Strategies, and future perspectives

1. Introduction

Food loss and waste is central to the food systems crisis, drawing widespread concern. Globally, approximately one-third of the total food produced is lost and wasted across multiple stages of the supply chain ("Food loss and waste," 2024). This issue is particularly evident in perishables, such as fresh meat. Meat spoilage driven by microbial growth and proliferation is one of the primary causes of meat loss and waste, to the negative sustainability impacts of meat products quality and human health (Shao, Chen, Wang, Zhang, Xu, & Wang, 2021). As the largest producer and consumer of meat, China faces growing concerns over meat loss and waste. According to a report from Chinese Institute of Food Science and Technology, meat spoilage dependent on microorganism account for up to 8% of meat losses in China, causing billions of dollars in losses for the meat industry (J. Chen, 2019). To extend the shelf life of fresh meat, various preservation technologies have been developed, among which active food packaging has gained increasing attention. Active food packaging is characterized as an innovative system that not only offers physical protection but also actively modulates the internal packaging environment through the integration of functional components or mechanisms. Unlike traditional packaging, this dynamic system engages in a continuous interaction with the food or its surrounding environment, effectively prolonging the shelf life and bolstering the safety of food products (Du, Sun, Chong, Yang, Zhu, & Wen, 2023).

1.1. Antimicrobial packaging

Antimicrobial packaging, a specialized form of active food packaging systems, is engineered through the integration of active compounds into polymer matrices to suppress microbial proliferation and consequently prolong the shelf life of perishable products. The concept of a ‘clean label’ has emerged as a growing trend in the food and packaging industries, referring to products formulated with natural, recognizable, and minimal ingredients, without synthetic additives or artificial preservatives. Plant-derived antimicrobial agents, such as essential oils (EOs), are considered promising natural functional ingredients that align with the clean label trend and can be strategically incorporated into antimicrobial packaging systems. EOs complex mixtures of secondary metabolites extracted from aromatic plants and flowers, comprising a diverse array of aromatic compounds (Ni, Wang, Shen, Thakur, Han, Zhang, et al., 2021). These natural substances have been shown to possess significant antibacterial properties, effectively inhibiting the growth of various microbial, including bacterial strains associated with meat spoilage (J. Ji, Shankar, Royon, Salmieri, & Lacroix, 2023). However, because of the low molecular weight characteristics, the release rates of EOs from antimicrobial packaging are potentially rapid, causing a loss of the prolonged activity of antimicrobial packaging during the application in food preservation (Figure1-1). Additionally, the localized high concentration of EOs produced by the rapid release behavior may have an impact on food flavor, nutritional content, and even consumer health. Nowadays, some researchers are dedicated to enhancing the performance of EOs in antimicrobial packaging systems and food preservation.

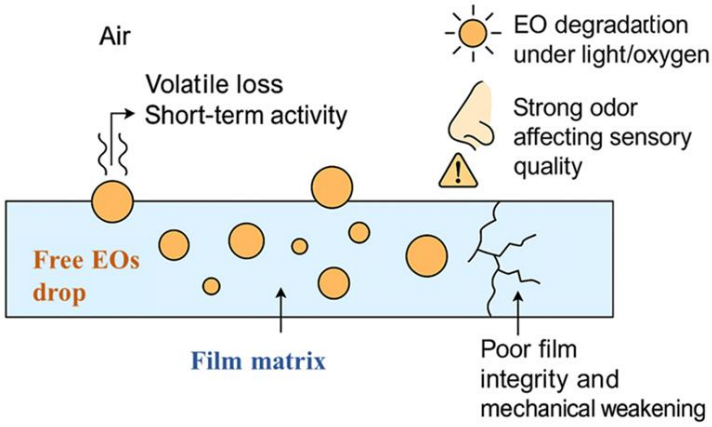

Figure 1-1 Changes of directly incorporating essential oils into food antimicrobial packaging.

1.2. Controlled release technology

Controlled release technology integrated with food packaging (CRP) offers a next-generation solution that ensures the slow and sustained release of active compounds (EOs in particular) over a predetermined period through precise material selection and structural design (Almasi, Jahanbakhsh Oskouie, & Saleh, 2021; X. Chen, Chen, Xu, & Yam, 2019; Kuai, Liu, Chiou, Avena-Bustillos, McHugh, & Zhong, 2021). CRP not only significantly extends the effective duration of EOs delivery but also enhances the predictability of release rates, thereby enhancing product efficiency and safety. Table 1-1 summarizes some approaches and application of CRP.

In response to the growing demand for innovative food preservation strategies, emulsion-based systems have emerged as a promising controlled release technology. Emulsions are biphasic systems consisting of dispersed oil droplets and a continuous aqueous phase, typically stabilized by emulsifiers or solid particles at the oil–water interface. Compared with traditional controlled release methods, emulsion-based systems offer notable advantages for incorporating bioactive compounds and modulating their release behavior. They feature mild, solvent-free preparation processes that help preserve the bioactivity and volatility of sensitive substances such as EOs.

Among the various emulsion types, Pickering emulsions (PEs) are particularly advantageous due to their stabilization by food-grade solid particles rather than conventional surfactants. Compared to traditional emulsions, PEs exhibit enhanced stability due to the presence of solid nanoparticles that stabilize the interface between two liquid phases. This leads to superior interfacial stability, lower toxicity, and greater compatibility with clean-label demands. Their enhanced stability and biocompatibility allow for effective protection of EOs from oxidation and volatilization, enabling a prolonged and tunable release during storage. Additionally,

active compound-loaded PEs can improve bioavailability and regulate release rates. Recently, PEs have been proposed as a strategy for CRP (Tavassoli, Khezerlou, Punia Bangar, Bakhshizadeh, Haghi, Moghaddam, et al., 2023). The following section explores their fundamental principles, advantages, and application in CRP for the controlled release of active compounds.

Table 1-1 Various approaches and application of controlled release packaging.

Approaches	Working principle	Advantages	Disadvantages	Reference
Modification polymers	Alters polymer structures through chemical or physical methods to control diffusion or degradation of active compounds.	Tunable release rates; compatibility with various active ingredients.	Release kinetics may be inconsistent; complex modification processes.	(Mulla, Ahmed, Al-Attar, Castro-Aguirre, Arfat, & Auras, 2017)
Multilayer structure	Combines multiple layers of materials to retain active compounds.	Precise control over release timing; customizable layer configurations.	Limited by layer adhesion and integrity; higher production complexity.	(Chenwei Chen, Li, Yang, Zhang, Yang, Tang, et al., 2019)
Micro encapsulation	Encapsulates active ingredients in microcapsules for gradual or triggered release.	Protects sensitive compounds; enables targeted and sustained release.	High production costs; potential burst release if capsules degrade.	(J. Wang, Li, Li, Song, Hu, Wang, et al., 2025)
Electrospinning technology	Creates nanofibrous mats with high surface area for controlled release of active agents.	High loading capacity; adjustable release profiles through fiber design.	Limited scalability; potential uneven distribution of active agents.	(Drago, Franco, Campardelli, De Marco, & Perego, 2022)
Nano-reinforcement	Incorporates nanoparticles to modulate the release of active compounds from polymer matrices.	Enhanced control over release kinetics; improved stability of active agents.	Risk of nanoparticle aggregation; potential regulatory and safety concerns.	(Dairi, Ferfera-Harrar, Ramos, & Garrigós, 2019)
Emulsion	Encapsulates active ingredients in emulsion droplets for controlled release.	Simple and scalable; suitable for both hydrophilic and hydrophobic compounds.	Limited stability; potential for premature release or phase separation.	(Ghadetaj, Almasi, & Mehryar, 2018)

2. Overview of PEs

2.1. Fundamental Principles

The concept of PEs dates back to the early 1900s when S.U. Pickering first reported that solid particles could stabilize emulsions (Pickering, 1907). He observed that these particles adhered to the oil-water interface, preventing droplet coalescence and forming a stable emulsion system. Traditional emulsions rely on surfactants to disperse oil droplets and maintain uniformity within the continuous water phase, whereas PEs are stabilized by the irreversible adsorption of solid particles at the oil-water interface. Thus, the dual affinity of particles for both two phases is a prerequisite for the formation of PEs. The classical type of PEs formed depends on the wettability of these particles (Figure 1-2). When the solid particles are preferentially wetted by water, they form oil-in-water (O/W) PEs; conversely, when they are preferentially wetted by oil, they form water-in-oil (W/O) PEs. More sophisticated version of PEs has also been reported in recent years, such as oil-in-water-in-oil double emulsion (Yajuan Sun, Wang, Jiang, Zhao, Yang, & Li, 2024) and water-in-oil-in-water double emulsion (Xie, Fang, Liu, Cong, Luo, Zhou, et al., 2024).

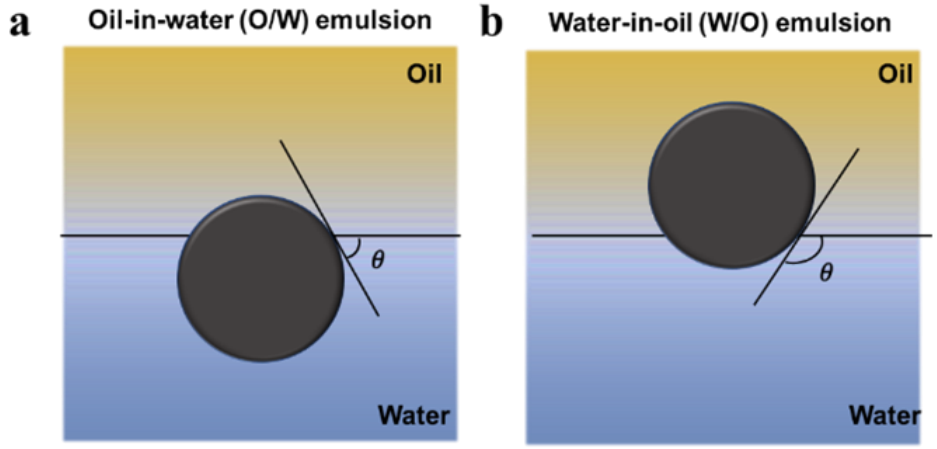

Figure 1-2 Graphical illustration of two classical types Pickering emulsions.

The particles create a steric barrier at the oil-water interface that blocks the droplet interaction through volume exclusion, preventing the aggregation of dispersed phases (Fredrick, Walstra, & Dewettinck, 2010; Low, Siva, Ho, Chan, & Tey, 2020). According to the classical stabilization theory of PEs, the desorption of these particles from the interface requires significant energy (as known as desorption energy, ΔE), providing PEs with excellent stability (Chevalier & Bolzinger, 2013; Schroën, Shen, Hasyyati, Deshpande, & van der Gucht, 2024) (Eq. 1.2.1).

$$\Delta E = \pi\gamma_{ow}R^2(1-|\cos\theta|)^2 \qquad (1.2.1)$$

Where ΔE represents the desorption energy (J), γOW denotes the interfacial tension of the pristine oil-water interface (N/m), R is the particle radius (m), and θ is the contact angle between the particle tangent and the water phase interface (°).

Although PEs are widely recognized for their high stability due to the irreversible adsorption of solid particles at the oil-water interface, they are still susceptible to various destabilization phenomena under certain conditions. Common instability mechanisms include flocculation, coalescence, creaming or sedimentation, and Ostwald ripening (Figure 1-3). Flocculation refers to the reversible aggregation of droplets caused by bridging or depletion interactions without the rupture of the interfacial layer (Fredrick, Walstra, & Dewettinck, 2010). In contrast, coalescence involves the fusion of adjacent droplets following the breakdown of the particle-stabilized interfacial film, leading to irreversible phase separation (Xu, Jia, Li, Sun, Cai, Wu, et al., 2024; Zhou, Chen, Chen, Wang, Cao, & Xiao, 2024). Creaming (or sedimentation) result from density differences between the dispersed and continuous phases, causing vertical migration and phase stratification; while reversible in theory, prolonged phase separation can accelerate coalescence. Ostwald ripening is a physicochemical process driven by the Laplace pressure difference between droplets of varying sizes, whereby dispersed phase molecules diffuse from smaller to larger droplets, resulting in a gradual increase in mean droplet size (Doan-Nguyen, Jiang, Koynov, Landfester, & Crespy, 2021; Trujillo-Cayado, Santos, Calero, Alfaro-Rodríguez, & Muñoz, 2020).

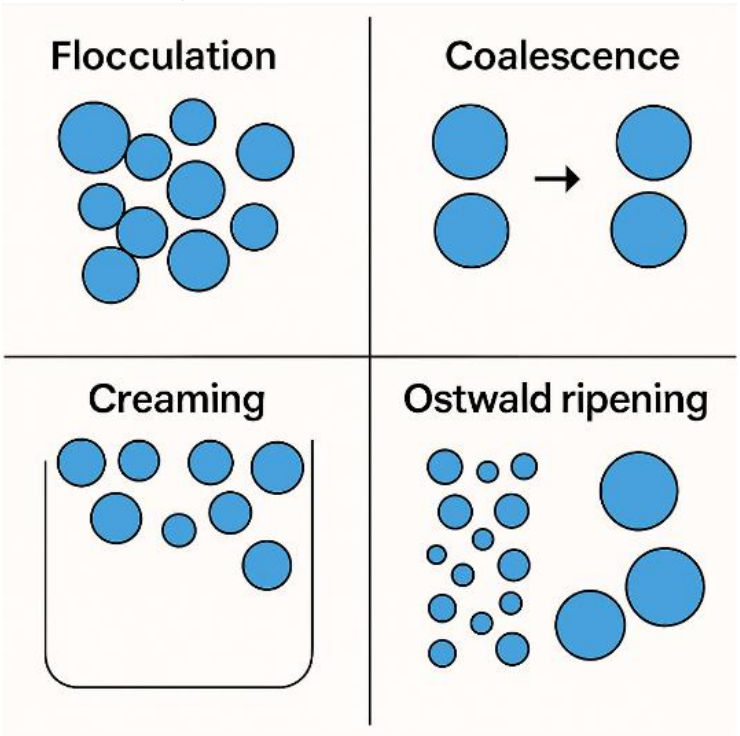

Figure 1-3 Destabilization mechanism of Pickering emulsions.

The occurrence of PEs destabilization is inherently linked to the physicochemical characteristics of the interfacial particles, particularly their size and concentration (Figure 1-4). Smaller particles can provide more efficient and dense coverage at the oil-water interface due to their higher specific surface area, enhancing the steric hindrance and mechanical barrier effect that resists droplet coalescence. However, particles that are too small may have insufficient adsorption energy to remain irreversibly anchored at the interface, leading to reduced stabilization efficiency. Conversely, particles that are too large may fail to uniformly cover the interface, resulting in exposed regions that are vulnerable to coalescence. In addition, insufficient particle concentration can lead to incomplete interfacial coverage, while excessively high concentrations may cause bridging flocculation or depletion-induced instability. Therefore, optimizing both particle size and concentration is critical for achieving a kinetically stable PEs system.

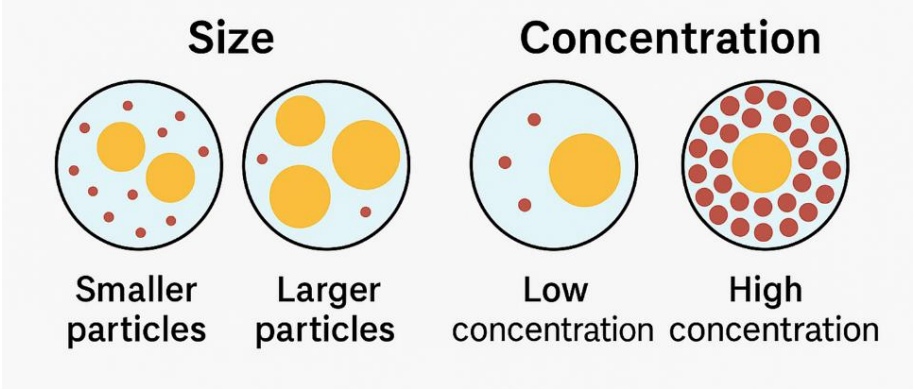

Figure 1-4 Destabilization of PEs are correlated to the size and concentration of particles.

These instability phenomena severely affect the functional performance of PEs in food packaging (Figure 1-5). For instance, flocculation or coalescence alters droplet size and distribution, impacting film-forming behavior and controlled-release properties. Ostwald ripening can lead to uncontrolled release kinetics of encapsulated actives, while creaming or sedimentation results in phase inhomogeneity, hindering downstream processing such as casting or spraying. Moreover, interfacial particle desorption may trigger burst release or loss of active compounds, compromising antimicrobial or antioxidant efficiency. Therefore, a comprehensive understanding of these instability mechanisms is crucial for tailoring PEs with enhanced stability and performance in active packaging applications.

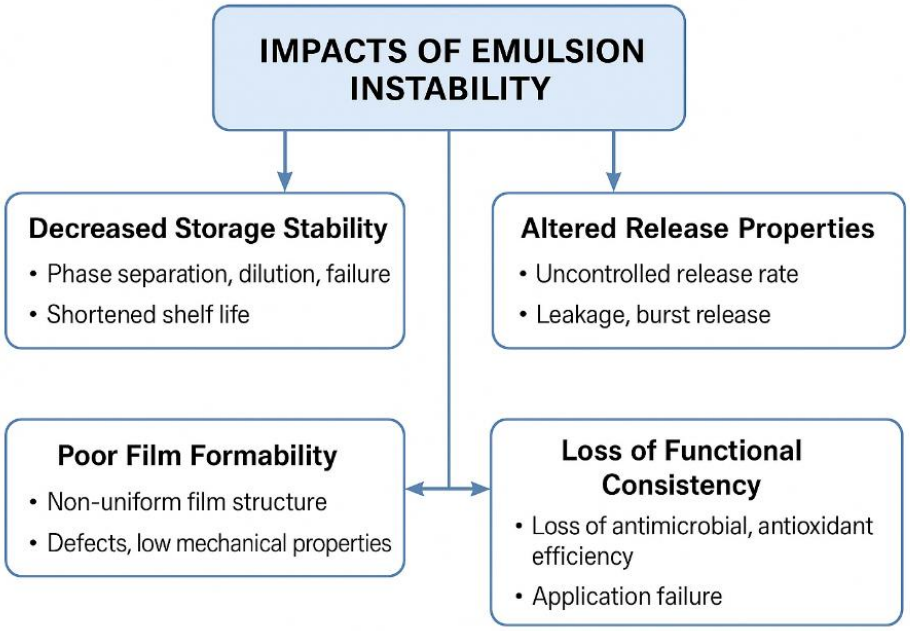

Figure 1-5 Impacts of Pickering emulsions instability in food packaging.

2.2. Preparation Methods

PEs can be prepared using several commonly used techniques (Cheng, Cai, Zhang, Zhao, Song, Xu, et al., 2024). Mechanical stirring involves adding particles to a mixture of the aqueous and oil phases, followed by high-shear mixing or homogenization to form an emulsion. For example, Yin et al. reported the fabrication of Zanthoxylum bungeanum oil-loaded PEs using a high-speed emulsification method (Yin, Chen, Han, Wang, Ding, Ding, et al., 2025). This method is simple to operate and suitable for large-scale production of PEs in food industry (H. Jiang, Yu, Guan, Jiang, Li, Liu, et al., 2024).

The ultrasonic emulsification method involves thoroughly mixing the oil phase, aqueous phase, and particles, followed by applying high frequency mechanical wave via an ultrasonic processor to facilitate emulsion formation. This method effectively produces emulsions with uniform droplet size distribution and excellent dispersion stability (Gao, Bu, Zhou, Wang, Bilal, Hassan, et al., 2022). Researchers have successfully prepared cinnamon essential oil-loaded PEs with uniformly dispersed droplets and high encapsulation efficiency using this method (Ly, Bui, Nguyen, Le, Tran, & Le, 2024).

Microfluidic technology is an innovative approach for PEs preparation. It employs a microfluidic chip that separately injects the oil and aqueous phases into distinct channels. Within the chip, these phases mix in the presence of particles, resulting in emulsions with precisely controlled droplet size and high monodispersity (Parvate, Vladisavljević, Leister, Spyrou, Bolognesi, Baiocco, et al., 2023). However, the

applicability of this approach remains limited to specific systems and conditions, requiring further research to broaden its potential applications (Nie, Wang, Zhou, Jiang, Fang, & Xiao, 2024).

Additionally, PEs can be prepared through a self-assembly (W. Meng, Sun, Mu, & Garcia-Vaquero, 2023). Particles pre-dispersed in either the oil or aqueous phase spontaneously migrate to the interface and assemble into a stable emulsion (W. Wu, Xu, Yang, Yang, Zhang, Wang, et al., 2022; Yu, Li, Ma, Wang, Zhu, & Wang, 2023). As a preparation method that does not require additional energy input, the self-assembly approach for preparing PEs is simple to operate and not constrained by complex equipment, making it highly promising for applications in the food industry (W. Meng, Sun, Mu, & Garcia-Vaquero, 2023).

2.3. Performance Influencing Factors

The properties of PEs are influenced by multiple factors. Based on PEs system composition, these factors can be categorized into the effects of solid particles, and the two phase (including the continuous phase and the dispersed phase). The following section provides a detailed discussion of these two aspects.

2.3.1 Solid Particles

Existing research highlights that the interfacial characteristics of solid colloidal particles are key determinants of both the formation and stability of PEs (Q. Zhao, Fan, Li, & Zhong, 2024). Solid particles typically need to be wetted by both the continuous and dispersed phases to ensure proper wettability and achieve sufficient interfacial adsorption. The three-phase contact angle serves as a qualitative indicator of the wettability of solid particles, reflecting the position of particles at the two-phase interface and dictating the type of PEs formed. Theoretically, as the particle contact angle approaches 90° (as see in Eq. (1)), the particles exhibit balanced wettability (neither too hydrophilic nor too hydrophobic), which maximizes their adsorption energy at the interface, significantly surpassing thermal energy. This strong interfacial anchoring ensures that particles remain firmly adsorbed, leading to highly stable PEs (C. Wang, Wu, Wang, Mu, Ngai, & Lin, 2022). Recent research has focused on developing biopolymer-based colloidal particles such as protein particles, polysaccharides particles and their hybrid particles to fabricate PEs (Q. Zhao, Fan, Li, & Zhong, 2024).

Once anchored at the interface, particles form a mechanical barrier known as the interfacial membrane (T. Liu, Chen, Zhao, Guo, Wang, Feng, et al., 2023). The properties of this interface membrane are determined by the particle size, concentration, and surface charge (Boostani, Sarabandi, Tarhan, Rezaei, Assadpour, Rostamabadi, et al., 2024). Particle size directly affects the coverage quality of the interfacial membrane. Smaller particles provide better coverage but may struggle to remain stably adsorbed due to strong Brownian motion, whereas larger particles create a more robust interfacial film but may lead to uneven coverage (Hollestelle, Michon, Fayolle, & Huc-Mathis, 2024; Shen, Wu, Zhao, & Zhou, 2024). Additionally, particle size determines the minimum concentration required for stable emulsion formation. However, excessive particle concentration can result in aggregation within the

continuous phase, hindering their adsorption at the interface (Tao, Zhu, Zhu, Lei, & Zhao, 2024). Surface charge plays a dual role in PEs. In terms of particle interactions, surface charge influences the dispersion state and adsorption behavior. For aspect of droplet interactions, surface charge ultimately determining emulsion stability and rheology properties (Wu, Zhang, Qiu, Pei, Li, Li, et al., 2021; Y. Zhao, Zhang, Chen, Liu, Zheng, Miao, et al., 2024).

2.3.2 Continuous and Dispersed Phase

Continuous phase and dispersed phase are the two main components of PEs. The polarity of the continuous phase dictates the emulsion type, with aqueous-continuous systems favoring oil-in-water (O/W) emulsions, which are common in food and pharmaceuticals. While non-polar oil phases promoting water-in-oil (W/O) emulsions, are prevalent in cosmetics (Schroën, Shen, Hasyyati, Deshpande, & van der Gucht, 2024). Typically, the stabilizing particles in PEs are dissolved in a continuous phase, the pH and ionic strength of the continuous phase further regulate the surface charge and wettability of stabilizing particles, impacting their adsorption behavior at the interface. A study on silica particles and soy hull polysaccharides have provided valuable insights into how pH and ionic strength influence the stability and rheological properties of PEs (Zhao, Wang, Yang, Wang, Han, & Liu, 2025). Additionally, the viscosity of the continuous phase plays a crucial role in controlling droplet mobility, where higher viscosity enhances stability by reducing coalescence and phase separation (Pires, Régnier, dos Santos, & Alves de Freitas, 2023).

The dispersed phase composition and concentration influence PEs properties including formation, stability and encapsulation efficiency. Polar of dispersed phase is factor that affects the emulsification process and the ability of particles to stabilize the interface. Hu et al. reported That under the same continuous phase conditions, a highly polar dispersed phase forms a more stable emulsion because the particles are more easily adsorbed onto the surface of highly polar oil droplets, leading to the formation of a stable interfacial film (Hu, Cao, Nguyen, Frank, Kalinowski, Li, et al., 2024).

High internal phase emulsions are a special type of emulsion in which the internal phase (dispersed phase) typically occupies more than 74% of the total volume. In these emulsions, the internal phase forms densely packed droplets, while the external phase (continuous phase) exists as a thin film, creating a continuous network that encapsulates the droplets and maintains emulsion stability. The rigid structure and high loading capacity of high internal phase emulsions provide promising solutions for food formulations, porous material, and 3D print technique (He & Lu, 2024; Rehman, Liang, Karim, Assadpour, Jafari, Rasheed, et al., 2024).

2.4. Advantages for essential oils encapsulation

PEs differ fundamentally from classical surfactant-stabilized emulsions in both stabilization mechanisms and physicochemical behavior. Classical emulsions rely on amphiphilic surfactants that dynamically adsorb and desorb at the oil-water interface to reduce interfacial tension and stabilize droplets. In contrast, PEs are stabilized by the irreversible adsorption of solid particles at the interface, forming a mechanically

robust and elastic interfacial film that effectively prevents droplet coalescence. This results in enhanced kinetic and, in some cases, thermodynamic stability.

Compared with traditional emulsions, PEs offer several advantages for the encapsulation and delivery of essential oils. First, their solid particle-based interfacial layer provides superior protection against coalescence, flocculation, and Ostwald ripening, ensuring long-term emulsion stability even under harsh conditions. Second, the use of food-grade and biocompatible particles-such as proteins, polysaccharides, and polyphenols-avoids potential toxicity concerns associated with low-molecular-weight surfactants, making PEs particularly suitable for food packaging applications.

Moreover, PEs offer significant tunability through the design of interfacial particles. By adjusting particle size, surface wettability, and concentration, the interfacial coverage and packing density can be precisely controlled. This tunability enables the regulation of release kinetics, allowing for sustained or stimuli-responsive release of encapsulated compounds. In the case of essential oils, this leads to improved retention of volatile components, enhanced oxidative stability, and controlled migration to the food surface-benefits that are difficult to achieve with conventional emulsions.

Given these advantages, PEs were selected over classical emulsions as the encapsulation platform in this study. A comparative overview of classical emulsions and Pickering emulsions, including their respective advantages and limitations, is presented in Table 1-2 to highlight their fundamental differences and application potential.

Table 1-2 Fundamental differences between classical and Pickering emulsions

Feature	Pickering Emulsion	Classical Emulsion
Stabilizer type	Solid particles	Molecular surfactants
Stabilization mechanism	Irreversible adsorption of particles	Adsorption of amphiphilic molecules
Interfacial energy	Strong reduction due to high desorption energy	Moderate reduction
Stability	Highly stable against coalescence and Ostwald ripening	Often kinetically stable, prone to coalescence
Environmental sensitivity	More robust but can be tuned by particle properties	Sensitive to pH, ionic strength, and temperature
Toxicological concern	Potentially food-grade or GRAS particles	Potential concerns with synthetic surfactants
Stimuli responsiveness	Possible but more complex (depends on particle design)	Easier to design for triggered release
Preparation complexity	Requires particle engineering	Relatively simple

3. PEs in Food Packaging

The utilization of PEs has garnered increasing research attention within the food packaging sector, primarily attributable to their distinctive structural stability and inherent natural functionality characteristic of particle-stabilized colloidal systems. This section specifically focuses on the functional convergence of PEs with advanced packaging matrices, particularly emphasizing nanoparticle-stabilized systems featured in sustainable packaging solutions. The current applications of PEs in food packaging are summarized in Table 1.2.

3.1. Encapsulation of Active Compounds

PEs are widely employed to encapsulate active compounds due to their compatible colloidal architectures and enhanced payload retention capabilities. There is a growing interest in applying natural antibacterial agents instead of synthetic ones to target foodborne bacteria, driven by the broad-spectrum antibacterial activity and good biocompatibility of natural extracts, as well as rising concerns over the potential risks of synthetic chemicals and the emergence of drug resistance. However, the inherent incompatibility between lipophilic phytochemical compounds and hydrophilic biopolymeric matrices presents significant technological challenges, particularly concerning functional instability manifested through volatilization and thermal degradation phenomena under processing conditions involving oxidative, photonic, and thermal stressors. PEs encapsulation strategy employs interfacial confinement mechanisms and molecular encapsulation architectures to mitigate these thermodynamic instabilities during bioactive film fabrication processes. In a comparative study about konjac glucomannan (KGM)-based active films incorporating different types of thyme essential oil emulsion, it was observed that thyme essential oils encapsulated in PEs exhibited improved dispersion within the KGM and provided enhanced protective effects (Zhe Liu, Lin, Li, & Yang, 2022). Moreover, a variety of bio-based nanoparticles are employed to construct stable encapsulating shells for the PEs, enhancing the overall stability and integrity of the encapsulated active compounds. For example, Liu et al. effectively addressed the poor solubility of curcumin by encapsulating it in PEs stabilized with octenyl succinic anhydride (OSA)-modified starch, which significantly improved the performance of the corn starch/polyvinyl alcohol films (D. Liu, Dang, Zhang, Munsop, & Li, 2021).

3.2. Controlled Release of Active Agents

When active substances are incorporated into food packaging films, two key processes occur before their functional activation. First, the active compounds and their carriers must migrate within the film matrix. Subsequently, after further diffusion, the active agents are gradually released from the film surface into the food or its surrounding environment (Kuai, Liu, Chiou, Avena-Bustillos, McHugh, & Zhong, 2021). PEs can enable the controlled/targeted release of loaded active agents, making them valuable for delivery systems in food packaging (Fan, Wang, Wen, Li, Fang, Richel, et al., 2023). Food spoilage is typically a gradual process rather than an instantaneous event. Therefore, if active agents in packaging materials are rapidly and

completely released during the early stages of storage, it may lead to excessive release at the beginning and insufficient protection in the later stages (Almasi, Jahanbakhsh Oskouie, & Saleh, 2021). This imbalance ultimately compromises the long-term preservation efficacy and fails to provide coverage throughout the entire shelf life. Moreover, an excessive number of active agents may negatively affect the sensory quality of food, including its flavor and texture. PEs offer excellent physical stability and act as effective carriers for active agents, enabling slow and sustained release (Ji & Wang, 2025). This makes them highly suitable for use in active food packaging to extend shelf life and preserve quality. This controlled release can be tailored by adjusting the properties of the PEs, including droplet size, the concentration of stabilizing particles, and the viscosity of the continuous phase (Dai, Chen, Chen, Fu, Ma, Wang, et al., 2023). Such tunability makes PEs a promising and versatile platform for the development of active packaging materials with customizable release profiles.

3.3. Effects of PEs on Packaging Systems

PEs have emerged as valuable components in the design of advanced packaging systems, owing to their proven ability to enhance the structural integrity, barrier efficiency, and functional performance of packaging films.

3.3.1 Mechanical Properties

The mechanical properties of packaging materials primarily refer to their resistance to external forces, typically assessed by tensile strength (TS), and their flexibility, which is commonly evaluated by elongation at break (EAB). Recent studies have indicated that the incorporation of PEs may have a positive effect on the TS of packaging materials. The polyvinyl alcohol/gelatin (PVA/Gel) films incorporated with perilla aldehyde-loaded PEs developed by Wen et al., (Wen, Wang, Xiao, Wei, Liu, Niu, et al., 2025) is an example. In this study, the incorporation of perilla aldehyde-loaded PEs improved the TS of PVA/Gel composite films. This enhancement can be attributed to the formation of extensive intermolecular reticulations, which reinforce the internal network structure. The resulting intermolecular network strengthens the interaction forces and improves the compatibility between film components, thereby contributing to the overall increase in mechanical strength. Xia et al. also observed an enhancement in TS during the study of bacterial cellulose nanocrystal-based three-phase PEs films (Xia, Sun, Jia, Li, Xu, Cao, et al., 2023). The improvement was attributed to the rigid structure of the bacterial cellulose nanocrystal stabilizers in PEs, which played a load-bearing role by effectively transferring tensile stress to the polymer chains, thereby reinforcing the mechanical performance of the film. However, in another study involving the incorporation of curcumin-loaded PEs into bacterial cellulose films, a reduction in TS was observed (Miao, Gu, Shi, Zhang, Yu, Xiao, et al., 2024), which was attributed to the disruption of the native bacterial cellulose chain density by the PEs droplets, weakened the cohesion of the polymer network and compromised the structural integrity of the film. In this study, the TS was also found to be influenced by the oil content in the internal phase of the PEs.

The incorporation of PEs has been shown to improve the EAB of polymer-based packaging films, primarily owing to their unique structural characteristics. The uniform dispersion of PEs in the film structure plays a critical role in determining EAB, as well-dispersed emulsions are generally associated with enhanced film flexibility and improved mechanical performance (Zhe Liu, Lin, Li, & Yang, 2022). Certain components (commonly found in essential oils) within the PEs may act as internal plasticizers, increasing the mobility of polymer chains and thereby contributing to the enhanced flexibility and extensibility of the films (Fan, et al., 2023). In an investigation of composite pectin coating films based on nanolignin citrus essential oil PEs (Zhang, Guo, Zhang, Ding, Li, Ai, et al., 2025), reported that the incorporation of nanolignin citrus essential oil PEs led to a significant increase in the EAB of coating films. This effect is believed to result from the plasticizing action of nanolignin citrus essential oil PEs, which improved the flexibility of the polymer network by increasing molecular chain mobility. Besides PEs containing essential oils, beeswax-loaded PEs have likewise been shown to enhance the EAB of polymer films (Trinh, Smith, & Mekonnen, 2022).

These findings suggests that the structural effects of PEs on film matrices are highly formulation-dependent, particularly with regard to droplet concentration, stabilizer, and oil phase content.

3.3.2 Barrier Properties

The barrier performance of food packaging materials typically encompasses three key aspects: resistance to water vapor, prevention of gas permeation, especially oxygen, and the ability to block light transmittance. In food packaging, the ability to resist water vapor transmission is essential for preventing moisture gain or loss in packaged foods, particularly in high-moisture or dry food products (Shah, Bhatia, Al-Harrasi, Tarahi, Almasi, Chawla, et al., 2024). The incorporation of PEs has been demonstrated to significantly enhance the water vapor barrier properties of packaging materials. For instance, Trinh et al. (Trinh, Smith, & Mekonnen, 2022) reported a 61.3% reduction in water vapor permeability (WVP) in a nanomaterial-stabilized beeswax PEs-starch film compared to the control starch film. This notable improvement was attributed not only to the uniform dispersion of hydrophobic beeswax within the matrix, but also to the increased tortuosity of the diffusion pathway for water molecules introduced by the presence of PEs. Yang et al. (W. Yang, Zhang, Hu, Fu, Cheng, Li, et al., 2024) investigated the WVP of pectin-based film incorporated with oregano essential oil PEs stabilized by carboxylate cellulose nanocrystals. Their results demonstrated that the WVP of the films decreased significantly, from 2.40 × 10-10 g/m·s·Pa to 1.40×10^{-10} g/m·s·Pa, as the PEs content increased from 0% to 10% (v/v). However, current research indicates that the incorporation of PEs into packaging matrices does not necessarily lead to significant enhancements in oxygen barrier properties, contrary to initial expectations. Trinh et al. (Trinh, Smith, & Mekonnen, 2022) observed the oxygen barrier property decreased of nanomaterial-stabilized beeswax PEs-starch film. The authors attributed this limited improvement to the diffusion of non-polar oxygen molecules through the hydrophobic beeswax channels, as well as their partial adsorption within the beeswax phase, which

collectively compromised the overall oxygen-blocking capability of the starch-films. In another study on chitosan/zein bilayer films containing cinnamon essential oil-loaded PEs (Fan, Yang, Zhu, Li, Richel, Fauconnier, et al., 2025), the oxygen permeability (OP) of the films increased from 6.76 to 11.02 g/(Pa·s·m) as the concentration of cinnamon essential oil-loaded PEs increased. The authors attributed this adverse effect on oxygen barrier performance to the evaporation of essential oil during the film-forming drying process. The light barrier properties of packaging materials incorporating PEs are largely dependent on the formulation of the emulsions, including the nature of the stabilizing particles and the dispersed phase. In a study involving PEs stabilized by lignin nanoparticles (LNPs) incorporated into pectin-based films, the addition of NLCPE significantly reduced UV transmittance, with nearly complete blockage in the ultraviolet region of the spectrum (Zhang, Guo, Zhang, Ding, Li, Ai, et al., 2025). This excellent UV-shielding performance was attributed to the unique phenolic hydroxyl groups and chromophoric structures present in lignin nanoparticles, which are capable of effectively absorbing UV radiation. PEs loaded with essential oils can reduce the light transmittance of packaging materials, primarily due to the presence of a high content of terpenoid compounds in the essential oils (Fan, Wang, Wen, Li, Fang, Richel, et al., 2023; Hou, Sun, Jia, Su, Cheng, Tan, et al., 2024).

3.3.3 Functional Properties

Beyond acting as carriers for active substances, PEs significantly contribute to the functional performance of packaging systems by imparting antimicrobial and antioxidant agents. Ji and Wang (Ji & Wang, 2025) demonstrated that the incorporation of PEs loaded with natural antibacterial agents significantly enhanced the antibacterial performance of the packaging films. In a study run by Liu et al.(J. Liu, Li, Chen, Ding, Wu, Gao, et al., 2022), the cinnamon oil was loaded into cellulose nanofiber-stabilized PEs and incorporated into gelatin/chitosan film applied in pork preservation. The results showed that the incorporation of cinnamon oil-loaded PEs significantly enhanced the antibacterial properties of the gelatin/chitosan films. The antibacterial inhibition zones against E. coli increased from 34.27 ± 3.65 mm^2 to 150.47 ± 12.86 mm^2, and those against S. aureus increased from 34.58 ± 2.15 mm^2 to 173.72 ± 11.91 mm^2. And these PEs films retained strong antibacterial activity even after 30 days of storage, demonstrating their potential for long-lasting antimicrobial effectiveness. Another zein/chitosan active film incorporating cinnamon essential oil-loaded PE was studied and applied in pork preservation (Fan, Yang, Zhu, Li, Richel, Fauconnier, et al., 2025). The study demonstrated that the high loading efficiency of the PEs enabled the film to exhibit outstanding antibacterial performance, achieving over 99% inhibition against P. paralactis MN10, A. pullicarnis MN21, and L. sakei VMR17. This pronounced antibacterial activity was attributed to the sustained release of cinnamon essential oil from both the PEs and the film matrix. The controlled release behavior ensured a prolonged antimicrobial effect, maintaining an effective concentration of active compounds over time. The small molecular constituents (such as cinnamaldehyde) of the cinnamon essential oil were capable of targeting bacterial cell walls, disrupting cell structures, and interfering with cellular metabolism. The

zein/chitosan active film also exhibited excellent antioxidant activity. Both the DPPH and ABTS radical scavenging capacities of the ZCPE films increased significantly ($P < 0.05$), with DPPH radical scavenging activity rising from 28.01% to 74.30%, and ABTS radical scavenging activity improving from 17.93% to 93.80%. These results highlight the strong antioxidant potential of the zein/chitosan active film, which also can be attributed to the sustained release of active compounds from the incorporated cinnamon essential oil-loaded PEs.

An advanced study conducted by Miao et al. further revealed that PEs can endow food packaging with freshness-indicating functionality (Miao, Gu, Shi, Zhang, Yu, Xiao, et al., 2024). This was achieved by incorporating pH-sensitive curcumin into the PE system, enabling the film to undergo visible color changes in basa fish perseveration, the color changed from light yellow to dark yellow as spoilage progressed during storage. Such a response provided a real-time visual indication of basa fish freshness, demonstrating the potential of PEs as multifunctional delivery systems in smart packaging applications.

Table 1-3 Current Applications of Pickering emulsions in Food Packaging

PEs	Stabilizer	Packaging matrix	Effect of PEs on packaging	Active properties	Preservation products	Reference
Citrus essential oil-loaded PEs	Nano lignin	Pectin	Enhanced mechanical properties, hydrophobicity, gas barrier performance	UV resistance, antioxidant and antimicrobial properties	Kiwifruit and strawberry	(Zhang, Guo, Zhang, Ding, Li, Ai, et al., 2025)
urcumin-embedded PEs	Protein-polysaccharide hybrid nanoparticles	Bacterial cellulose	Enhanced thermal stability, mechanical properties hydrophobicity, water vapor barrier	UV shielding properties, antioxidant and antimicrobial properties	Basa fish	(Miao, Gu, Shi, Zhang, Yu, Xiao, et al., 2024)
Perilla aldehyde-loaded PEs	Zein-octenylsuccinic anhydride-modified starch composite nanoparticles	Polyvinyl alcohol/gelatin	Reduced mechanical properties, Enhanced water vapor barrier	Antioxidant and antimicrobial properties	Strawberry	(Wen, Wang, Xiao, Wei, Liu, Niu, et al., 2025)
Three-phase Carnosic acid and ε-polylysine PEs	Bacterial cellulose nanocrystal	Gelatin	Enhanced thermal stability, hydrophobicity, water vapor barrier	UV-shielding, antioxidant and antibacterial properties	Cheese	(Xia, Sun, Jia, Li, Xu, Cao, et al., 2023)
Cornstarch-beeswax PEs	Cellulose nanocrystals	Nanomaterial-stabilized starch-beeswax PEs	Robust mechanical strength, simultaneous oxygen, and moisture barrier properties	/	Bananas, strawberries, and fresh-cut apples	(Trinh, Smith, & Mekonnen, 2022)
Cinnamon essential oil-loaded PEs	Cellulose nanocrystals	Chitosan/silk fibroin	Enhanced thermal stability, mechanical properties hydrophobicity, water	Antioxidant and antimicrobial properties	Strawberries	(J.-D. Wang, Yang, Liu, Zhou, Fu, Gu, et al.,

			vapor barrier			2024)
Cinnamon essential oil-loaded PEs	Bacterial cellulose	Chitosan	Improved thermal stability, mechanical strength, and barrier properties.	Antioxidant activity (up to 60%), antibacterial efficacy (up to 65%)	Fresh walnuts	(Chen, Deng, Tian, Yu, Huang, Lou, et al., 2025)
Thyme essential oil-loaded PEs	Oxidized chitin nanocrystalline	Konjac gum and hydroxypropyl methyl cellulose	Improved mechanical properties	Antioxidation, antibacterial effects, and ultraviolet radiation protection	Salmon	(Hou, Sun, Jia, Su, Cheng, Tan, et al., 2024)
Cinnamon essential oil-based	Soy protein isolates and chitosan	Collagen	Improved light-blocking, mechanical properties, and water resistance.	Anti-bacterial activity, anti-oxidant activity, and pH sensitivity.	Fish	(Ran, Xiong, Zheng, Tang, Zhang, Yang, et al., 2024)
Litsea cubeba oil Pickering emulsion	ZnO nanoparticles	Gelatin	Improve the biological, mechanical, and water-barrier properties	Electrochemical writing property	Mango	(Z. Yang, Li, Li, Li, Huang, Wang, et al., 2023)
Oregano essential oil-loaded PEs	Zein/tannic acid composite colloidal particles	Konjac glucomannan and carrageenan	Good mechanical strength, thermal stability, light blocking, and water vapor and oxygen permeability.	Antibacterial and antioxidant activity, pH sensitive	Fruit/shrimp	(Li, Liu, Yang, Wang, Yuan, Yue, et al., 2025)
Thyme essential oil-	Soybean lipophilic proteins	Soybean lipophilic	Oxidation resistance, water barrier	Antioxidant and bacteriostatic	Salmon	(Sun, Jia, Hou, Cheng,

loaded PEs		proteins	properties, thermal stability, and biodegradability.	activities		Tan, Zhu, et al., 2025)
Tea tree essential oil-loaded PEs	Soybean separation protein and carboxymethyl cellulose	Chitosan	Enhanced thermal stability, mechanical properties hydrophobicity, water vapor barrier	Antioxidant, antimicrobial	Pork	(H. Wang, Xu, Jin, Hu, Tao, Lu, et al., 2025)
Thymol-loaded PEs	γ-CD-MOF	Polyvinyl alcohol	Remarkable physical-mechanical performance	Antimicrobial efficacy	Basa (Pangasius) fish	(Cheng, Ying, Cai, Chen, Xu, Song, et al., 2025)
Baobab seed oil-loaded PEs	β-Cyclodextrin/persimmon pectin	Sodium alginate/guar gum	Enhanced mechanical, barrier, and biological properties	Antibacterial and antioxidant properties	Mushroom	(Z. Yang, Li, Li, Huang, Li, Zhai, et al., 2024)

4. Key Point for Successful Design of Antibacterial Packaging Film Based on PEs

Currently, considerable research attention has been directed toward the incorporation of PEs into active food packaging films. The integration of PEs into packaging matrices presents significant potential for the controlled release of bioactive compounds, particularly essential oils, thereby enhancing the antimicrobial and antioxidant functionalities of the packaging system. Nevertheless, to achieve optimal performance and ensure long-term stability, several critical factors must be carefully considered in the design and formulation of such PE-based food packaging.

4.1. PE stability

4.1.1 Particle characteristics

The characteristics of interface particles, including the wettability, shape, size of the particles, as well as their concentration fundamentally determine the properties of PEs, (Ming, Wu, Liu, Naeem, Dong, Fan, et al., 2023). The wettability of particles determines the type of PEs (O/W or W/O type), which commonly characterized by the three-phase contact angle. In food packaging, the encapsulated active compounds are typically hydrophobic, necessitating the formation of oil-in-water (O/W) emulsions for effective delivery and stabilization. The polymers such as chitin (Jiménez-Saelices, Trongsatitkul, Lourdin, & Capron, 2020), cellulose (Dai, Wu, Zhang, Chen, Ma, Huang, et al., 2020), starch (Zhu, 2019), and zein (E. M. C. Souza, Ferreira, & Soares, 2022) are usually considered stabilizers for active compounds. However, most polymeric particles used as stabilizers inherently possess hydrophilic domains (such as hydroxy group) in their molecular structures, which may limit their ability to effectively stabilize emulsions when used alone. To overcome this limitation, hybridization with other compounds (polysaccharides, proteins, and polyphenols) has been demonstrated to modulate their physicochemical properties, particularly wettability, thereby enhancing the overall stability and performance of the resulting PEs. Tao et al explored the stability of PEs stabilized by zein nanoparticles (ZNPs) in the presence of colloidal lignin particles (CLPs) (Tao, Zhu, Zhu, Lei, & Zhao, 2024). Their findings revealed that the incorporation of CLPs significantly improved the performance of ZNP-based PEs. The stabilizing effect of CLPs was primarily attributed to their electrostatic interactions with ZNPs, which enhanced the single ZNPs wettability, promoted interfacial adsorption, increased steric hindrance, and reinforced the formation of a dense, viscous interfacial network. This study highlights the role of composite particles in promoting the stability of PEs.

Although spherical particles are the most commonly used stabilizers in PEs, the morphology of stabilizing particles is not limited to spheres. Studies have shown that non-spherical particles, such as fibrous (Ji & Wang, 2023), rod-like (Ji, Wei, & Wang, 2024), and anisotropic shapes (Iwashita, 2020), can also effectively stabilize PEs. The geometry of particles significantly influences their arrangement and adsorption behavior at the oil-water interface, thereby affecting the stability of PEs. From the perspective of desorption energy, non-spherical particles exhibit higher desorption

energies compared to spherical particles with the same surface properties (i.e., similar wettability) (Low, Siva, Ho, Chan, & Tey, 2020). In terms of interparticle interactions, in addition to electrostatic forces and van der Waals interactions, non-spherical particles also experience capillary forces, which further contribute to the stability of the PE (Danov & Kralchevsky, 2010). This characteristic of shape is crucial for the encapsulation and protection of active compounds. Particularly in food packaging applications, non-spherical particles often provide stronger interfacial barriers and more complex structural networks, which can effectively slow down the diffusion of active substances from the emulsion to the external environment. In a study comparing lemon essential oil PEs stabilized by different types of cellulose with β-cyclodextrin (T. Liu, Chen, Zhao, Guo, Wang, Feng, et al., 2023), it was found that cellulose nanocrystals and β-cyclodextrin formed irregularly shaped particles anchored at the oil-water interface. These particles effectively enhanced interfacial tension and interfacial dilatational modulus, thereby creating a more substantial barrier against the diffusion of lemon essential oil.

To achieve more stable PEs, the particle size and concentration are also critical factors that must be taken into account. Generally, the particle size needs to be much smaller than the droplet size to effectively stabilize PEs. Smaller particles can more efficiently cover the oil-water interface, thereby offering better emulsion stability. For example, Kim et al. (2016) investigated the effect of silica nanoparticles with different sizes on the stability of PEs. They found that silica particles with a diameter of 5 nm could form a dense interfacial layer, providing stronger steric hindrance protection. The particle size determines the droplet size of the PEs. In food active packaging, smaller PE droplets are generally preferred, as larger droplets may disrupt the continuity of the polymer network, thereby negatively affecting the mechanical properties of the packaging materials. The concentration of particles can also modulate the stability of PE. A stable PE can only be formed when the particle concentration meets the minimum surface coverage required at the oil-water interface. Jiang et al. found that, in the case of PEs stabilized by zein/pectin composite nanoparticles, a stable PE could only be formed when the particle concentration exceeded 0.125% (Jiang, Wang, Li, Li, & Huang, 2020). This study also found that as the particle concentration increased to 2%, the droplet size decreased accordingly. Higher particle concentrations generally lead to the formation of smaller droplets due to more efficient coverage of the oil-water interface, which in turn enhances emulsion stability (Feng, Dai, Ma, Fu, Yu, Zhou, et al., 2020). The size and concentration of stabilizing particles must be synergistically optimized to achieve a balance in PEs performance.

In summary, the characteristics of stabilizing particles are the most critical considerations in the preparation of PEs for active compound delivery. Researchers must seek a balance among several key factors to develop PEs with optimal stability and functionality.

4.1.2 Emulsion formulation

Most studies on the stability of PEs have primarily focused on the role of solid particles. However, the type and content of the oil phase also play a crucial role in

determining stability of PEs. Oils with different polarities can significantly influence the positioning and adsorption strength of particles at the oil-water interface, thereby affecting interfacial energy and particle wettability. These variations ultimately impact the formation, structure, and long-term stability of PEs. In the field of active food packaging, plant essential oils are commonly used as the oil phase in PEs. These essential oils generally exhibit medium to low polarity, which primarily depends on their chemical composition. As complex mixtures, plant essential oils contain a variety of compounds, including terpenes, esters, aldehydes, and ketones, all of which influence their overall polarity and interaction with stabilizing particles at the oil-water interface. In a comparative study investigating the properties of PEs loaded with three different essential oils (cardamom, cinnamon cassia, and ho wood essential oil), the authors found that, despite being stabilized by the same nanofibrils, the PEs exhibited distinct differences in droplet size, rheological behavior, and stability (A. G. Souza, Ferreira, Paula, Setz, & Rosa, 2020). These variations were attributed to the polarity and chemical characteristics of the essential oils, which significantly influence their interfacial behavior and interactions with stabilizing particles. Cardamom and cinnamon oils possess relatively stable chemical structures (benzene ring and cyclohexene group), contributing to effective steric stabilization of the PEs. In contrast, ho wood oil, with its more reactive chemical structure (linalool that contains an alcohol end group), formed additional hydrogen bonds upon the introduction of cellulose nanofibrils (CNF), which disrupted the interfacial balance and promoted droplet coalescence. Moreover, oil phases containing specific functional groups may interact with the stabilizing particles, thereby influencing the adsorption behavior of particles at the interface. Tang et al. indicate that cinnamaldehyde in the oil phase of cinnamon essential oil interacted with the chitosan-gum Arabic coacervated complex via Schiff base reactions, hydrophobic interactions, and in situ hydrogen bonding (Tang, Gao, & Tang, 2023). These interactions significantly enhanced the adsorption of the chitosan-gum Arabic coacervated complex particles at the oil-water interface, resulting in the formation of a dense interfacial layer and ultimately yielding a stable PE. The type and content of the oil phase in PEs also influence the performance of food packaging films. For instance, Dai et al. prepared PEs containing cinnamon essential oil (CEO) and applied them to enhance the properties of gelatin-based films (Dai, Chen, Chen, Fu, Ma, Wang, et al., 2023). The study demonstrated that by adjusting the CEO ratio in the emulsion, various properties of the resulting latex films could be modulated, including color, morphology, mechanical strength, barrier properties, and functional characteristics. Additionally, the mechanical properties, including tensile strength (TS) and elongation at break (EB), were improved after CEO incorporation. As the CEO content in oil phase increased, the surface structure of the films became more uniform and compact, and the flexibility of films was improved. Increasing the oil phase content typically enhances the flexibility of packaging materials while reducing their rigidity. Moreover, an appropriate amount of oil phase can effectively fill micropores within the packaging matrix, thereby improving its barrier properties.

4.2. Polymer matrix compatibility

The compatibility between PEs and the polymer matrix is a critical factor in the design of active food packaging. Since the emulsion is typically incorporated into a continuous polymer network to form composite films, poor compatibility can lead to phase separation, non-uniform dispersion, and compromised mechanical or barrier properties of the final material. The physical and chemical interactions between the stabilizing particles, the encapsulated active compounds, and the polymer chains determine the structural integrity and performance of the film. Dai et al. found that the incorporation of PEs loaded with cinnamon essential oil (CEO) into gelatin films significantly influenced the microstructure of the resulting materials (Dai, et al., 2023). As the CEO proportion in the emulsions increased, the gelatin-based emulsion films exhibited progressively smoother, denser, and more homogeneous surfaces. This was attributed to the nano-filling effect and additional intermolecular hydrogen bonds between of the emulsion droplets within the polymer matrix, which contributed to the formation of a more compact and structurally refined film network.

From the perspective of emulsion droplets, the surface chemistry of the emulsion-stabilizing particles must be compatible with the polymer matrix to ensure uniform droplet dispersion and effective interfacial anchoring. This compatibility facilitates the retention of the stable interfacial structures formed by the PEs during the film-forming process. For example, Liu et al., reported that the cross-sectional morphology of konjac glucomannan (KGM) films transformed into a densely packed, uniform, and stratified porous structure following the incorporation of PEs stabilized by tannic acid-functionalized zein nanoparticles (Z. Liu, Ma, Hao, Bian, Zhang, Wang, et al., 2024). This structural refinement was ascribed to the excellent interfacial compatibility between the protein-based self-assembled nanoparticles and the KGM matrix, which not only facilitated homogeneous dispersion but also established robust interfacial networks that impeded the flocculation and coalescence of oil droplets within the polymeric framework. In contrast, an opposite trend was observed in gelatin films incorporated with PEs stabilized by bacterial cellulose nanofibers (BCNs) (Xia, et al., 2023). Due to the intramolecular hydrogen bonding and electrostatic repulsion between the similarly charged BCNs and gelatin (GL), significant aggregation of BCNs within the film matrix was observed. However, this issue was mitigated by increasing the content of positively charged ε-Polylysine in the dispersed phase of the PEs, which improved the compatibility and dispersion of PEs within the gelatin matrix.

In addition, a well-compatible system can synergistically delay the migration of active substances through the interaction between the particles and the polymer matrix. Fan et al. incorporated cinnamon essential oil (CEO)-loaded PEs into chitosan/gelatin (CS/GL) films and investigated the release behavior in a 50% ethanol food simulant system (Fan, Wang, Wen, Li, Fang, Richel, et al., 2023). It was observed that the release rate of CEO from the CS/GL self-assembled films was significantly lower than that from the CS/GL bilayer films. This phenomenon was attributed to the extensive hydrogen bonding network formed between chitosan and gelatin molecules, which

stabilized the spatial structure of the film matrix and effectively regulated the controlled release of CEO.

Consequently, the design of PE-based food packaging films systems must involve a comprehensive, multidimensional evaluation of polymer matrix to achieve optimal integration and performance.

4.3. Controlled Release Behavior

The primary purpose of loadng active compounds, such as essential oils, into PEs is to achieve a sustained and targeted release, thereby prolonging the antimicrobial effects and enhancing food preservation. The release profile is influenced by several factors, including the structure and composition of the stabilizing particles, the type of polymer matrix, and environmental conditions such as temperature, humidity, and pH (Pandita, de Souza, Gonçalves, Jasińska, Jamróz, & Roy, 2024). Ideally, the release should be gradual and responsive to the storage environment or food spoilage signals, rather than occurring rapidly and uncontrollably (Westlake, Tran, Jiang, Zhang, Burrows, & Xie, 2022). This suggests that researchers could integrate environmental factors with material properties when designing antimicrobial packaging based on PEs. For instance, Meng et al. reported the development of pH-responsive PEs by grafting cationic polymer polyethyleneimine (PEI) onto TEMPO-oxidized cellulose nanocrystals (CNCs), creating nanoparticles with both amino and carboxyl groups (Meng, Xue, Chen, Wu, & Lu, 2023). These particles were used to stabilize oregano essential oil, resulting in a stable and intelligent antimicrobial PE with pH-responsive release behavior. The emulsion exhibited rapid release under both acidic (pH 4.0) and alkaline (pH 8.0) conditions, enabling on-demand and targeted delivery of antimicrobial agents. This approach not only enhanced the efficacy of the antimicrobial agents but also minimized their required dosage, making it a promising strategy for designing more efficient and sustainable active food packaging.

To further enhance the controlled release performance of PE-based films, several advanced strategies have been explored. One approach involves increasing the degree of crosslinking within the polymer matrix, which enhances the density of the film network, thereby creating a more effective barrier to the release of active compounds. This modification helps to regulate the release rate by restricting the diffusion of active agents and improving the overall stability of the film (Thungphotrakul & Prapainainar, 2024; H. Yang, Xu, Li, Li, Tao, Lu, et al., 2025). For example, mulberry extract was incorporated into gelatin-based films containing PE to enhance the internal crosslinking of the film matrix (Ran, et al., 2024). The phenolic compounds present in the mulberry extract interacted with the gelatin chains through hydrogen bonding and covalent interactions, leading to a denser and more compact network structure. This improved network not only enhanced the mechanical strength and barrier properties of the films but also effectively slowed down the release rate of the active compounds. Another promising strategy is the incorporation of nanoparticles to form tortuous diffusion pathways within the film. The addition of nanoparticles, such as cellulose nanocrystals or nanoclays, increases the surface area and creates a more complex network that hinders the direct diffusion of active substances, leading

to a more gradual and controlled release profile. Additionally, composite loading techniques can be employed to form multiple diffusion barriers within the packaging material. By combining different functional materials, such as polymers with varying permeability or incorporating layers with different release characteristics, researchers can create a multilayer system that provides enhanced control over the release behavior (Fan, Yang, Zhu, Li, Richel, Fauconnier, et al., 2025; Li, et al., 2025).

These strategies can further optimize PE-incorporated packaging film systems, thereby improving food preservation and reducing the reliance on chemical preservatives.

4.4. Environmental and safety factors

Since the packaging materials come into direct contact with food, it is essential to ensure that all components—including emulsifiers, stabilizing particles, and polymer matrices, are non-toxic, biocompatible, and compliant with relevant food safety regulations. The use of food-grade or naturally derived particles, such as cellulose nanocrystals, chitosan, or plant proteins, is preferred to minimize potential health risks and regulatory barriers.In addition to safety, environmental sustainability is a growing concern. Packaging materials should ideally be biodegradable, recyclable, or derived from renewable resources to reduce environmental impact. The development of eco-friendly PEs using natural solid particles and biodegradable polymers aligns with the increasing demand for sustainable food packaging solutions. A study developed a biodegradable multifunctional packaging film by incorporating a PE stabilized with cellulose nanocrystals and loaded with cinnamon essential oil into a chitosan/silk fibroin matrix (J.-D. Wang, et al., 2024). The resulting film demonstrated nearly complete degradation within approximately two weeks under composting conditions. Furthermore, the authors assessed the environmental impact of the film during its production process. Compared to conventional polypropylene (PP) and polyethylene (PE) films, the newly developed film reduced fossil resource consumption by over 68% and mitigated global warming potential and ozone formation by more than 50%. This study highlights the potential of PE-based packaging to not only improve food preservation but also significantly contribute to environmental sustainability. Furthermore, production processes should be designed to minimize energy consumption and solvent use, ensuring that the overall environmental footprint of the packaging system is as low as possible.

5. Conclusion and future perspectives

The synergistic integration of PE-based antimicrobial delivery systems with bio-based materials has emerged as an innovative strategy to overcome the traditional bottlenecks of low active ingredient utilization and uncontrolled release in food packaging. The core mechanism lies in the hierarchical physical barriers formed by the interfacial self-assembly of PEs, which not only minimize the loss of antimicrobial agents during film formation but also regulate their sustained release through modulation of diffusion pathways. This significantly enhances the spatial and temporal utilization efficiency of active compounds. Furthermore, this system can

simultaneously improve the mechanical properties, barrier performance, and antimicrobial/antioxidant functionality of the packaging films, creating a multidimensional synergistic enhancement of food packaging material properties. In addition, this review systematically elucidates that the stability of PEs and the compatibility with polymer matrices are key factors in regulating the controlled release behavior of antimicrobial packaging systems.

To further advance PE-based food packaging technologies and their application performance, future research should focus on the following areas:

i) Construction of multifunctional synergistic systems: Harnessing the multiphase interfacial characteristics of PEs to develop composite carriers with dual or multiple functions (e.g., antimicrobial and antioxidant), thereby achieving coordinated preservation effects through the spatiotemporal distribution control of active compounds;

ii) Development of stimuli-responsive precision delivery systems: Engineering stimuli-responsive particles by chemical modifications (e.g., Schiff base linkages, disulfide bonds) in response to specific food spoilage microenvironmental factors (such as pH changes, enzymes, or metabolites) to establish intelligent on-demand release mechanisms for active ingredients;

iii) Structure-function integrated packaging development: Overcoming the limitations of traditional film materials by integrating microfluidic molding and 3D printing technologies to create novel formats such as controlled-release antimicrobial pads, smart hydrogel dressings, and porous topological cushioning materials, thereby achieving precise programming of active loading sites and release kinetics;

iv) Analysis of migration behavior and safety risks: Systematically investigating the migration kinetics of active compounds from packaging matrices into food systems and assessing their biological safety, in order to establish a comprehensive lifecycle risk assessment framework based on nanoparticle-biointerface interactions.

In summary, due to their unique interfacial stability and high-efficiency loading capacity for active ingredients, PEs offer innovative solutions for the food packaging field. Their technological advantages in targeted delivery and controlled release of bioactives are expected to drive breakthrough improvements in food preservation performance. With continuous technological advancements and deeper mechanistic insights, such as optimization of particle/matrix interactions and environmental responsiveness, PE-based systems hold great promise to transition from laboratory research to large-scale applications, becoming a core driving force for the green and functional upgrading of the food packaging industry.

6. Reference

Almasi, H., Jahanbakhsh Oskouie, M., & Saleh, A. (2021). A review on techniques utilized for design of controlled release food active packaging. Critical Reviews in Food Science and Nutrition, 61(15), 2601-2621.

Boostani, S., Sarabandi, K., Tarhan, O., Rezaei, A., Assadpour, E., Rostamabadi, H., Falsafi, S. R., Tan, C., Zhang, F., & Jafari, S. M. (2024). Multiple Pickering

emulsions stabilized by food-grade particles as innovative delivery systems for bioactive compounds. Advances in Colloid and Interface Science, 328, 103174.

Chen, C., Deng, S., Tian, H., Yu, H., Huang, J., Lou, X., & Yuan, H. (2025). Enhanced fresh walnut preservation using chitosan films reinforced with cinnamon essential oil and bacterial cellulose pickering emulsion. Food Hydrocolloids, 165, 111267.

Chen, C., Li, C., Yang, S., Zhang, Q., Yang, F., Tang, Z., & Xie, J. (2019). Development of New Multilayer Active Packaging Films with Controlled Release Property Based on Polypropylene/Poly (Vinyl Alcohol)/Polypropylene Incorporated with Tea Polyphenols. Journal of Food Science, 84(7), 1836-1843.

Chen, J. (2019). Food science and technology in China: from 2020 to 2035. Journal of Chinese Institute of Food Science and Technology, 19(12), 1-5.

Chen, X., Chen, M., Xu, C., & Yam, K. L. (2019). Critical review of controlled release packaging to improve food safety and quality. Critical Reviews in Food Science and Nutrition, 59(15), 2386-2399.

Cheng, Y., Cai, X., Zhang, X., Zhao, Y., Song, R., Xu, Y., & Gao, H. (2024). Applications in Pickering emulsions of enhancing preservation properties: Current trends and future prospects in active food packaging coatings and films. Trends in Food Science & Technology, 151, 104643.

Cheng, Y., Ying, X., Cai, X., Chen, Y., Xu, Y., Song, R., & Gao, H. (2025). Characterization of γ-CD-MOF-stabilized thymol Pickering emulsion films with enhanced preservation properties for Basa (Pangasius) fish. Food Chemistry, 476, 143273.

Chevalier, Y., & Bolzinger, M.-A. (2013). Emulsions stabilized with solid nanoparticles: Pickering emulsions. Colloids and Surfaces A: Physicochemical and Engineering Aspects, 439, 23-34.

Dai, H., Chen, Y., Chen, H., Fu, Y., Ma, L., Wang, H., Yu, Y., Zhu, H., & Zhang, Y. (2023). Gelatin films functionalized by lignocellulose nanocrystals-tannic acid stabilized Pickering emulsions: Influence of cinnamon essential oil. Food Chemistry, 401, 134154.

Dai, H., Wu, J., Zhang, H., Chen, Y., Ma, L., Huang, H., Huang, Y., & Zhang, Y. (2020). Recent advances on cellulose nanocrystals for Pickering emulsions: Development and challenge. Trends in Food Science & Technology, 102, 16-29.

Dairi, N., Ferfera-Harrar, H., Ramos, M., & Garrigós, M. C. (2019). Cellulose acetate/AgNPs-organoclay and/or thymol nano-biocomposite films with combined antimicrobial/antioxidant properties for active food packaging use. International Journal of Biological Macromolecules, 121, 508-523.

Danov, K. D., & Kralchevsky, P. A. (2010). Capillary forces between particles at a liquid interface: General theoretical approach and interactions between capillary multipoles. Advances in Colloid and Interface Science, 154(1), 91-103.

Doan-Nguyen, T. P., Jiang, S., Koynov, K., Landfester, K., & Crespy, D. (2021). Ultrasmall Nanocapsules Obtained by Controlling Ostwald Ripening. Angewandte Chemie International Edition, 60(33), 18094-18102.

Drago, E., Franco, P., Campardelli, R., De Marco, I., & Perego, P. (2022). Zein electrospun fibers purification and vanillin impregnation in a one-step supercritical process to produce safe active packaging. Food Hydrocolloids, 122, 107082.

Du, H., Sun, X., Chong, X., Yang, M., Zhu, Z., & Wen, Y. (2023). A review on smart active packaging systems for food preservation: Applications and future trends. Trends in Food Science & Technology, 141, 104200.

Fan, S., Wang, D., Wen, X., Li, X., Fang, F., Richel, A., Xiao, N., Fauconnier, M.-L., Hou, C., & Zhang, D. (2023). Incorporation of cinnamon essential oil-loaded Pickering emulsion for improving antimicrobial properties and control release of chitosan/gelatin films. Food Hydrocolloids, 138, 108438.

Fan, S., Yang, Q., Zhu, C., Li, X., Richel, A., Fauconnier, M.-L., Fang, F., Zhang, D., & Hou, C. (2025). Zein/chitosan Janus film incorporated with tannic acid and cinnamon essential oil co-loaded Pickering emulsion for sustained controlled release and pork preservation. International Journal of Biological Macromolecules, 286, 138429.

Feng, X., Dai, H., Ma, L., Fu, Y., Yu, Y., Zhou, H., Guo, T., Zhu, H., Wang, H., & Zhang, Y. (2020). Properties of Pickering emulsion stabilized by food-grade gelatin nanoparticles: influence of the nanoparticle's concentration. Colloids and Surfaces B: Biointerfaces, 196, 111294.

Food loss and waste. (2024). Nature Food, 5(8), 639-639.

Fredrick, E., Walstra, P., & Dewettinck, K. (2010). Factors governing partial coalescence in oil-in-water emulsions. Advances in Colloid and Interface Science, 153(1), 30-42.

Gao, J., Bu, X., Zhou, S., Wang, X., Bilal, M., Hassan, F. U., Hassanzadeh, A., Xie, G., & Chelgani, S. C. (2022). Pickering emulsion prepared by nano-silica particles – A comparative study for exploring the effect of various mechanical methods. Ultrasonics Sonochemistry, 83, 105928.

Ghadetaj, A., Almasi, H., & Mehryar, L. (2018). Development and characterization of whey protein isolate active films containing nanoemulsions of Grammosciadium ptrocarpum Bioss. essential oil. Food Packaging and Shelf Life, 16, 31-40.

He, X., & Lu, Q. (2024). A review of high internal phase Pickering emulsions: Stabilization, rheology, and 3D printing application. Advances in Colloid and Interface Science, 324, 103086.

Hollestelle, C., Michon, C., Fayolle, N., & Huc-Mathis, D. (2024). Co-stabilization mechanisms of solid particles and soluble compounds in hybrid Pickering emulsions stabilized by unrefined apple pomace powder. Food Hydrocolloids, 146, 109184.

Hou, Y., Sun, Y., Jia, S., Su, W., Cheng, S., Tan, M., & Wang, H. (2024). Double-layer films based on konjac gum and hydroxypropyl methyl cellulose loaded with thyme essential oil Pickering emulsion: Preparation, characterization, and application. Food Hydrocolloids, 157, 110459.

Hu, Y., Cao, Y., Nguyen, F. M., Frank, B. D., Kalinowski, M. J., Li, M., Rajani, S., & Marelli, B. (2024). Antibody-Targeted Phytohormone Delivery Using Foliar Sprayed Silk Fibroin Pickering Emulsions. Advanced Functional Materials, 34(38), 2402618.

Iwashita, Y. (2020). Pickering–Ramsden emulsions stabilized with chemically and morphologically anisotropic particles. Current Opinion in Colloid & Interface Science, 49, 94-106.

Ji, C., & Wang, Y. (2023). Nanocellulose-stabilized Pickering emulsions: Fabrication, stabilization, and food applications. Advances in Colloid and Interface Science, 318, 102970.

Ji, C., & Wang, Y. (2025). Recent advances in Pickering emulsions for inhibiting foodborne bacteria. Current Opinion in Food Science, 61, 101265.

Ji, C., Wei, J., & Wang, Y. (2024). Cinnamaldehyde-enriched Pickering emulsions stabilized by modified cellulose I and II nanocrystals recycled from maple leaves for shrimp preservation. Carbohydrate Polymers, 326, 121590.

Ji, J., Shankar, S., Royon, F., Salmieri, S., & Lacroix, M. (2023). Essential oils as natural antimicrobials applied in meat and meat products—a review. Critical Reviews in Food Science and Nutrition, 63(8), 993-1009.

Jiang, H., Yu, H., Guan, X., Jiang, W., Li, Y., Liu, W., Yang, C., Jiang, J., Binks, B. P., & Ngai, T. (2024). Harnessing the Power of Nature: Monodisperse Pickering Emulsion Droplets and Yolk-Shell Microcapsules Utilizing Bee Pollen Particles. Advanced Functional Materials, 34(25), 2316510.

Jiang, Y., Wang, D., Li, F., Li, D., & Huang, Q. (2020). Cinnamon essential oil Pickering emulsion stabilized by zein-pectin composite nanoparticles: Characterization, antimicrobial effect and advantages in storage application. International Journal of Biological Macromolecules, 148, 1280-1289.

Jiménez-Saelices, C., Trongsatitkul, T., Lourdin, D., & Capron, I. (2020). Chitin Pickering Emulsion for Oil Inclusion in Composite Films. Carbohydrate Polymers, 242, 116366.

Kim, I., Worthen, A. J., Johnston, K. P., DiCarlo, D. A., & Huh, C. (2016). Size-dependent properties of silica nanoparticles for Pickering stabilization of emulsions and foams. Journal of Nanoparticle Research, 18, 1-12.

Kuai, L., Liu, F., Chiou, B.-S., Avena-Bustillos, R. J., McHugh, T. H., & Zhong, F. (2021). Controlled release of antioxidants from active food packaging: A review. Food Hydrocolloids, 120, 106992.

Li, S., Liu, L., Yang, S., Wang, X., Yuan, Y., Yue, T., Cai, R., & Wang, Z. (2025). Designing double-layer smart packaging with sustained-release antibacterial and antioxidant activities for efficient preservation and high-contrast monitoring. Food Hydrocolloids, 158, 110559.

Liu, D., Dang, S., Zhang, L., Munsop, K., & Li, X. (2021). Corn starch/polyvinyl alcohol based films incorporated with curcumin-loaded Pickering emulsion for application in intelligent packaging. International Journal of Biological Macromolecules, 188, 974-982.

Liu, J., Li, K., Chen, Y., Ding, H., Wu, H., Gao, Y., Huang, S., Wu, H., Kong, D., Yang, Z., & Hu, Y. (2022). Active and smart biomass film containing cinnamon oil and curcumin for meat preservation and freshness indicator. Food Hydrocolloids, 133, 107979.

Liu, T., Chen, Y., Zhao, S., Guo, J., Wang, Y., Feng, L., Shan, Y., & Zheng, J. (2023). The sustained-release mechanism of citrus essential oil from cyclodextrin/cellulose-based Pickering emulsions. Food Hydrocolloids, 144, 109023.

Liu, Z., Lin, D., Li, N., & Yang, X. (2022). Characterization of konjac glucomannan-based active films loaded with thyme essential oil: Effects of loading approaches. Food Hydrocolloids, 124, 107330.

Liu, Z., Ma, W., Hao, Y., Bian, J., Zhang, Y., Wang, H., Li, L., & Wang, Y. (2024). Development of antimicrobial and antioxidant film by incorporation of modified protein self-assembled nanoparticles into Pickering emulsion. Food Packaging and Shelf Life, 41, 101236.

Low, L. E., Siva, S. P., Ho, Y. K., Chan, E. S., & Tey, B. T. (2020). Recent advances of characterization techniques for the formation, physical properties and stability of Pickering emulsion. Advances in Colloid and Interface Science, 277, 102117.

Ly, T. B., Bui, B. T. A., Nguyen, Y. T. H., Le, K. A., Tran, V. T., & Le, P. K. (2024). Innovative ultrasonic emulsification of cinnamon essential oil pickering emulsion stabilized by rice straw-derived cellulose nanocrystals. International Journal of Biological Macromolecules, 276, 134084.

Meng, Q., Xue, Z., Chen, S., Wu, M., & Lu, P. (2023). Smart antimicrobial Pickering emulsion stabilized by pH-responsive cellulose-based nanoparticles. International Journal of Biological Macromolecules, 233, 123516.

Meng, W., Sun, H., Mu, T., & Garcia-Vaquero, M. (2023). Pickering emulsions with chitosan and macroalgal polyphenols stabilized by layer-by-layer electrostatic deposition. Carbohydrate Polymers, 300, 120256.

Miao, W., Gu, R., Shi, X., Zhang, J., Yu, L., Xiao, H., & Li, C. (2024). Indicative bacterial cellulose films incorporated with curcumin-embedded Pickering emulsions: Preparation, antibacterial performance, and mechanism. Chemical Engineering Journal, 495, 153284.

Ming, L., Wu, H., Liu, A., Naeem, A., Dong, Z., Fan, Q., Zhang, G., Liu, H., & Li, Z. (2023). Evolution and critical roles of particle properties in Pickering emulsion: A review. Journal of Molecular Liquids, 388, 122775.

Mulla, M., Ahmed, J., Al-Attar, H., Castro-Aguirre, E., Arfat, Y. A., & Auras, R. (2017). Antimicrobial efficacy of clove essential oil infused into chemically modified LLDPE film for chicken meat packaging. Food Control, 73, 663-671.

Ni, Z.-J., Wang, X., Shen, Y., Thakur, K., Han, J., Zhang, J.-G., Hu, F., & Wei, Z.-J. (2021). Recent updates on the chemistry, bioactivities, mode of action, and industrial applications of plant essential oils. Trends in Food Science & Technology, 110, 78-89.

Nie, C., Wang, W., Zhou, Z., Jiang, Z., Fang, S., & Xiao, J. (2024). A microfluidic and Langmuir approach to unveil the interplay between hydroxypropyl methylcellulose and zein nanoparticles on the stability of Pickering emulsions. Food Hydrocolloids, 157, 110382.

Nimaming, N., Sadeghpour, A., Murray, B. S., & Sarkar, A. (2023). Hybrid particles for stabilization of food-grade Pickering emulsions: Fabrication principles and interfacial properties. Trends in Food Science & Technology, 138, 671-684.

Pandita, G., de Souza, C. K., Gonçalves, M. J., Jasińska, J. M., Jamróz, E., & Roy, S. (2024). Recent progress on Pickering emulsion stabilized essential oil added biopolymer-based film for food packaging applications: A review. International Journal of Biological Macromolecules, 269, 132067.

Parvate, S., Vladisavljević, G. T., Leister, N., Spyrou, A., Bolognesi, G., Baiocco, D., Zhang, Z., & Chattopadhyay, S. (2023). Lego-Inspired Glass Capillary Microfluidic Device: A Technique for Bespoke Microencapsulation of Phase Change Materials. ACS Applied Materials & Interfaces, 15(13), 17195-17210.

Pickering, S. U. (1907). Cxcvi.—emulsions. Journal of the Chemical Society, Transactions, 91, 2001-2021.

Pires, C., Régnier, B. M., dos Santos, M. J. R., & Alves de Freitas, R. (2023). Effect of sulfate-ester content and nanocellulose allomorph on stability of amylopectin-xyloglucan water-in-water emulsions. Food Hydrocolloids, 141, 108700.

Ran, R., Xiong, Y., Zheng, T., Tang, P., Zhang, Y., Yang, C., & Li, G. (2024). Active and intelligent collagen films containing laccase-catalyzed mulberry extract and pickering emulsion for fish preservation and freshness indicator. Food Hydrocolloids, 147, 109326.

Rehman, A., Liang, Q., Karim, A., Assadpour, E., Jafari, S. M., Rasheed, H. A., Virk, M. S., Qayyum, A., Rasul Suleria, H. A., & Ren, X. (2024). Pickering high internal phase emulsions stabilized by biopolymeric particles: From production to high-performance applications. Food Hydrocolloids, 150, 109751.

Schroën, K., Shen, X., Hasyyati, F. I., Deshpande, S., & van der Gucht, J. (2024). From theoretical aspects to practical food Pickering emulsions: Formation, stabilization, and complexities linked to the use of colloidal food particles. Advances in Colloid and Interface Science, 334, 103321.

Shah, Y. A., Bhatia, S., Al-Harrasi, A., Tarahi, M., Almasi, H., Chawla, R., & Ali, A. M. M. (2024). Insights into recent innovations in barrier resistance of edible films for food packaging applications. International Journal of Biological Macromolecules, 271, 132354.

Shao, L., Chen, S., Wang, H., Zhang, J., Xu, X., & Wang, H. (2021). Advances in understanding the predominance, phenotypes, and mechanisms of bacteria related to meat spoilage. Trends in Food Science & Technology, 118, 822-832.

Shen, P., Wu, J., Zhao, M., & Zhou, F. (2024). Does particle size matter for soy protein nanoparticles in the fabrication and lipolysis of pickering-like emulsions? Food Hydrocolloids, 153, 110005.

Souza, A. G., Ferreira, R. R., Paula, L. C., Setz, L. F. G., & Rosa, D. S. (2020). The effect of essential oil chemical structures on Pickering emulsion stabilized with cellulose nanofibrils. Journal of Molecular Liquids, 320, 114458.

Souza, E. M. C., Ferreira, M. R. A., & Soares, L. A. L. (2022). Pickering emulsions stabilized by zein particles and their complexes and possibilities of use in the food industry: A review. Food Hydrocolloids, 131, 107781.

Sun, Y., Jia, S., Hou, Y., Cheng, S., Tan, M., Zhu, B., & Wang, H. (2025). Novel thyme essential oil-loaded biodegradable emulsion film based on soybean lipophilic proteins for salmon preservation. Food Hydrocolloids, 160, 110790.

Sun, Y., Wang, C., Jiang, H., Zhao, B., Yang, C., & Li, Y. (2024). Biocompatible oil-in-water-in-oil double emulsion stabilized synergistically by phytosterol/chitosan complex particle and gelatin. Food Hydrocolloids, 147, 109419.

Tang, Y., Gao, C., & Tang, X. (2023). In situ rapid conjugation of chitosan-gum Arabic coacervated complex with cinnamaldehyde in cinnamon essential oil to stabilize high internal phase Pickering emulsion. Food Hydrocolloids, 134, 108103.

Tao, J., Zhu, L., Zhu, L., Lei, L., & Zhao, G. (2024). Colloidal lignin particle reinforces the stability of Pickering emulsions prepared with zein nanoparticle. Food Chemistry, 460, 140581.

Tavassoli, M., Khezerlou, A., Punia Bangar, S., Bakhshizadeh, M., Haghi, P. B., Moghaddam, T. N., & Ehsani, A. (2023). Functionality developments of Pickering emulsion in food packaging: Principles, applications, and future perspectives. Trends in Food Science & Technology, 132, 171-187.

Thungphotrakul, N., & Prapainainar, P. (2024). Development of polyvinyl alcohol/carboxymethylcellulose-based bio-packaging film with citric acid crosslinking and clove essential oil encapsulated chitosan nanoparticle pickering emulsion. International Journal of Biological Macromolecules, 282, 137223.

Trinh, B. M., Smith, M., & Mekonnen, T. H. (2022). A nanomaterial-stabilized starch-beeswax Pickering emulsion coating to extend produce shelf-life. Chemical Engineering Journal, 431, 133905.

Trujillo-Cayado, L. A., Santos, J., Calero, N., Alfaro-Rodríguez, M.-C., & Muñoz, J. (2020). Strategies for reducing Ostwald ripening phenomenon in nanoemulsions based on thyme essential oil. Journal of the Science of Food and Agriculture, 100(4), 1671-1677.

Wang, C., Wu, J., Wang, C., Mu, C., Ngai, T., & Lin, W. (2022). Advances in Pickering emulsions stabilized by protein particles: Toward particle fabrication, interaction and arrangement. Food Research International, 157, 111380.

Wang, H., Xu, Z., Jin, X., Hu, J., Tao, Y., Lu, J., Xia, X., Tan, M., Du, J., & Wang, H. (2025). Structurally robust chitosan-based active packaging film by Pickering emulsion containing tree essential oil for pork preservation. Food Chemistry, 466, 142246.

Wang, J.-D., Yang, S.-L., Liu, G.-S., Zhou, Q., Fu, L.-N., Gu, Q., Cai, Z.-H., Zhang, S., & Fu, Y.-J. (2024). A degradable multi-functional packaging based on

chitosan/silk fibroin via incorporating cellulose nanocrystals-stabilized cinnamon essential oil pickering emulsion. Food Hydrocolloids, 153, 109978.

Wang, J., Li, L., Li, Y., Song, Q., Hu, Y., Wang, Q., & Lu, S. (2025). Characterization of thyme essential oil microcapsules and potato starch/pectin composite films and their impact on the quality of chilled mutton. Food Chemistry, 464, 141692.

Wen, J., Wang, B., Xiao, Y., Wei, L., Liu, Y., Niu, W., Wang, H., Yan, H., Niu, B., & Li, W. (2025). Spherical nanoparticle-stabilized perilla aldehyde picolin emulsion functionalized polyvinyl alcohol/gelatin composite film for strawberry preservation. Chemical Engineering Journal, 511, 161638.

Westlake, J. R., Tran, M. W., Jiang, Y., Zhang, X., Burrows, A. D., & Xie, M. (2022). Biodegradable Active Packaging with Controlled Release: Principles, Progress, and Prospects. ACS Food Science & Technology, 2(8), 1166-1183.

Wu, W., Xu, J., Yang, L., Yang, M., Zhang, T., Wang, X., & Zhong, J. (2022). Self-assembled hydrolyzed gelatin nanoparticles from silver carp spine bones for Pickering emulsion stabilization. Food Bioscience, 48, 101735.

Wu, Y., Zhang, X., Qiu, D., Pei, Y., Li, Y., Li, B., & Liu, S. (2021). Effect of surface charge density of bacterial cellulose nanofibrils on the rheology property of O/W Pickering emulsions. Food Hydrocolloids, 120, 106944.

Xia, J., Sun, X., Jia, P., Li, L., Xu, K., Cao, Y., Lü, X., & Wang, L. (2023). Multifunctional sustainable films of bacterial cellulose nanocrystal-based, three-phase pickering nanoemulsions: A promising active food packaging for cheese. Chemical Engineering Journal, 466, 143295.

Xie, F., Fang, Y., Liu, X., Cong, X., Luo, Y., Zhou, J., Din, Z.-u., Cheng, S., & Cai, J. (2024). Transformation of W/O/W emulsions and O/W/O emulsions for co-loading selenium-enriched peptide and vitamin E: Design and characteristics. Journal of Food Engineering, 360, 111702.

Xu, W., Jia, Y., Li, J., Sun, H., Cai, L., Wu, G., Kang, M., Zang, J., & Luo, D. (2024). Pickering emulsion with high freeze-thaw stability stabilized by xanthan gum/lysozyme nanoparticles and konjac glucomannan. International Journal of Biological Macromolecules, 261, 129740.

Yang, H., Xu, Z., Li, L., Li, C., Tao, Y., Lu, J., Hu, J., Xia, X., Tan, M., Du, J., & Wang, H. (2025). Boosting the loading dosage of cinnamon essential oil within edible packaging film via the multiple cross-linking strategy for effective shrimp preservation. Food Hydrocolloids, 158, 110490.

Yang, W., Zhang, S., Hu, Y., Fu, Q., Cheng, X., Li, Y., Wu, P., Li, H., & Ai, S. (2024). Pectin-based film activated with carboxylated cellulose nanocrystals-stabilized oregano essential oil Pickering emulsion. Food Hydrocolloids, 151, 109781.

Yang, Z., Li, M., Li, Y., Huang, X., Li, Z., Zhai, X., Shi, J., Zou, X., Xiao, J., Sun, Y., Povey, M., Gong, Y., & Holmes, M. (2024). Sodium alginate/guar gum based nanocomposite film incorporating β-Cyclodextrin/persimmon pectin-stabilized baobab seed oil Pickering emulsion for mushroom preservation. Food Chemistry, 437, 137891.

Yang, Z., Li, M., Li, Y., Li, Z., Huang, X., Wang, X., Shi, J., Zou, X., Zhai, X., Povey, M., & Xiao, J. (2023). Improving properties of Litsea cubeba oil Pickering emulsion-loaded gelatin-based bio-nanocomposite film via optimizing blending ratio: Application for mango preservation. Food Hydrocolloids, 145, 109052.

Yin, X., Chen, F., Han, B., Wang, X., Ding, W., Ding, B., & You, J. (2025). Chitin nanowhiskers-stabilized Pickering emulsions for encapsulating flavor compounds in Zanthoxylum bungeanum oil. Food Hydrocolloids, 163, 111067.

Yu, X., Li, X., Ma, S., Wang, Y., Zhu, W., & Wang, H. (2023). Biomass-Based, Interface Tunable, and Dual-Responsive Pickering Emulsions for Smart Release of Pesticides. Advanced Functional Materials, 33(27), 2214911.

Zhang, S., Guo, H., Zhang, B., Ding, K., Li, H., Ai, S., Shan, Y., & Ding, S. (2025). A composite coating film based on the interfacial interlocking symbiosis of nanolignin Pickering emulsion and pectin matrix for perishable fruit preservation. Chemical Engineering Journal, 507, 160886.

Zhao, G., Wang, S., Yang, L., Wang, P., Han, L., & Liu, H. (2025). Stability of electrostatically stabilized Pickering emulsion of silica particles and soy hull polysaccharides: Mechanism of pH and ionic strength. Food Chemistry, 471, 142804.

Zhao, Q., Fan, L., Li, J., & Zhong, S. (2024). Pickering emulsions stabilized by biopolymer-based nanoparticles or hybrid particles for the development of food packaging films: A review. Food Hydrocolloids, 146, 109185.

Zhao, Y., Zhang, F., Chen, M., Liu, F., Zheng, B., Miao, W., Gao, H., & Zhou, R. (2024). Cellulose nanofibrils-stabilized food-grade Pickering emulsions: Clarifying surface charge's contribution and advancing stabilization mechanism understanding. Food Hydrocolloids, 152, 109920.

Zhou, Z., Chen, M., Chen, Z., Wang, W., Cao, Y., & Xiao, J. (2024). Formation and properties of zein Particle-GMS Co-stabilized pickering emulsions: Insights into the complex interface. Food Hydrocolloids, 149, 109518.

Zhu, F. (2019). Starch based Pickering emulsions: Fabrication, properties, and applications. Trends in Food Science & Technology, 85, 129-137.

Chapter 2

Objective and outline

1. Research Questions

This study seeks to address the following scientific questions:

i) How can interfacial engineering strategies be employed to efficiently encapsulate cinnamon essential oil (CEO) into Pickering emulsions (PEs), thereby enhancing their long-term physical stability and enabling sustained antimicrobial release?

ii) How can CEO-loaded PEs be effectively incorporated into biodegradable packaging films through rational structural design, and how does the resulting film architecture govern the CEO diffusion and controlled release behavior?

iii) To what extent can the CEO-loaded films inhibit microbial proliferation and maintain the quality of fresh meat during refrigerated storage?

2. Hypothesis

This study hypothesizes that encapsulating CEO in PEs and structurally integrating them into biodegradable packaging films will enable sustained CEO release by modulating interfacial properties and diffusion pathways, thereby enhancing antimicrobial efficacy, prolonging the shelf life of fresh meat, and contributing to the development of sustainable food packaging systems.

3. Objective

The primary objective of this study is to develop a biodegradable packaging film system with controlled release antimicrobial functionality by integrating CEO-loaded PEs through rational structural design. Specifically, this study aims to:

i) Formulate physically stable CEO-loaded PEs with high encapsulation efficiency and tunable release profiles.

ii) Incorporate CEO-loaded PEs into biodegradable films using structure-oriented strategies to ensure controlled CEO diffusion and release.

iii) Elucidate the diffusion mechanisms of CEO within the film matrix based on interfacial properties and film architecture.

iv) Evaluate the antimicrobial activity and preservation performance of the developed films in real fresh meat systems under refrigerated storage conditions.

4. Research Outline

The research outline is shown in Figure 2-1. There are three main experiment parts (chapter 3, 4, 5), that answer the research question above.

In chapter 3, a sire of zein and tannic acid hybrid particles (ZT) were fabricated in different pH value, and these ZT hybrid particles were used to stabilized CEO-loaded PEs, aiming to improve the encapsulation efficiency, physical stability and antimicrobial activity of emulsion. The measurements including morphology, structure, size, wettability, interfacial tension, was used to evaluate their potential in

enhancing physical stability, encapsulation efficiency, and antimicrobial activity. The high-performance CEO-loaded PEs was considered for next part.

In chapter 4, the CEO-loaded PEs (prepared in chapter 3) incorporated with multilayer system, aim to target sustained release. A zein/chitosan Janus film was developed by combining CEO-loaded PEs/chitosan loading layer and zein barrier layer, aiming to sustained antimicrobial release and enhanced meat preservation. The comprehensive characterization of films involves morphology structure mechanical barrier properties and antimicrobial activity. Then, the release behavior of CEO was evaluated using food simulation and kinetics mathematical. Final, the high-performance film was used to packaging fresh meat.

In chapter 5, the quercetin nanocrystals (QNs) were used to adjusted the internal structure of CEO-loaded PEs/chitosan/PVA film, aim to improve the control release and other properties of film, and enhanced meat preservation. The comprehensive characterization measurements were carried out and release behavior of films was evaluated. Final, the high-performance film was used to packaging fresh meat.

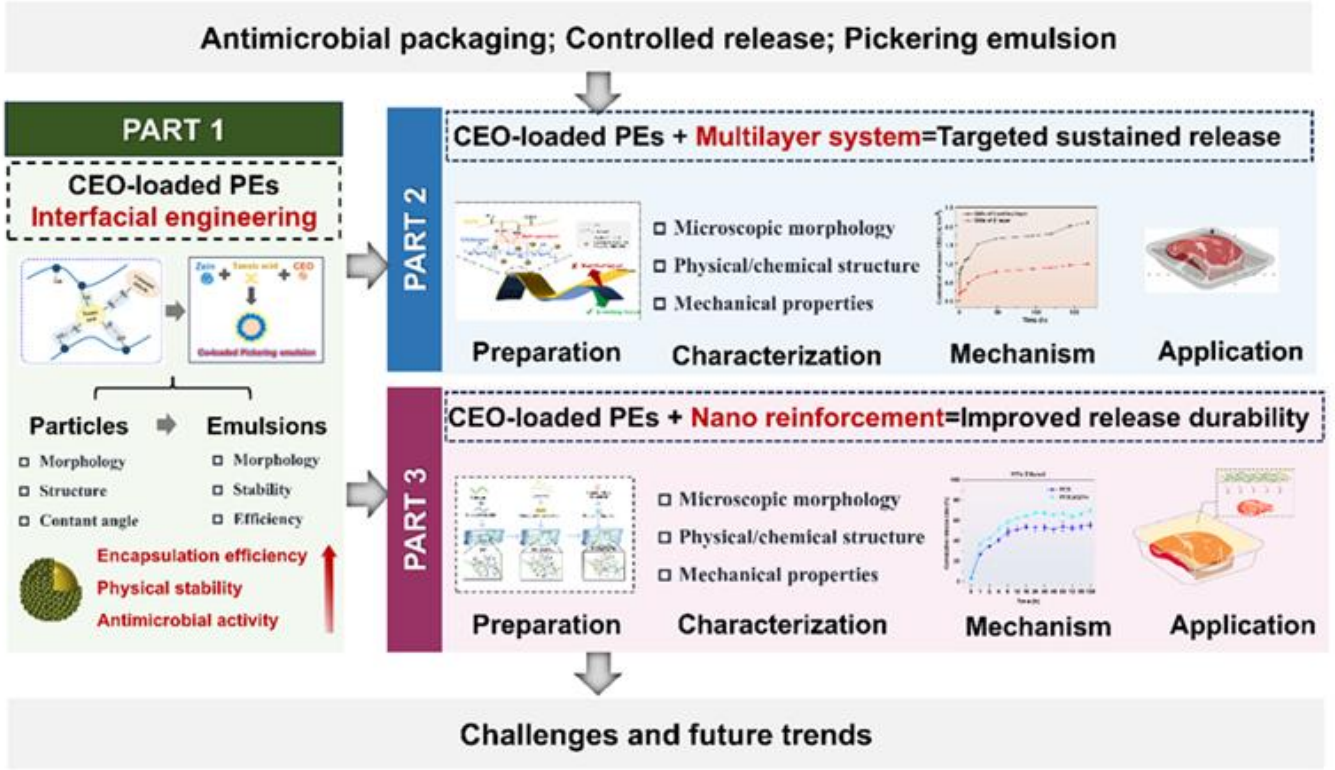

Figure 2-1 Research outline of thesis

Chapter 3

Zein and tannic acid hybrid particles improving physical stability, controlled release properties, and antimicrobial activity of cinnamon essential oil loaded Pickering emulsions

Short overview

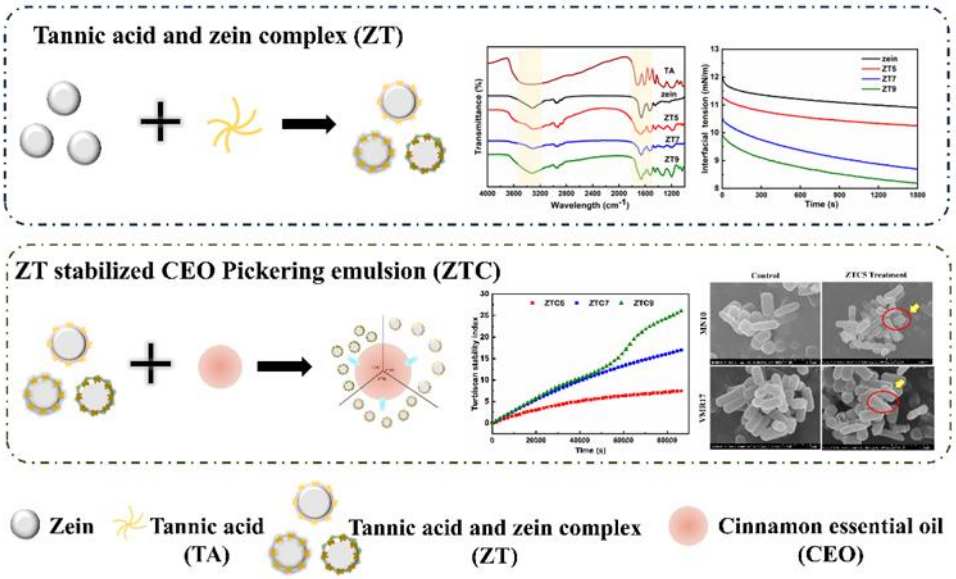

Graphical abstract: Zein and tannic acid hybrid particles improving physical stability, controlled release properties, and antimicrobial activity of cinnamon essential oil loaded Pickering emulsions

The research content of this chapter has been published in the international peer-reviewed journal ***Food Chemistry***, to which readers are referred for more comprehensive details by **Fan, S.,** Yang, Q., Wang, D., Zhu, C., Li, X., Richel, A., Fauconnier, M.-L., Yang, W., Hou, C., & Zhang, D. (2024). Zein and tannic acid hybrid particles improving physical stability, controlled release properties, and antimicrobial activity of cinnamon essential oil loaded Pickering emulsions. *Food Chemistry*, 446, 138512.

Abstract

Pickering emulsion loading essential oil has demonstrated a promising strategy as delivery system in food preservation, but localization in stability and antimicrobial activity limits application. In this study, Pickering emulsions co-loaded with tannic acid and cinnamon essential oil (ZTC) have been developed based on zein and tannic acid complexes (ZT) mediated interfacial engineering. Fourier transform infrared, fluorescence spectroscopy, and molecular docking results indicated tannic acid altered the structural of zein. Interfacial tension results indicated that tannic acid accelerated the adsorbed speed of zein particles by decreased interfacial tension (11.99-9.96 mN/m). ZT5 formed a viscoelastic and dense layer in oil-water interface than that for other ZTs, which improved stability and control release performance of ZTC. Furthermore, the ZTC showed an effective antimicrobial activity against spoilage organisms *P. paralactis* MN10 and *L. sakei* VMR17. These findings provide new insight for developing co-loaded multiple antimicrobial agents within Pickering emulsion as a delivery system.

Keywords: Function Pickering emulsion; Tannic acid; Zein; Interfacial engineering; Antimicrobial activity

1. Introduction

Microbiology in food preservation has always been a concerned topic, emerging tremendous research attention. Natural antimicrobial substances, typically represented by essential oils (EOs), are well-known for their natural source and environmental compatibility (da Silva et al., 2022; Vilela et al., 2018). Many studies found that plant-derived EOs are effective in defending a wide range of bacteria and fungi (da Silva et al., 2022). For example, cinnamon essential oil (CEO), extracted from cinnamon branches, leaves and bark, has been shown to possess strong antimicrobial activity on spoilage organisms (Fan et al., 2023; Shao et al., 2021; Ran et al., 2023), which could be used to prolong the shelf life and maintain quality of fresh agricultural products. However, the volatility, instability, and environmental sensitivity to light, high temperature, and oxygen of EOs lead to decreased antimicrobial function, which limits their application in food preservation. Thus, it is necessary to develop a sustainable technique to overcome the limitations of instabilities and improve the antimicrobial performance of EOs (Ma et al., 2022; Zhang et al.,2019).

Pickering emulsion is one of the most important delivery systems for loading and encapsulating EOs, have been extensively used in food, pharmaceutical, and cosmetic applications (Mwangi et al., 2020). Compared to conventional emulsions, Pickering emulsion is stabilized by solid particles instead of synthetic surfactants, which emphasizes environmental compatibility of the delivery systems. In addition, the colloidal particles anchor at oil-water interface of Pickering emulsions droplet, forming a barrier to block the coalescence of droplets and Ostwald maturation phenomenon. Moreover, the stability and encapsulation effect of Pickering emulsion could be optimized elaborately by designing the behavior of particles at the oil-water interface (Liu et al., 2023).

Recently, interfacial engineering has been developed to enhance the stability of Pickering emulsion systems (Reitzer et al., 2018). Zein, the main storage protein in corn, contains a high percentage of hydrophobic amino acid residues, with a unique self-assembly character. Zein has been studied as a stabilizer for Pickering emulsion systems attributed to its emulsifying properties and ability to self-organize at the oil-water interface (Souza, Ferreira, & Soares, 2022). However, the single zein particles failed to effectively stabilize the dispersed systems due to the adequate interfacial properties. Some modification strategies have achieved in improving interfacial properties and led to an enhancement in emulsion stabilization, as establish molecular interactions between zein and polyphenols for example (Ge et al., 2022; Xu, Wei, & Xue, 2023; Wang et al., 2022a; Zhu et al., 2021). Particularly emphasis be given to the function of polyphenols at oil-water interface. Tannic acid (TA) is a kind of plant-derived polyphenol with multiple hydroxyl groups (around 25 hydroxyl groups) in its structure, providing abundant interaction sites with biomacromolecules (such as protein, polysaccharides and mixtures). TA can form complexes with proteins through its hydroxyl groups and phenolic rings, which improves the interfacial functionalities of proteins. For example, Zhu et al. (2021) found that the addition of TA improved the emulsifying properties of gliadin. TA and soy isolate protein complex as Pickering

emulsion stabilizer was able to inhibit the accumulation of oil droplets and improved the physical stability of the emulsions (Li et al., 2023). Both noncovalent and covalent interactions between zein and TA are known to affect the interfacial behavior of complexs. Moreover, TA has been recognized for its antimicrobial and antioxidant bioactivity (Zhang et al., 2023). Therefore, it can be hypothesized above that TA might improve not only the stability property of zein-based Pickering emulsion but also the antimicrobial effects of EOs loaded Pickering emulsions.

In this work, we constructed Pickering emulsions co-loaded with TA and CEO (ZTCs) based on the zein-TA (ZT) complexes mediated interfacial engineering. The impact of structural features and interfacial properties generated by interactions between zein and TA were investigated by Fourier transform infrared, fluorescence spectroscopy, molecular docking analysis, wettability, and interfacial tension. Furthermore, the stability, rheological, control releases properties of prepared emulsions was investigated. Finally, the antimicrobial effect was evaluated against food spoilage organisms. The findings in our work will provide novel insight into developing Pickering emulsions loaded with binary bioactive compounds and for their subsequent application in food preservation.

2. Materials and methods

2.1. Materials and reagents

Zein (CAS 9010-66-6) was purchased from Sigma-Aldrich (St. Louis, MO, USA). TA (CAS 5424-20-4, purity ⩾96%) was obtained from Yuanye Bio-Technology Co., Ltd. (Shanghai, China). CEO was sourced from Jiangxi Taicheng Natural Perfume Co., Ltd. (Ji'an, China). 5,5′-dithiobis-(2-nitrobenzoic acid) (DTNB) and bromophenol blue (BPB) were sourced from Sigma-Aldrich (St. Louis, MO, USA). All reagents and chemicals in this work were analytical grade. The strain *Pseudomonad paralactis* MN10 (*P. paralactis* MN10) and *Lactobacillus sakei* VMR17 (*L. sakei* VMR17) were provided by the Meat Laboratory of the Institute of Food Science and Technology at the Chinese Academy of Agricultural Sciences (Beijing, China).

2.2. Preparation of the ZT complexes

ZT complexes were prepared using the procedure of Wang et al. (2022a) with slight modifications. Briefly, 1 g of zein powder and 0.2 g of TA were dissolved in 100 mL of an ethanol water solution (70%, v/v), then the solutions were adjusted to pH 5, pH 7, and pH 9 with 1 M HCl and 1 M NaOH forming ZT complexes dispersions. The dispersions were noted as ZT5, ZT7, and ZT9, respectively. Before further characterization, the dispersions were storage at 4℃ and part of them were freeze-dried to obtain ZT complex powders.

2.3. Characterization of the ZT complexes

2.3.1. Average size, zeta-potential and polydispersity index (PDI)

The average size, zeta-potential and PDI of ZT complexes were measured using a Zetasizer Nano ZS (Malvern Instrument Inc., Malvern, UK). Before measurements, each ZT complex dispersion solution was diluted 100-fold with ultrapure water.

2.3.2. Scanning electron microscope (SEM)

The morphology of ZT complex were observed using a SEM (SU 1510, HITACHI, Japan) at 10.0 kV. Briefly, a droplet of the ZT complex dispersions (about 10.0 μL) were directly dropped on a silicon slide (5.0 × 5.0 mm), then mounted on a copper tape and coated with gold for microscopic observation at 50,000-magnification.

2.3.3. Fluorescence spectroscopy

The fluorescence spectra of the ZT complexes were performed on a F-2500 spectrofluorometer (Hitachi, Japan). Each ZT complex dispersion was diluted with ultrapure water before measurements. The excitation wavelength, emission wavelength range, and excitation slit widths were 280 nm, 290-400 nm, and 2.5 nm, respectively.

2.3.4. Fourier transform infrared (FTIR) spectroscopy

The FTIR spectroscopy of the ZT complexes were detected using an FTIR spectrometer (Tensor 27, Bruker, Germany). The ZT complex powders were mixed with KBr and pressed steadily, then the FTIR spectra were acquired three times and averaged. Peakfit 4.12 software (SPSS Inc., Chicago, IL, USA) was used to calculate the secondary structure of the samples using the amide I band (1660 - 1700 cm-1).

2.3.5. Surface hydrophobicity and free sulfhydryl content

The surface hydrophobicity was determined using a BPB method according to the procedure of Wang et al., (2022a) with some modifications. To be specific, 10.0 mg of ZT complex powder was dissolved in 1.0 mL of phosphate buffer saline (PBS; 50 mM, pH 7) and added to 200 μL BPB (1 mg/mL), then the mixtures were centrifuged at 4,000 g for 15 min. The absorbance of the supernatant was determined using a microplate reader at 595 nm (Spark, Tecan Ltd, Switzerland).

The free sulfhydryl content was measured using the methods of Cheng et al. (2023) with some adjustments. 0.5 mL of ZT complex dispersion solution, 50 μL of DTNB (4.0 mg/mL), and 5 mL of Tris-glycine buffer solution (0.09 mol/L Tris, 0.09 mol/L glycine, 4 mmol/L ethylene diamine tetraacetic acid, 8 mol/L urea at pH 8.0) were mixed and incubated in the dark of 60 min. Then, the absorbance of the mixture was detected at 412 nm using a microplate reader. The free sulfhydryl content was calculated using Eq. (3.2.1):

$$\text{-SH}(\mu\text{mol/g}) = \frac{73.53 \times A \times D}{C} \qquad (3.2.1)$$

where A is the absorbance at 412 nm, D is the dilution factor, and C is the sample concentration in mg/mL.

2.3.6 Molecular docking

AutoDock 4.0 and AutoDock vina 1.1.2 (The Scripps Research Institute, La Jolla, CA, USA) were used to provide binding information between zein and TA using the procedure described by Wang et al., (2022a). The structure of zein was obtained by

homologous modeling using Alphafold 2. The 3D structures of TA were download from Pubchem (https://pubchem.ncbi.nlm.nih.gov/). PyMol 2.5 (http://www.pymol.org/) was used to analyze the interactions between zein and TA.

2.4. Evaluation of ZT complexes as potential Pickering emulsion stabilizer

2.4.1. Wettability

The wettability of ZT complexes was measured using a contact angle meter (OCA40, DataPhysics Instruments Ltd., Germany) according to Liu et al., (2022). The ZT complex powders were compressed into tablets of 1 mm thickness and 10 mm diameter. A droplet (~5 μL) of distilled water was gently deposited on the sample surface, by a high precision injector. The profiles of the drop were recorded by a high-speed camera 3 times.

2.4.2. Interfacial tension

The interfacial tension of ZT complexes was measured using a tensiometer (Sigma 701, Biolin Scientific, Sweden) via the Wilhelmy plate method at 25 ℃ (Liu et al., 2023). The width of the Wilhelmy plate was 20 mm. The principle relies on the balance of forces acting on a vertically suspended plate partially immersed in the liquid interface. The calibration factor of corn oil (density ≈ 0.92 g/mL, food-grade, purchased from local supermarket) was determined before taking the measurements. Prior to use, it was filtered using a 0.45 μm membrane to remove any suspended impurities. Briefly, 30 mL of the ZT complex solutions and 30 mL of corn oil were added into a standard vessel (70 mm), standing for 30 min. The dynamic interfacial tension of the two liquids was record.

2.4.3. Interfacial dilational rheology

The interfacial dilational rheology of ZT complexes were probed at the oil-water interface using a OCA50 optical contact angle meter (Dataphysics, Germany) based on oscillatory area deformations of the droplet shape (Dai et al., 2023). A droplet of ZT complex solution (aqueous phase) was formed in corn oil, and sinusoidal oscillations in droplet surface area were applied at a fixed frequency (0.1 Hz) and amplitude (10%). The measurements were conducted after allowing the system to equilibrate for 30 minutes to ensure sufficient adsorption of interfacial particles. Three sinusoidal oscillation cycles were performed by a time corresponding to 30 cycles.

The interfacial dilatational modulus (E), dilatational elasticity modulus (E_d), and dilatational viscosity modulus (E_v) were calculated automatically by SCA20 software from the oscillation cycles, based on the following Eq. (3.2.2):

$$E=\sqrt{Ed^2 + Ev^2} \qquad (3.2.2)$$

where E_d represents the storage (elastic) modulus and E_v represents the loss (viscous) modulus.

2.5. Preparation of ZTCs

The ZTCs were prepared using the method of Cheng, et al., (2020) and Xie, et al., (2022) with some modifications. Briefly, the ZT complex dispersions were mixed

with 10% (v/v) CEO and sheared by a high-speed machine (HR-500, Shanghai Huxi Industry Co., Ltd, China) at 8,000 rpm for 2 min at room temperature. Pickering emusions were obtained by adding ultrapure water into oil-dispersion mixture at a ratio of 50:50 (v/v). The final concentrations of zein, TA, and CEO were 0.05% (w/v), 0.01%(w/v), and 5%, respectively. The ZTCs stabilized by ZT5, ZT7, and ZT9 were recorded as ZTC5, ZTC7, and ZTC9, respectively.

2.6. Characterization of ZTCs

2.6.1. Droplet size and zeta-potential

The droplet size and zeta-potential of the ZTCs were measured using a Zetasizer Nano ZS (Malvern Instruments Inc., Malven, UK). Before measurements, the samples were diluted 100-fold with ultrapure water.

2.6.2. Transmission electron microscopy (TEM)

The microstructures of ZTCs were observed by TEM (H-7500, Hitachi, Japan). Before observation, 10 μL of emulsion were pipetted onto a carbon-coated copper grid and staind with 15 g/L phosphotungstic acid for 30 s.

2.6.3. Confocal laser scanning microscopy (CLSM)

The microstructures of the ZTCs were observed using CLSM (Leica TCS SP8, Leica microsystems Inc., Wetzlar, Germany) according to our previous method (Fan et al., 2023). Nile red (0.1 wt%) and Nile blue (0.1 wt%) were used in the pre-stained oil phase and aqueous phase in the dark, respectively. The excitations wavelengths of Nile red and Nile blue were 488 nm and 633 nm, respectively, and the images of the emulsion were recorded by CLSM.

2.6.4. Stability evaluation

The stability of the ZTCs was evaluated by Turbiscan TOWER Stability Analyzer (Formulaction Inc., France), and the results were presented as profiles of the Turbiscan Stability Index (TSI). 20 mL of prepared emulsion was placed in a glass test tube and scanned with pulsed near-infrared light (λ = 880 nm) every 1 h, continuously for 24 h.

2.6.5. Rheological properties

The rheological properties of fresh Pickering emulsions were measured by rheometer (MCR502, Anton Paar, Germany) with a 50 mm diameter parallel plate and a gap of 1 mm at 25 °C. Before measurements, the linear viscoelastic region (LVR) of the emulsion was investigated by a strain sweep test ranging from 0.01% to 100% with 10 rad/s of frequency. Then, the viscosity was measured as the shear rate increased from 0.1 to 100 s-1. For the frequency sweep mode, the storage modulus (G′) and loss modulus (G″) were obtained with the strain of 0.1%.

2.6.6 Encapsulation efficiency (EE)

The EE (%) of the CEO in the Pickeirng emulsion was measured spectrophotometrically and calculated using following equation according to Liu et al. (2024) with a slight modifaction. Briefly, the eumslion (2 mL) was added an equal volume of N-hexane. After centrifugation at 5,000 rpm for 10 min, the concentration of CEO in the supernatant was measured using CEO calibration curve and the EE (%)

of CEO in the Pickeirng emulsion was calculated according to the following Eq. (3. 2. 2):

$$\text{EE (\%)} = \frac{Encapsulated\ CEO}{Total\ CEO} \times 100 \qquad (3.2.2)$$

The measurement was repeated three times for each sample group.

2.6.7 Release behavior

The release behavior of CEO from Pickering emulsion was carried out through a dynamic test method. 2 mL eumslion was added an equal volume of N-hexane and set aside at room temperature. At each specific time, 200 uL of the N-hexane phase was removed to measure the absorbance of CEO. The cumulative release rate was calculated as following Eq. (3. 2. 3):

$$\text{Cumulative release rate (\%)} = \frac{Release\ CEO}{Total\ CEO} \times 100 \qquad (3.\ 2.\ 3)$$

2.7. Antimicrobial assays of the ZTCs

2.7.1. Antimicrobial properties

The plate counting method was used to test the antimicrobial effect of the ZTCs (Meng et al., 2023), and the viability of bacteria was used to evaluate the antimicrobial properties. Briefly, 100 μL of emulsion were added to 10 mL of liquid medium, then 100 μL of tested bacteria (approximately 10^6 CFU/mL) were added to the liquid medium, and the liquid medium containing the emulsion and bacterial was incubated at 30℃ for 12 h. Thereafter, 100 μL of bacteria suspension was spread on the surface of the agar plate uniformly, and incubation at 30°C for 24 h. A control group consisting of a bacterial suspension with equal volume normal saline solution was also included in the test. The viability of surviving cells was counted.

2.7.2. Minimum inhibitory concentration (MIC)

The MIC of ZTCs were conducted against *P. paralactis* MN10 and *L. sakei* VMR17 using the reported echelon dilution method with some modifications (Zhou, et al., 2018). Briefly, 600 μL of emulsion were added to 6 mL of liquid medium as the first broth tube, then 2-fold dilutions were used to prepared a series of liquid medium tubes; the final concentrations of emulsion of a series of broth tube were 100, 50, 25, 12.5, 6.25, and 3.13 μL/mL, respectively. Then 100 μL of tested bacterial suspension (approximately 10^6 CFU/mL) were added to each tube. The broth tubes were incubated at 30°C for 24 h. The MIC was defined as the concentration in the lowest serial dilution of emulsions that resulted in the lack of visible microorganism growth in the tubes (Hu, et al., 2023).

2.7.3. Antimicrobial mechanism

The mechanism of ZTCs against *P. paralactis* MN10 and *L. sakei* VMR17 was examined by observing microstructure of cell structure using a SEM (SU 1510, Hitachi, Japan). The logarithmic growth phase cells (approximately 106 CFU/mL) were treated with MIC of ZTCs, and were incubated for 4 h at 30℃. Then, the sediment bacteria were collected by centrifugation at 4 ℃, and fixed with 3.5 wt%

glutaraldehyde. Before observation, a gradient dehydration process was applied to the fixed bacteria, using ethanol solutions of 30%, 50%, 70%, 90%, and 100%.

2.8. Statistical analysis

Results were expressed as mean ± standard deviation in triplicates for all experiments. Statistical analysis was conducted by SPSS 26.0 software (SPSS Inc., Chicago IL, USA), and Duncan's multiple tests at 95% confidence intervals were used to assess significance of differences.

3. Results and discussion

3.1. TA altered the apparent of zein

SEM provided information about the morphological feature of ZT complexes. According to Figure 3-1A, ZT complexes are presented as spherical particles, which are promoted by the self-assembly process of zein (Wang et al., 2022a). Compared with ZT complex prepared in different pH conditions, the appearance of ZT9 was relatively rough, which could be attributed to different interactions of zein and TA at pH 9. Previous studies also reported that the zein-polyphenol complexes prepared in an alkaline environment appeared to have smooth surface (Liu et al., 2017). The self-assembly process of zein and the interaction force between zein and polyphenol mainly involved hydrogen bonding, hydrophobic and electrostatic forces. However, these interaction forms weakened in alkaline environment, which finally resulted in the obvious change in the ZT complex's morphology.

The average size, zeta-potential and PDI of different ZT complexes were closely associated with their characteristics. As shown in Table 3-1, the hydrodynamic average size of ZT5, ZT7 and ZT9 were 293.53 nm, 192.30 nm and 149.77 nm, respectively. The small size of ZT complexes was beneficial to adsorb on the oil-water interface quickly. Notably, the particle size of ZT5 was larger than the others. This phenomenon could be attributed to pH 5 is close to isoelectric point of zein, which more easily to form large particles and decrease of charge repulsion when upon binding with TA. The smaller zeta-potential absolute value (-22.70 mV) provided the evidence. In addition, polyphenols could drive the protein chains folding or unfolding by regulating the interaction force, which could alter the particle size of the complex (Zhang et al., 2023). These observed results indicate that pH conditions modulated the appearance and particle size of ZT complexes.

Table 3-1 The average size, Zeta potential and polydispersity index (PDI) of zein-TA (ZT) complexes prepared at various conditions and CEO loaded Pickering emulsions stabilized by different ZT complexes.

Sample	Average size (nm)	Zeta potential (mV)	PDI
ZT5	293.53±4.01^{d}	-22.70±0.66^{d}	0.37±0.01^{b}
ZT7	192.30±1.35^{e}	-39.00±0.96^{e}	0.23±0.02^{d}
ZT9	149.77±7.39^{f}	-44.77±1.04^{f}	0.32±0.03^{c}
ZTC5	353.60±5.19^{a}	24.67±0.57^{a}	0.50±0.03^{a}

ZTC7	336.60±6.30[b]	19.43±0.49[b]	0.52±0.00[a]
ZTC9	311.20±2.51[c]	-12.03±0.67[c]	0.53±0.00[a]

Values are expressed as means ± SD (n = 3). Different superscripts in the same column indicate significant differences between groups ($P < 0.05$).

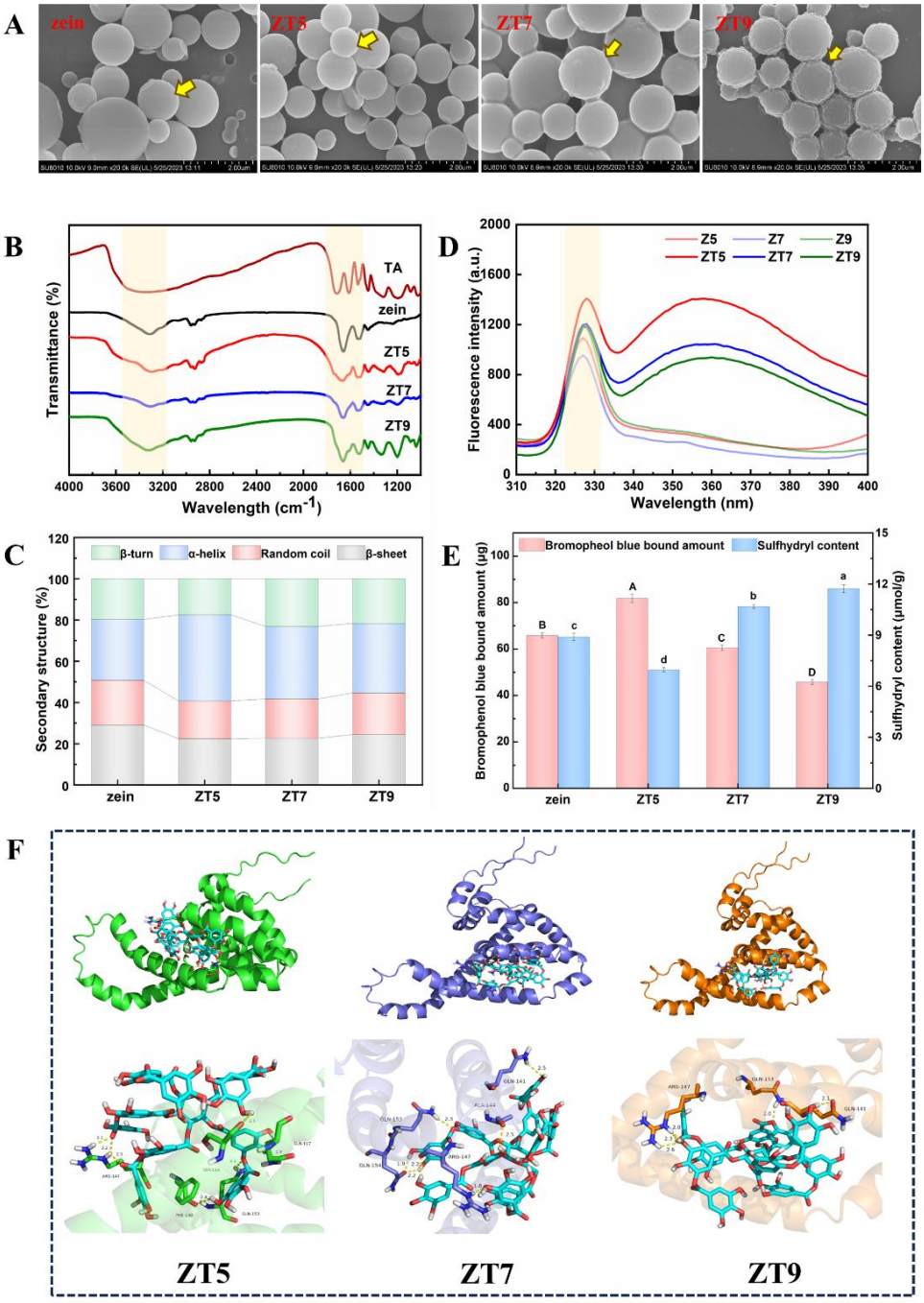

Figure 3-1 Characteristics of zein and their complexes with tannic acid (ZT). Microscopic morphology was observed by scanning electron microscope at a magnification of × 20 k (A).

FTIR spectroscopy (B), secondary structures contents (C), fluorescence spectroscopy (D), surface hydrophobicity and sulfhydryl content (E). The molecular docking of zein and tannic acid at different pH conditions (F). ZT5, ZT7 and ZT9 represent zein combine with TA at pH 5, pH 7 and pH 9. Different letters above the bars in same measurement indicate significant differences among fractions ($P < 0.05$).

3.2. TA altered the conformation of zein

3.2.1. FTIR spectroscopy

To analyze the interactions between zein and TA, the FTIR spectrum of ZT complexes was recorded (Figure 3-1B). It was seen that the broad characteristic peak in the wavelength region of 3200-3400 cm^{-1} was shifted after the formation of ZT complexes compared to the zein, demonstrating that the interaction between zein and TA was highly related to hydrogen bonding coupled with N-H stretching vibration. The characteristic peak at 2980 cm^{-1} was caused by a C-H stretching vibration. It can be seen a slight shift, indicating that there was hydrophobic interaction between the zein and TA. By contrastive analysis of three ZT complexes, it can be seen that ZT5, which was prepared in acidic pH conditions (pH 5), had strong hydrogen bonding and hydrophobic interactions between the zein and TA while ZT9 (prepared in alkaline pH conditions) was weaker. These differences are mainly attributed to the non-covalent or covalent interaction between zein and polyphenols (Liu et al., 2017). The analysis of FTIR in the amide I band region (1600-1700 cm^{-1}) provided more information about the secondary structure change of zein and their TA complex (Wang et al., 2022a). As shown in Figure 3-1C, the major secondary structures of zein were α-helix, which was also observed by Wang, et al. (2022b). Upon binding with TA, a slight increase in α-helix in ZT complexes were recorded. The α-helix was mainly correlated to inter-molecular hydrogen bonds formed between C=O and N-H. There are a large number of phenolic hydroxyl groups in TA, which provide more hydrogen bond site between zein and TA. Thus, affecting the α-helix content of zein. The similar result was observed by Wang et al. (2022a) in zein-ferulic acid complexes. Wen et al. (2023) considered that these changes in secondary structure may contribute to enhanced the interfacial performance of proteins.

3.2.2. Fluorescence spectroscopy

To further investigate the interactions between zein and TA, fluorescence spectroscopy was used to probe the tertiary structure of the ZT complexes (Figure 3-1D). Since zein lacks tryptophan (Typ), tyrosine (Tyr) and phenylalanine (Phe) residues were the intrinsic fluorophores in zein. The fluorescence intensity of zein (Z5, Z7, and Z9) increased with increasing pH, and the emission peak showed a slight red shift with decreasing pH, indicating the chromophores environmental polarity was changed by pH condition. Zein was dissolved in aqueous ethanol solution (70%, v/v) to form ZT complexes. In this higher ethanol content solution system, the complexes exposed more hydrophobic amino acids to adapt to the polar environment (Li et al., 2023). In the case of ZT complexes, the fluorescence intensity increased with the addition of TA. These results suggested that the addition of TA led to the exposure of

intrinsic fluorophores, whereas a opposite result was reported by Liu et al. (2017) in zein-chlorogenic acid system, it might be the effect of polyphenol types. In addition, the stronger fluorescence intensity was observed in ZT5, revealing that the interaction between the intrinsic fluorophores of zein and TA was greater in an acid microenvironment.

3.2.3. Surface hydrophobicity and sulfhydryl content

The hydrophobic sites of proteins could bind to the BPB. The increased BPB bounding amount was reflective of the conformational and hydrophobicity changes of proteins. As shown in Figure 3-1E, the BPB bound number of ZT5 increased compared to zein, implying that more hydrophobic amino acid residues were exposed in ZT5 structure, the solution polarity altered embedded state of hydrophobic amino acid residues of zein. Another reason for this result was that TA could drive exposed hydrophobic groups of zein aggregation by hydrogen bond and hydrophobic interaction in acid condition. Wang et al., (2023) reported similar results by analysing the interaction between soy isolate protein and TA complexes. In addition, the free sulfhydryl content was also used to reflect the structure change of ZT in our work (Figure 3-1F). The significant differences ($P < 0.05$) of free sulfhydryl content were detected between different ZT complexes, demonstrating the pH conditions changed the conformation of ZT complexes. The increased content of free sulfhydryl was due to rupturation of the S-S bond. The free sulfhydryl content of ZT9 was higher than that of ZT5 and ZT7, which might be associated with the unfolding of the protein in alkaline condition (Pi et al., 2023; Wei et al., 2023). To some extent, the phenomenon in surface hydrophobic and free sulfhydryl content had an influence on the wettability of protein-polyphenol complexes, which finally changed the interfacial properties (Chao et al., 2023).

3.2.4. Molecular docking simulation

Combining experimental data with computational models could provide detailed information on functional groups and molecular forces (Li et al., 2023). A theoretical analysis was carried out by docking the zein with TA and optimized binding sites as illustrated in Figure 3-1F. The dominant binding forces between zein and TA were hydrogen bonds and hydrophobic interactions, which were consistent with the FTIR results. TA was located in the hydrophobic pocket of zein, forming strong hydrophobic interactions. The phenolic hydroxyl group of TA interacts with the amino acid residues of zein by hydrogen bonding. Table 3-2 provided the number of hydrogen bonds and involved amino acid residues. Specifically, TA formed five hydrogen bonds with amino acid residues of zein in pH5 and pH7, involved ARG147, GLN117, SER114, PHE156, and GLN153 of zein in pH5; GLN153, GLN154, ARG147, ALA144 and GLN141 of zein in pH7. In pH9, there were three hydrogen bonds formed between TA and zein involved GLN153, GLN141 and ARG147. The binding affinity of zein and TA was arranged in the order ZT7(-8.3 kcal/mol) > ZT9(-8.5 kcal/mol) > ZT5(-8.6 kcal/mol), implying the favorable affinity of zein and TA in pH5 compare to pH7 and pH9. These results could help us to understand the structural change information of ZT complexes before emulsification and mainly adsorbs at the oil-water interface (Gong, et al., 2022)

Table 3-2 Number of hydrogen bonds and hydrophobic interactions, and the involved amino acids in different zein and tannic acid complex were listed.

	Binding energy	Number of hydrogen bond	Residues involved in hydrogen bonds
ZT5	-8.6	5	ARG147, GLN117, SER114, PHE156, GLN153
ZT7	-8.3	5	GLN153, GLN154, ARG147, ALA144, GLN141
ZT9	-8.5	3	GLN153, GLN141, ARG147

3.3. Potential of ZT complex stabilizing Pickering emulsions

3.3.1. Wettability

The wettability of ZT complexes was evaluated by determining the contact angle. It was observed in Figure 3-2A, that the contact angles of ZT5, ZT7 and ZT9 were 74.38°, 73.15° and 45.63°, respectively. Notably, the contact angles had no significant difference ($P>0.05$) between the three pairings (zein, ZT5, ZT7), implying that zein, ZT5 and ZT7 exhibit similar hydrophobicity. According to the stabilization mechanism of the Pickering emulsion, the emulsion was more stable when the contact angle of stabilizer close to 90°. Previous studies reported that zein nanoparticles had ability to stabilize Pickering emulsion due to their hydrophobic features (Souza et al., 2022). Although most polyphenols are hydrophilic, the introduction of TA under acidic conditions maintained the potential of ZT complexes as Pickering emulsion stabilizers. These results were attributed to the hydrogen bonds between the zein and TA, which reduced the exposure of hydrophilic groups of the zein (Zhu et al., 2021). These observations indicated that the addition of TA contributed to the improved performance of ZT complexes as stabilizer in Pickering emulsions, especially in acidic condition.

3.3.2. Interfacial tension

To further investigate the stabilizing potential of the ZT complexes in loading the CEO to form a Pickering emulsion, the interfacial tension of ZT complexes were determined. Theoretically, there are two stages when colloid emulsifiers stabilized Pickering emulsion. First, the colloid emulsifiers reduce the interfacial tension at the droplet surface rapidly due to the formation of the interfacial layer. Then, the colloid emulsifiers anchored at oil-water interface, with the interfacial tension decreases gradually as a relatively stable value (Liu et al., 2022). As displayed in Figure 3-2B, the interfacial tension of ZT complexes decreased more than that of zein, implying that the interfacial activity of complex was improved by the addition of TA, which was consistent with the research of Chen et al. (2020). As reported by Xu et al. (2023), the zein/polyphenol complexes decrease the interfacial tension due to the formation of a homogeneous and cohesive film, which could improve the stability of the emulsion. The initial interfacial tension value in the presence of ZT9 (9.96 mN/m) was significantly lower than that of ZT5 (11.31 mN/m) and ZT7 (10.49 mN/m), indicating that ZT9 had the strongest interfacial adsorption capacity. As the measurement time prolonged, the interfacial tension of ZT complexes tends to remain

stable, demonstrating that they anchor at the oil-water interface. These results indicate that ZT complexes have great potential as Pickering emulsion stabilizers.

3.3.3. Interfacial dilational rheology

The interface dilatational viscoelasticity of ZT complexes particles is crucial to examine the formation of Pickering emulsion interfacial layer, including dilatational modulus (E), dilatational elasticity modulus (E_d), and dilatational viscosity modulus (E_v), as this property could reflect the mechanical strength of interfacial layer. The time-dependent dilatational elasticity and viscosity modulus of ZT complexes were shown in Figure 3-2C. In measurement range, the E_d was dominant compared E_v, and indicating that all ZT complexes could form viscoelastic interfacial layers. To be more specific, the E_d of ZT9 was large than ZT5 and ZT7, implying superior viscoelasticity and stronger mechanical strength of the interfacial layer formed by ZT9 compared to ZT5 and ZT7. The resulting slope of E-π curve further indicated the equilibrium state of complexes at the oil-water interface. In Figure 3-2D, the slope of all samples is greater than 1, signifying an ideal adsorption state. The slope of E-π curve of ZT complexes were around 1.91, 2.89, and 3.64, respectively, highlighting the intensive adsorption of ZT complexes at interface. The observed interfacial elasticity is attributed to the formation of a viscoelastic interfacial film, resulting from the adsorption of ZT complexes at the oil-water interface. These complexes form a densely packed, physically crosslinked network, which resists interfacial deformation and contributes to the elastic behavior of the film. Meng et al. (2024) elucidated that this enhanced mechanical strength of the interfacial film could be attributed to the addition of polyphenol that increasing flexibility of protein structure, effectively preventing the coalescence of droplet. The result of interface dilatational viscoelasticity confirms that the mechanical strength of the interfacial layer is enhanced, which can respond to the interfacial tension in section 3.3.2.

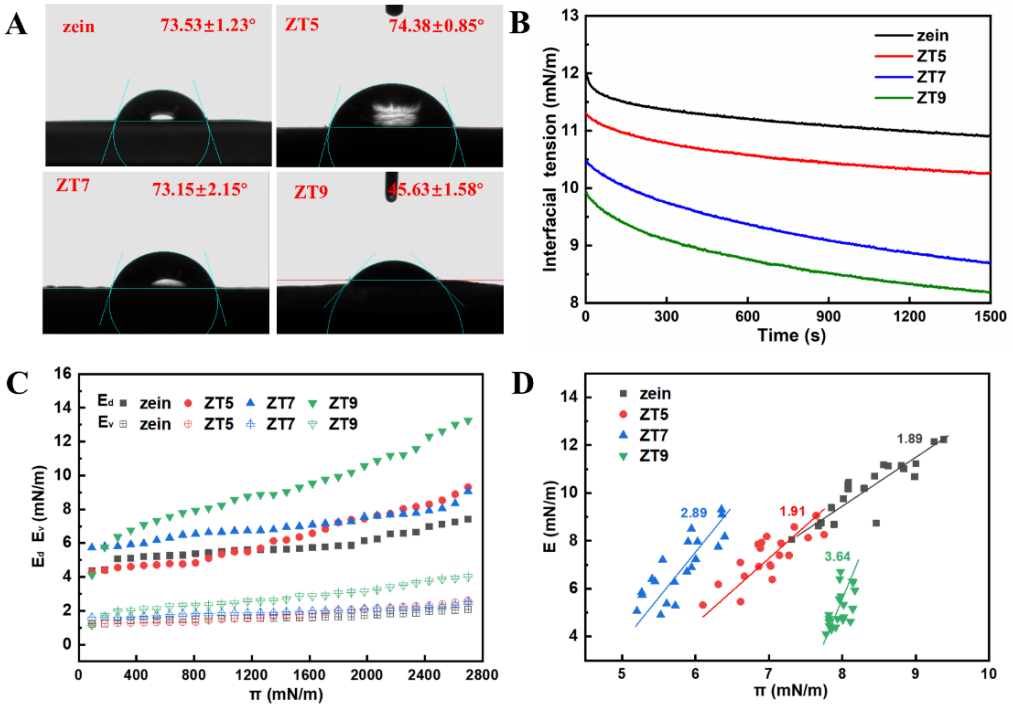

Figure 3-2 Potential of zein and their complexes with tannic acid (ZT) stabilizing Pickering emulsion. Water contact angle (A), interfacial tension (B), time-dependent dilatational elasticity modulus (Ed) and dilatational viscosity modulus (Ev) (C), and dilatational modulus as a function of surface pressure (π) (D) of different ZT as Pickering emulsion stabilizer.

3.4. Characterization of ZTCs

3.4.1. Morphological observation

After evaluating the potential of ZT complexes as Pickering emulsion stabilizers, the ZTCs were constructed by loading CEO. As displayed in Figure 3-3A, the morphology of ZTCs were presented using a TEM. The interfacial layer of emulsions was obviously observable, which was characterized by a slightly dark outer region, implying the formation of a Pickering emulsion. The absorption of ZT complexes onto droplets resulted in a thicker interface of steric hindrance that prevented stabilizer from desorbing (Wei et al., 2019). The droplets stabilized by ZT5 or ZT7 were spherical, while the droplet stabilized by ZT9 did not have a well-defined shape, which could be attributed to the promoted flocculation of small droplets by strong electrostatic attraction. In addition, the CLSM also provided the microstructures of ZTC with three different ZT complex (Figure 3-3B). The images of overlay showed the stacked state of CEO and ZTs phase, which were shown in yellow (superimposed color of green and red). The overlapping fluorescence micrograph showed that the CEO was wrapped by dense ZTs complexes. Similar phenomena were also observed in CEO Pickering emulsion stabilized by zein/carboxylated cellulose nanocrystals

composite nanoparticles (Qin et al., 2024). The CLSM images of ZTCs showed spherical dispersion of emulsion droplets with different sizes. Notably, it was obvious that a clear boundary of the ZTC5 wrapping layer, indicating ZT5 adsorpted onto the oil-water interface stably. However, ZTC9 emulsion system had a lot of dissociative ZT9 particle, suggesting poor stabilization of ZT9. Consistent with the TEM observations, the droplets of ZTC5 displayed dispersive and uniform characteristics, while the droplets of ZTC9 showed a partial aggregation. These results suggest that the structures of ZTCs could be regulated by interfacial compositions.

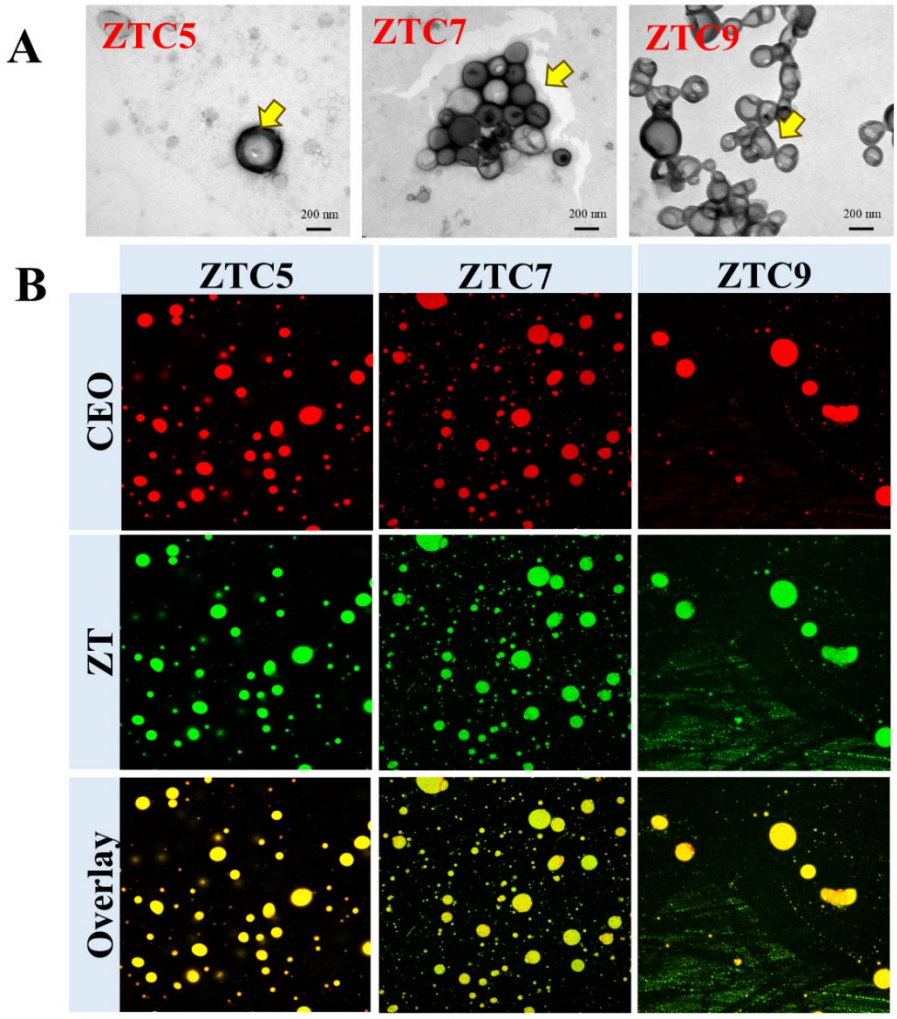

Figure 3-3 Microscopic morphology of Pickering emulsions co-loaded tannic acid and cinnamon essential oil, which observed by transmission electron microscope (A) and confocal laser scanning microscope (B). ZTC5, ZTC7, and ZTC9 represented the CEO loaded Pickering emulsion stabilized by ZT5, ZT7 and ZT9, respectively.

3.4.2. Droplet size and zeta-potential

The droplet size and zeta potential of ZTCs are listed in Table 3-1. The average droplet size of ZTCs was between 300 and 400 nm, and also in line with the TEM report. Similar results were observed in an algal oil Pickering emulsion stabilized by zein-gallic acid nanoparticles (Xu et al., 2023). As larger particles adsorb at the oil-water interface for longer periods of time, the diameter of the emulsion droplets increases. The zeta potential defined the net surface charge of oil droplets which represented aggregation possibility. The zeta potentials of ZTC5, ZTC7, and ZTC9 were 24.67 mV, 19.42 mV, and -12.03 mV, respectively. The highter absolute value of zeta potential improved its properties against flocculation because of the electrostatic repulsion among the emulsion droplets (Xu, et al., 2023).

3.4.3 Physical stability

The physical stability of a series of ZTCs was evaluated by TSI measurements. An increase in TSI values expressed a decline in emulsion stability (Fan et al., 2023; Liu et al., 2023). The dynamic curve of TSI values is displayed in Figure 3-4A. During the test period, the ZTCs displayed slow-growing TSI values, illustrating the suitability of protein-polyphenol complexes as stabilizers, which was probably related to the cross-linked network of the continuous phase at the oil-water interface. Xu, et al. (2023) observed a similar trend in TSI values of emulsion stabilized by gelatin and catechin complexes. Comparably, the emulsion stabilized by ZT5 showed a lower TSI value in the middle and late measurement, indicating better stability. Based on the stabilization potential of ZT complexes prepared in different pH conditions, ZT5 possessed appropriate wettability and anchored to the oil-water interface to form a homogeneous network film as a barrier, thus reducing the aggregation and coagulation of droplets and showing better stability.

The rheological properties reflected the stability and functionality of the emulsions. Figure 3-4B illustrated the viscosity with the shear rate of CEO loaded Pickering emulsions stabilized by ZT5, ZT7, and ZT9. It was obvious that the viscosity of all emulsions decreased gradually with an increase in shear rate from 0.1 to 100 s-1, implying that the prepared emulsions showed shear thinning behavior and were defined as typical non-Newtonian fluid, a well-known rheological property of complex fluids (Chen et al., 2023). Interestingly, ZTC5 exhibited significantly higher viscosity than that of ZT7 and ZT9. The viscosity was related to the tight distributions of particles in continuous phase. The reason for this high viscosity could be case that the strong intermolecular force in ZT5, which made ZT5 anchored at the of oil-water interface easily, lead to more ZT5 particles in the continuous phase. This result was in agreement with the study reported by Xu et al. (2023). It was reported that high viscosity can reduce the collision frequency of droplets in the continuous phase, which was beneficial to improve the stability of emulsions (Liu, et al., 2023). These results about rheological properties of ZTCs provides a supplementary explanation for the stability.

3.4.4 EE and release performance

The EE of emulsion are important to efficient delivery system from the perspective of economically and functional, which could culminate beneficial effects of bioactive agents. Figure 3-4C showed the EE percentage of emulsion stabilized by ZT complex. The emulsion prepared from ZT5 complex showed a significantly higher ($P < 0.05$) value (86.83%) in comparison with ZTC7 (77.24%) and ZTC9 (76.14%), indicating ZT5 complex confers more protection on the encapsulated by provides a higher viscoelastic oil-water interface. This result was consistent with rheological properties of prepared Pickering emulsion. Moreover, this excellent encapsulation performance of ZTC5 also reflected in release behavior (Figure 3-4D). All Pickering emulsions (stabilized by single zein particle and by ZT complex) exhibited a control release characteristic, which showed a slowly rising cumulative release rate in initial period. With the extension of time, ZTC5 remained a low cumulative release rate in comparison with ZTC7 and ZTC9, implying that the higher viscoelastic oil-water interface barrier (ZT5) has a delayed effect on the release of active substances in the interior. The oil-water interface is the key to blocking the migration of volatile molecules (Liu et al., 2023). There is abundance hydrogen bond reciprocity between tannic acid and various volatiles molecules at the oil-water of the droplet, reducing the content of free CEO in the aqueous. However, zein and tannic acid bonded covalently under alkaline conditions, with a large number of hydrogen bonding sites were buried, thus ZC and ZTC9 showed a similar release curve.

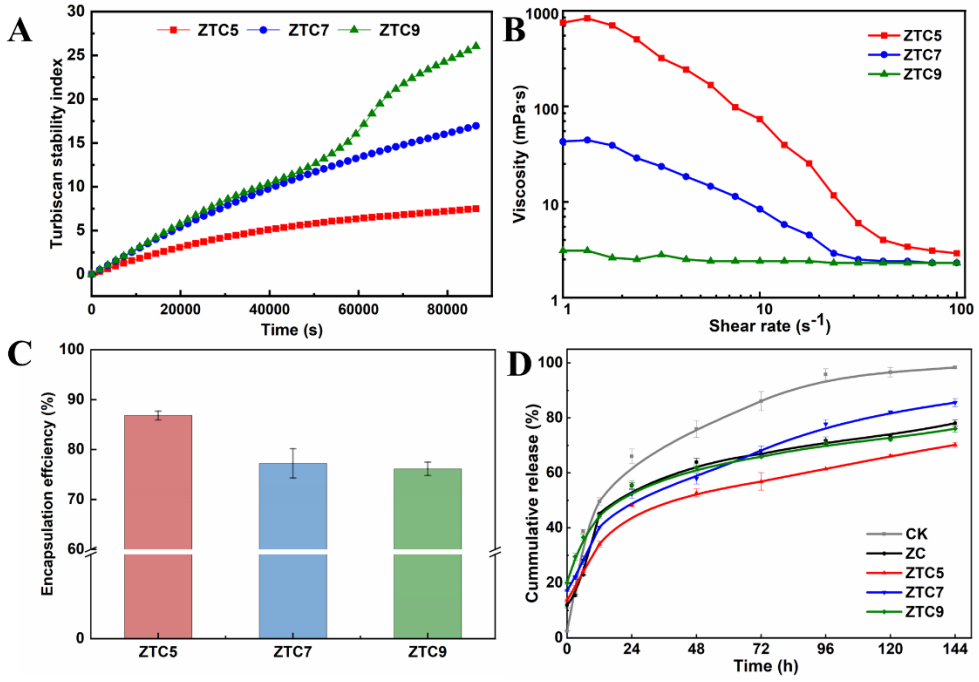

Figure 3-4 Stability evaluation of Pickering emulsion co-loaded tannic acid and cinnamon essential oil by Turbiscan stability index values (C). Rheological properties of Pickering emulsion loaded tannic acid and cinnamon essential oil, viscosity as a function of shear rate

(D). Encapsulation efficiency of Pickering emulsion co-loaded tannic acid and cinnamon essential oil (A) and release behavior of CEO from emulsion. Different letters above the bars in same measurement indicate significant differences among fractions ($P < 0.05$).

3.5. Formation mechanisms of ZTCs

The possible formation mechanisms of ZTCs are schematically described in Figure 3-5. The ZT complexes at the oil-water interface was the dominant factor that determined the formation of the Pickering emulsion in this work. However, the different interactions between zein and TA in different conditions changed the conformation of the ZT complexes. The ZT complexes exhibit adjusted wettability and interfacial tension, which affected the properties of the complex as a Pickering emulsion stabilizer (Zhao et al., 2024). Subsequently, there were two steps of the Pickering emulsion formation: adsorption and stabilization. As evidenced by interfacial tension, the interfacial adsorption capacity of the ZT complexes decreased in the following order: ZT9 > ZT7 > ZT5, which could be attributed to the high charge on ZT9. With the prolonging of time, the adsorption of ZT complexes reached equilibrium and the emulsion reached a stable state. At this moment, the ZT complexes anchors to the oil-water interface to form a film, which against the occur of aggregation and flocculation. Among the three ZT complexes, the contact angle of ZT5 particles was closest to 90° and the particle size was relatively larger, indicating that ZT5 had a strong anchoring effect and the formed interface film was thicker. The microstructure and stability characterization proved this view. Xu et al. (2023) demonstrated that the composite types between zein and polyphenols had a significant impact on the properties of prepared Pickering emulsions. Zhu, et al. (2021) made the same point and suggested that it can be achieved by tuning the molecular interaction between proteins and polyphenols.

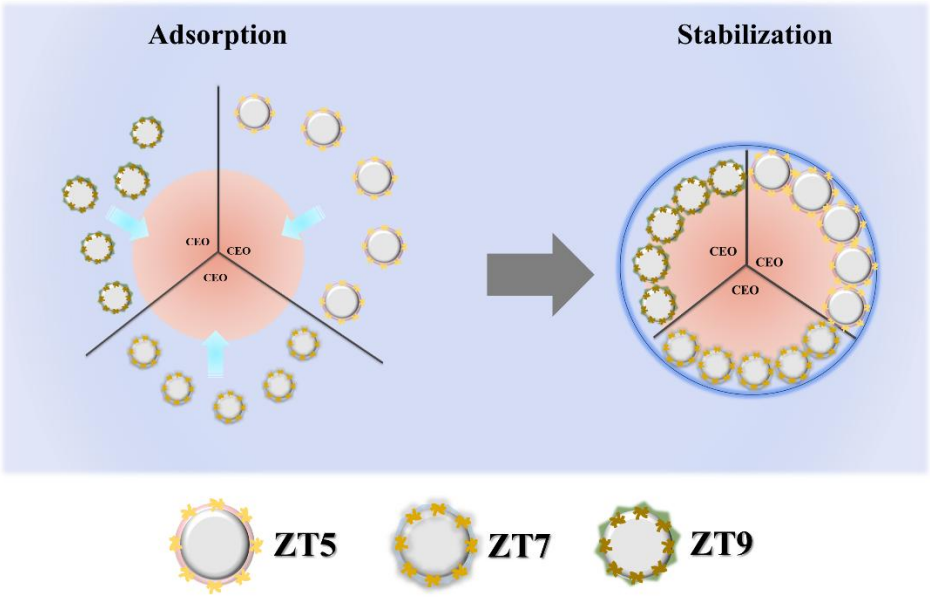

Figure 3-5 Schematic illustration of two formation steps of Pickering emulsion co-loaded TA and CEO. ZT5, ZT7, and ZT9 were represent zein and tannic acid complexes prepared in pH 5, pH 7 and pH 9; ZTC5, ZTC7, and ZTC9 were represent tannic acid and cinnamon essential oil co-loaded Pickering emulsion stabilized by ZT5, ZT7, and ZT9.

3.6. Antimicrobial activity of ZTCs

3.6.1 Antimicrobial activity testing

The antimicrobial effect of ZTCs against foodborne spoilage bacteria were confirmed by agar plate tests which are displayed in Figure 3-6. ZT complexes showed antimicrobial effects as described digitally by viability in Figure 3-6B, which may be attributed to efficient adhesion to bacterial membranes. It is worth noting that ZT complexes prepared in different pH conditions performed different inhibition effects. A number of phenolic hydroxyl groups in TA contribute to the bacteriostatic properties of ZT complexes, however, polyphenols of TA are easily oxidized under alkaline conditions which decreases the bio-abilities (Nassarawa, et al., 2022). The bacteriostasis between emulsions was different due to the encapsulation efficiency of the prepared Pickering emulsion, which will inevitably affect the antibacterial efficiency. The ZTC5 stabilized by ZT5 had a strong anchoring effect and a thicker interface film, which improved the encapsulation efficiency of CEO in the Pickering emulsion. Subsequently, we evaluated the MIC of ZT complexes and ZTCs (Table 3.3). The MIC value of ZTC5 against *P. paralactis* MN10 (A) and *L. sakei* VMR17 were both 12.5 μL/mL, which were lower than that of ZC (emulsion stabilized by zein). This result indicated that the ZTCs had enhanced antimicrobial activity.

Table 3-3 Determination of minimum inhibitory concentration of of zein-TA(ZT) complexes prepared at various conditions and CEO loaded Pickering emulsion stabilized by different ZT complexes against *P. paralactis* MN10 and *L. sakei* VMR17.

Sample	MIC (μL/mL)	
	***P. paralactis* MN10**	***L. sakei* VMR17**
Zein	-	-
ZT5	50^{b}	50^{b}
ZT7	50^{b}	50^{b}
ZT9	100^{a}	100^{a}
ZC	25^{b}	25^{c}
ZTC5	12.5^{d}	12.5^{d}
ZTC7	12.5^{d}	12.5^{d}
ZTC9	25^{c}	25^{c}

Values are expressed as means ± SD (n = 3). Different superscripts in the same column indicate significant differences between groups ($P < 0.05$). '-'means no recordable data results within measurement condition.

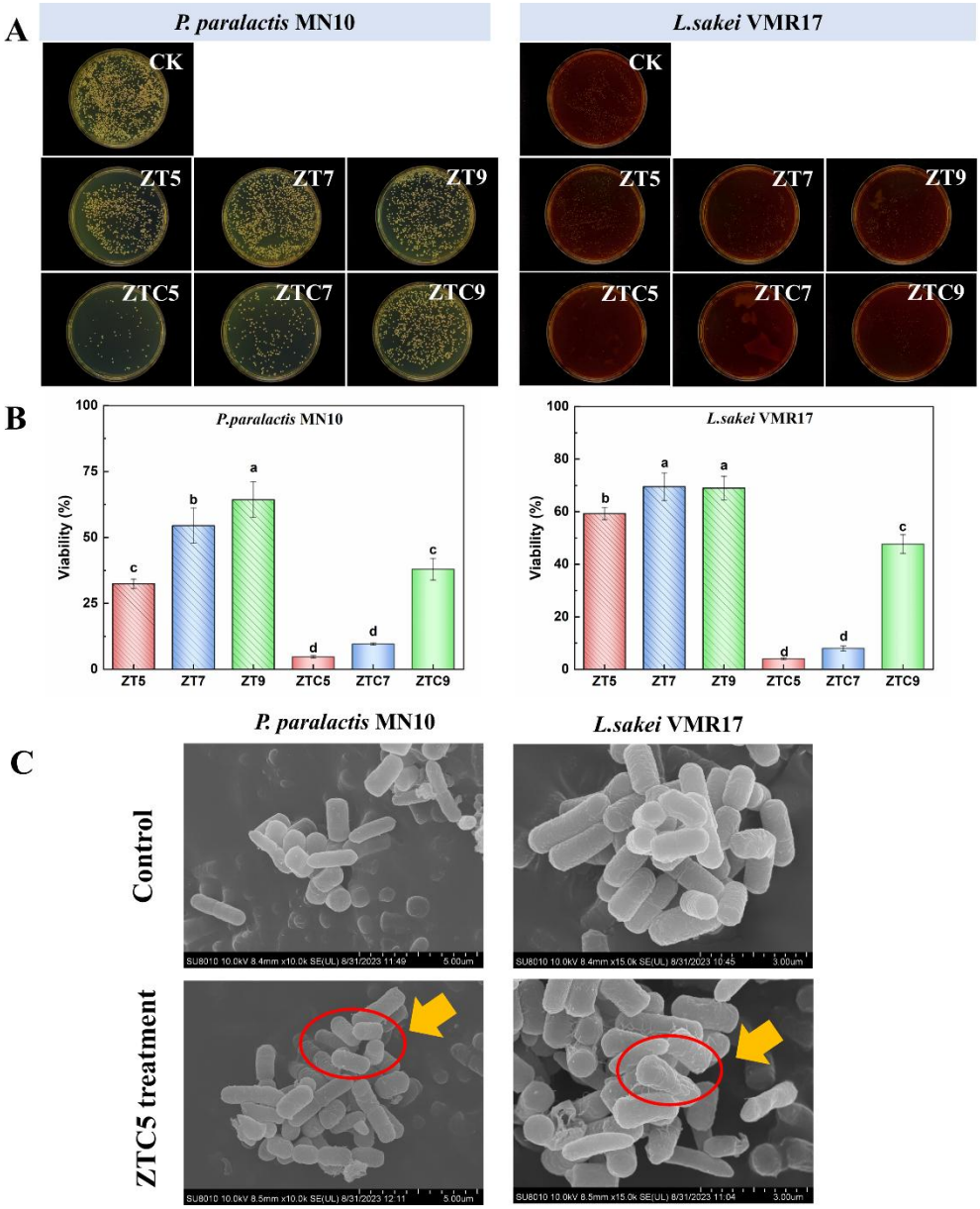

Figure 3-6 Antimicrobial effect (in vitro) of Pickering emulsion co-loaded tannic acid and cinnamon essential oil against *P. paralactis* MN10 and *L. sakei* VMR17. Survival clone on agar culture plates (A), viability of tested bacteria (B), and changes in cell structure of *P. paralactis* MN10 and *L. sakei* VMR17 after treated with minimum inhibitory concentration of ZTC5 by scanning electron microscope with 15000-magnifications (C). Different lowercase letters indicate significant differences ($P < 0.05$).

3.6.2. Antimicrobial mechanism

We employed SEM to observed the microstructure of *P. paralactis* MN10 and *L. sakei* VMR17, and ZTC5 was selected as the emulsion model at the previously established MIC values (Figure 3-6C). In the control group, the bacterial cell had the typical structure of themselves, however, folds and depressions on the cell surface were observed in the treated group. There are a lot of active compounds in CEO, which could interact with the cell membrane of bacteria, leading to the disruption of the cell structure (Zhou, et al., 2018). Further, EOs' lipophilicity facilitates their targeted diffusion and interaction with the membranes and intracellular components of cells. In addition, the role of TA in the oil-water interface should not be overlooked either. When emulsion droplets adsorbed around the bacteria, the phenol hydroxyl group of TA changed the permeability of the cell, leading to the disruption of the cell structure. These results demonstrated that the ZTCs caused the permeabilization of the cells and disrupted the membrane integrity.

Despite the great promise of zein and TA complexes in functional Pickering emulsion, considering the complexity of food emulsion, the ongoing challenge is to maintain the stability of zein and TA complexes-based Pickering emulsions in multi-component food systems and at various conditions, such as temperatures, ionic strengths, and pH values. Additionally, more studies on applications of this hybrid particle still expected, for example, combining bio-based materials to develop food active packaging.

4. Conclusions

In the present work, the Pickering emulsion co-loaded TA and CEO had been successfully prepared based on the ZT complexes mediated interfacial engineering. The addition of TA in zein at different pH conditions was regular the structural properties of zein, and hydrogen bonding and hydrophobic effects were the main driving forces. Introducing TA decreased the interfacial tension of the ZT complexes, implying the dominant role of TA in improving the interfacial stabilization of the ZT complexes. The TEM images confirmed the formation of a stronger interfacial layer film of ZTC5, corresponding to the high physical stability. The ZTC showed an effective antimicrobial property against spoilage organisms *P. paralactis* MN10 and *L. sakei* VMR17 by destroying cell structure. These findings provide new insight for developing co-loading multiple antimicrobial agents within Pickering emulsion as a delivery system via interfacial engineering.

5. References

Chao Song, Z., Zhang, H., Fei Niu, P., Shi, L. S., Yan Yang, X., Hong Meng, Y., Yu Wang, X., Gong, T., & Rong Guo, Y. (2023). Fabrication of a novel antioxidant emulsifier through tuning the molecular interaction between soy protein isolates and young apple polyphenols. Food Chemistry, 420, 136110.

Chen, H., Wang, Q., Rao, Z., Lei, X., Zhao, J., Lei, L., & Ming, J. (2023). The linear/nonlinear rheological behaviors of Pickering emulsion stabilized by Zein

and Xanthan gum: Effect of interfacial assembly strategies. Food Hydrocolloids, 145, 109116.

Chen, S., Shen, X., Tao, W., Mao, G., Wu, W., Zhou, S., Ye, X., & Pan, H. (2020). Preparation of a novel emulsifier by self-assembling of proanthocyanidins from Chinese bayberry (Myrica rubra Sieb. et Zucc.) leaves with gelatin. Food Chemistry, 319, 126570.

Cheng, H., Khan, M. A., Xie, Z., Tao, S., Li, Y., & Liang, L. (2020). A peppermint oil emulsion stabilized by resveratrol-zein-pectin complex particles: Enhancing the chemical stability and antimicrobial activity in combination with the synergistic effect. Food Hydrocolloids, 103, 105675.

Cheng, J., Dudu, O. E., Zhang, J., Wang, Y., Meng, L., Wei, W., Li, X., & Yan, T. (2023). Impact of binding interaction modes between whey protein concentrate and quercetin on protein structural and functional characteristics. Food Hydrocolloids, 142, 108787.

da Silva, B. D., do Rosário, D. K. A., Weitz, D. A., & Conte-Junior, C. A. (2022). Essential oil nanoemulsions: Properties, development, and application in meat and meat products. Trends in Food Science & Technology, 121, 1-13.

Dai, H., Sun, Y., Feng, X., Ma, L., Chen, H., Fu, Y., Wang, H., & Zhang, Y. (2023). Myofibrillar protein microgels stabilized high internal phase Pickering emulsions with heat-promoted stability. Food Hydrocolloids, 138, 108474.

Fan, S., Wang, D., Wen, X., Li, X., Fang, F., Richel, A., Xiao, N., Fauconnier, M.-L., Hou, C., & Zhang, D. (2023). Incorporation of cinnamon essential oil-loaded Pickering emulsion for improving antimicrobial properties and control release of chitosan/gelatin films. Food Hydrocolloids, 138, 108438.

Ge, S., Jia, R., Li, Q., Liu, W., Liu, M., Cai, D., Zheng, M., Liu, H., & Liu, J. (2022). Pickering emulsion stabilized by zein/Adzuki bean seed coat polyphenol nanoparticles to enhance the stability and bioaccessibility of astaxanthin. Journal of Functional Foods, 88, 104867.

Gong, T., Chen, B., Hu, C. Y., Guo, Y. R., Shen, Y. H., & Meng, Y. H. (2022). Resveratrol inhibits lipid and protein co-oxidation in sodium caseinate-walnut oil emulsions by reinforcing oil-water interface. Food Research International, 158, 111541.

Li, S., Wang, X., Zhang, X., Zhang, H., Li, S., Zhou, J., & Fan, L. (2023). Interactions between zein and anthocyanins at different pH: Structural characterization, binding mechanism and stability. Food Research International, 166, 112552.

Li, X., Hu, S., Rao, W., Ouyang, L., Zhu, S., Dai, T., Li, T., & Zhou, J. (2023). Study on the interaction mechanism, physicochemical properties and application in oil-in-water emulsion of soy protein isolate and tannic acid. Journal of Food Engineering, 357, 111626.

Li, Z., Wang, Y., Song, B., Li, J., Bao, Y., Jiang, Q., Chen, Y., Yang, S., Yang, Y., Tian, J., & Li, B. (2023). The comparison between zein-anthocyanins complex and nanoparticle systems: Stability enhancement, interaction mechanism, and in silico approaches. Food Chemistry, 420, 136136.

Liu, F., Ma, C., McClements, D. J., & Gao, Y. (2017). A comparative study of covalent and non-covalent interactions between zein and polyphenols in ethanol-water solution. Food Hydrocolloids, 63, 625-634.

Liu, T., Chen, Y., Zhao, S., Guo, J., Wang, Y., Feng, L., Shan, Y., & Zheng, J. (2023). The sustained-release mechanism of citrus essential oil from cyclodextrin/cellulose-based Pickering emulsions. Food Hydrocolloids, 144, 109023.

Liu, X., Xie, F., Zhou, J., He, J., Din, Z.-u., Cheng, S., & Cai, J. (2023). High internal phase Pickering emulsion stabilized by zein-tannic acid-sodium alginate complexes: β-Carotene loading and 3D printing. Food Hydrocolloids, 142, 108762.

Liu, Z., Shi, A., Wu, C., Hei, X., Li, S., Liu, H., Jiao, B., Adhikari, B., & Wang, Q. (2022). Natural Amphiphilic Shellac Nanoparticle-Stabilized Novel Pickering Emulsions with Droplets and Bi-continuous Structures. ACS Applied Materials & Interfaces, 14(51), 57350-57361.

Ma, Q., Xu, Y., Xiao, H., Mariga, A. M., Chen, Y., Zhang, X., Wang, L., Li, D., Li, L., & Luo, Z. (2022). Rethinking of botanical volatile organic compounds applied in food preservation: Challenges in acquisition, application, microbial inhibition and stimulation. Trends in Food Science & Technology, 125, 166-184.

Meng, Q., Xue, Z., Chen, S., Wu, M., & Lu, P. (2023). Smart antimicrobial Pickering emulsion stabilized by pH-responsive cellulose-based nanoparticles. International Journal of Biological Macromolecules, 233, 123516.

Meng, Y., Wei, Z., & Xue, C. (2024). Correlation among molecular structure, air/water interfacial behavior and foam properties of naringin-treated chickpea protein isolates. Food Hydrocolloids, 147, 109309.

Mwangi, W. W., Lim, H. P., Low, L. E., Tey, B. T., & Chan, E. S. (2020). Food-grade Pickering emulsions for encapsulation and delivery of bioactives. Trends in Food Science & Technology, 100, 320-332.

Nassarawa, S. S., Nayik, G. A., Gupta, S. D., Areche, F. O., Jagdale, Y. D., Ansari, M. J., Hemeg, H. A., Al-Farga, A., & Alotaibi, S. S. (2022). Chemical aspects of polyphenol-protein interactions and their antibacterial activity. Critical Reviews in Food Science and Nutrition, 1-24.

Pi, X., Liu, J., Sun, Y., Ban, Q., Cheng, J., & Guo, M. (2023). Protein modification, IgE binding capacity, and functional properties of soybean protein upon conjugation with polyphenols. Food Chemistry, 405, 134820.

Qin, W., Tang, S., Chen, C., & Xie, J. (2024). Preparation and characterization of cinnamon essential oil Pickering emulsion stabilized by zein/carboxylated cellulose nanocrystals composite nanoparticles. Food Hydrocolloids, 147, 109321.

Ran, R., Zheng, T., Tang, P., Xiong, Y., Yang, C., Gu, M., & Li, G. (2023). Antioxidant and antimicrobial collagen films incorporating Pickering emulsions of cinnamon essential oil for pork preservation. Food Chemistry, 420, 136108.

Reitzer, F., Allais, M., Ball, V., & Meyer, F. (2018). Polyphenols at interfaces. Advances in Colloid and Interface Science, 257, 31-41.

Shao, P., Yu, J., Chen, H., & Gao, H. (2021). Development of microcapsule bioactive paper loaded with cinnamon essential oil to improve the quality of edible fungi. Food Packaging and Shelf Life, 27, 100617.

Souza, E. M. C., Ferreira, M. R. A., & Soares, L. A. L. (2022). Pickering emulsions stabilized by zein particles and their complexes and possibilities of use in the food industry: A review. Food Hydrocolloids, 131, 107781.

Vilela, C., Kurek, M., Hayouka, Z., Röcker, B., Yildirim, S., Antunes, M. D. C., Nilsen-Nygaard, J., Pettersen, M. K., & Freire, C. S. R. (2018). A concise guide to active agents for active food packaging. Trends in Food Science & Technology, 80, 212-222.

Wang, J., Zhang, L., Tan, C., Ying, R., Wang, Y., Hayat, K., & Huang, M. (2022). Pickering emulsions by regulating the molecular interactions between gelatin and catechin for improving the interfacial and antioxidant properties. Food Hydrocolloids, 126, 107425.

Wang, Q., Tang, Y., Yang, Y., Lei, L., Lei, X., Zhao, J., Zhang, Y., Li, L., Wang, Q., & Ming, J. (2022a). The interaction mechanisms, and structural changes of the interaction between zein and ferulic acid under different pH conditions. Food Hydrocolloids, 124, 107251.

Wang, Q., Tang, Y., Yang, Y., Lei, L., Lei, X., Zhao, J., Zhang, Y., Li, L., Wang, Q., & Ming, J. (2022b). Interactions and structural properties of zein/ferulic acid: The effect of calcium chloride. Food Chemistry, 373, 131489.

Wang, T., Wang, N., Yu, Y., Yu, D., Xu, S., & Wang, L. (2023). Study of soybean protein isolate-tannic acid non-covalent complexes by multi-spectroscopic analysis, molecular docking, and interfacial adsorption kinetics. Food Hydrocolloids, 137, 108330.

Wei, L., Song, K., Shao, D., Dong, C., Wang, L., & Jiang, J. (2023). The effect of endogenous phenol and gallic acid on structure and functionalities of mung bean protein in aerated emulsion system. Food Hydrocolloids, 143, 108942.

Wei, Y., Sun, C., Dai, L., Mao, L., Yuan, F., & Gao, Y. (2019). Novel Bilayer Emulsions Costabilized by Zein Colloidal Particles and Propylene Glycol Alginate. 2. Influence of Environmental Stresses on Stability and Rheological Properties. Journal of Agricultural and Food Chemistry, 67(4), 1209-1221.

Wen, H., Zhang, D., Ning, Z., Li, Z., Zhang, Y., Liu, J., & Zhang, T. (2023). How do the hydroxyl group number and position of polyphenols affect the foaming properties of ovalbumin? Food Hydrocolloids, 140, 108629.

Xie, H., Ni, F., Gao, J., Liu, C., Shi, J., Ren, G., Tian, S., Lei, Q., & Fang, W. (2022). Preparation of zein-lecithin-EGCG complex nanoparticles stabilized peppermint oil emulsions: Physicochemical properties, stability and intelligent sensory analysis. Food Chemistry, 383, 132453.

Xu, Y., Wei, Z., & Xue, C. (2023). Pickering emulsions stabilized by zein–gallic acid composite nanoparticles: Impact of covalent or non-covalent interactions on storage stability, lipid oxidation and digestibility. Food Chemistry, 408, 135254.

Zhang, M., Fan, L., Liu, Y., & Li, J. (2023). Migration of gallic acid from the aqueous phase to the oil–water interface using pea protein to improve the physicochemical stability of water–in–oil emulsions. Food Hydrocolloids, 135, 108179.

Zhang, W., Roy, S., Ezati, P., Yang, D.-P., & Rhim, J.-W. (2023). Tannic acid: A green crosslinker for biopolymer-based food packaging films. Trends in Food Science & Technology, 136, 11-23.

Zhang, W., Shu, C., Chen, Q., Cao, J., & Jiang, W. (2019). The multi-layer film system improved the release and retention properties of cinnamon essential oil and its application as coating in inhibition to penicillium expansion of apple fruit. Food Chemistry, 299, 125109.

Zhao, Q., Fan, L., Li, J., & Zhong, S. (2024). Pickering emulsions stabilized by biopolymer-based nanoparticles or hybrid particles for the development of food packaging films: A review. Food Hydrocolloids, 146, 109185.

Zhou, Y., Sun, S., Bei, W., Zahi, M. R., Yuan, Q., & Liang, H. (2018). Preparation and antimicrobial activity of oregano essential oil Pickering emulsion stabilized by cellulose nanocrystals. International Journal of Biological Macromolecules, 112, 7-13.

Zhu, X., Chen, Y., Hu, Y., Han, Y., Xu, J., Zhao, Y., Chen, X., & Li, B. (2021). Tuning the molecular interactions between gliadin and tannic acid to prepare Pickering stabilizers with improved emulsifying properties. Food Hydrocolloids, 111, 106179.

Summary

In this work, we constructed Pickering emulsions co-loaded with TA and CEO (ZTCs) based on the zein-TA (ZT) complexes mediated interfacial engineering. The impact of structural features and interfacial properties generated by interactions between zein and TA were investigated. Furthermore, the stability, rheological, control releases properties of prepared emulsions was investigated. Finally, the antimicrobial effect was evaluated against food spoilage organisms. The insights into interfacial structure and stability gained in this study provide not only a theoretical basis for designing stable essential oil-loaded Pickering emulsions, but also a material platform for their integration into functional food packaging films. This work lays a critical foundation for the further development of PEs-based controlled-release packaging systems.

Chapter 4

Zein/chitosan Janus film incorporated with tannic acid and cinnamon essential oil co-loaded Pickering emulsion for sustained controlled release and pork preservation

Short overview

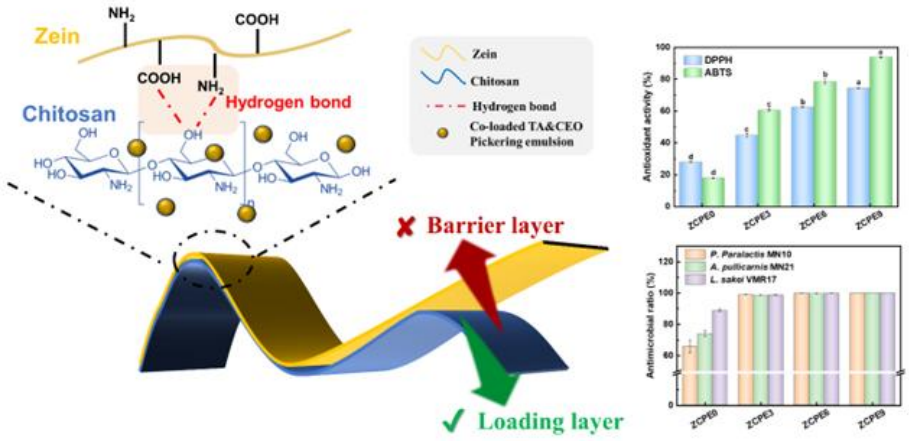

Graphical abstract: Zein/chitosan Janus film incorporated with tannic acid and cinnamon essential oil co-loaded Pickering emulsion for sustained controlled release and pork preservation

The research content of this chapter has been published in the international peer-reviewed journal ***International Journal of Biological Macromolecules***, to which readers are referred for more comprehensive details by **Fan, S.**, Yang, Q., Zhu, C., Li, X., Richel, A., Fauconnier, M.-L., Fang, F., Zhang, D., & Hou, C. (2024). Zein/chitosan Janus film incorporated with tannic acid and cinnamon essential oil co-loaded Pickering emulsion for sustained controlled release and pork preservation. International Journal of Biological Macromolecules, 286, 138429.

Abstract

The development of active packaging offers a promising approach to reducing food waste. However, challenges remain, particularly in achieving efficient release dynamics of active compounds and balancing the barrier properties. Herein, a Janus structure zein/chitosan film is custom designed by layer-by-layer casting method to achieve sustainable and unidirectional release performance of antimicrobial agent, which comprises an inner loading layer of tannic acid (TA) and cinnamon essential oil (CEO) co-loaded Pickering emulsion incorporated with chitosan and an outer barrier layer of zein. The good interfacial compatibility between the entities of Pickering emulsion/chitosan loading layer and zein barrier layer had be confirmed via physicochemical structure characterization. The lower swelling rate of Pickering emulsion/chitosan film (47.61% ~ 51.71%) indicated the sustained and stable release rate of substances from the inner loading layer, while the zein barrier layer restricted the diffusion of active molecules due to the high swelling rate (162.52%). In addition, the films showed excellent antimicrobial activity (> 99% against key foodborne pathogens) and radical scavenging activity (2.5-fold enhancement). Moreover, the film loading layer showed predominantly controlled by a quasi-Fickian diffusion, and prolonged the shelf life of pork by 6 days under the unidirectional sustained release. Our work presents a promising fabrication strategy of antimicrobial packaging film with sustainable release performance for food preservation.

Keywords: Antimicrobial packaging; Pickering emulsions; Sustained release properties; Food preservation

1. Introduction

Annually, approximately 1.3 billion tons of food are wasted or lost at various stages of the supply chain, especially manifest in perishable items such as fruits, vegetables and meat. This phenomenon has raised widespread concerns about the food safety and environmental sustainability (Asgher, Qamar, Bilal, & Iqbal, 2020; Snyder, Martin, & Wiedmann, 2024). Hence, it is imperative to adopt resolute measures in enhancing global endeavors aimed at mitigating food waste (Chang, Xu, Macqueen, Aytac, Peters, Zimmerman, et al., 2022; Tian, Liu, Yang, & Wan, 2023). Package plays a crucial role in safeguarding food items, shielding them from potential damage and effectively prolonging their shelf life. Conventional packaging made from petroleum-based plastics has presented significant challenges in terms of resource consumption and environmental pollution, which persist throughout the entire life cycle of petroleum-based packaging materials (Qu, Wang, Zhang, Chen, Wang, Xue, et al., 2023; Yadav, Silvenius, Katajajuuri, & Leinonen, 2024). Currently, researcher engaged in active investigation on modern packaging technologies that exhibit eco-environmental attributes and possess the potential to enhance the shelf life of food (Cheng, Cai, Zhang, Zhao, Song, Xu, et al., 2024; Hassoun, Boukid, Ozogul, Aït-Kaddour, Soriano, Lorenzo, et al., 2023; Priyadarshi, Roy, Ghosh, Biswas, & Rhim, 2022; Tian, Liu, Yang, & Wan, 2023; T. Wang & Su, 2024).

Recent studies have shown that cinnamon essential oil (CEO), natural substances extracted from the bark or leaves of the Cinnamomum zeylanicum, has utilized as an antimicrobial agent due to its significant inhibitory effect on foodborne microorganisms and inherent naturalness, which has great development in food active packaging (Ezzaky, Elmoslih, Silva, Bonilla-Luque, Possas, Valero, et al., 2023; W. Zhang, Ezati, Khan, Assadpour, Rhim, & Jafari, 2023). The chemical composition of CEO comprises over 20 compounds, with cinnamaldehyde being the most predominant (>70%), other constituents include eugenol, cinnamyl acetate, and α-pinene (Lucas-González, Yilmaz, Mousavi Khaneghah, Hano, Shariati, Bangar, et al., 2023; J. Sun, Leng, Zang, & Zhao, 2024). The antimicrobial activity of CEO is attributed to the strong interact between hydrophobic molecules mentioned above and the microbial cell membrane. Antimicrobial packaging films containing CEO have been successfully fabricated and employed in reducing the waste of food items (Lucas-González, et al., 2023). However, current packaging films containing CEO face challenges related to inefficient release dynamics, involves three stages: (a) the hydrophobicity of CEO renders it incompatible with bio-polymeric materials and the thermal sensitivity of CEO results in the inactivation of components during the film-forming process(W. Zhang, Ezati, Khan, Assadpour, Rhim, & Jafari, 2023); (b) blending CEO in bio-polymeric materials directly may result in a reduction of availability within the packaging cause of 'burst effect'(Malekjani, Karimi, Assadpour, & Jafari); (c) the CEO is released along both sides of packaging film, nearly half of the CEO was released into the surroundings(L. Wang, Yuan, Sun, Wu, Lv, Zhang, et al., 2023). It is crucial to explore ways to develop a packaging film that solves both issues at once.

Pickering emulsion is a promising method to encapsulate and deliver bioactive compounds. It can maximize the retention of essential oils during the film-forming process through the barrier effect, and control the release of bioactive compounds (Tavassoli, Khezerlou, Punia Bangar, Bakhshizadeh, Haghi, Moghaddam, et al., 2023; Zhao, Fan, Li, & Zhong, 2024). Additionally, Pickering emulsion is regarded as safer than conventional emulsion because the elimination in molecular surfactants. In our previous studies, we developed a CEO loaded Pickering emulsion enabled by zein-TA hybrid particles, which had regulated for good physical stability and enhanced antimicrobial activity against spoilage bacteria. However, whether this TA and CEO co-loaded Pickering emulsion strategy is suitable for food active packaging has not been confirmed.

In addition, to further achieve sustained release of CEO from packaging film, it is an ideal method to design the structure of films. A Janus structure based on multilayer film crosslinking, involves creating a bifunctional material with distinct properties on each side of the film, has been proposed in some studies due to their asymmetric structure and multifunctional properties. Natural polymeric materials (i.e., starch, carrageenan, pectin, gelatine, zein and so on) are potential alternatives for the production of packaging materials owing to their excellent film-forming properties and environmentally friendly (Yao, Huang, Lu, Huang, Ali, Jia, et al., 2024). In which, chitosan (CS) is one of the most renewable polymers in nature, mainly extracted from crustaceans. CS is a positively charged polyelectrolyte in solution, which is suitable for forming a loading layer with negatively charged TA and CEO co-loaded Pickering emulsion via electrostatic interactions. Zein is a prolamin found in corn gluten meal waste. Compared with CS, zein exhibits batter water and gas barrier properties, thereby presenting an opportunity to preventing the excessive diffusion of CEO. It is hypothesized that enhanced physical stability of Pickering emulsion and tightly cross-linking of chitosan with zein are benefit for sustained release of CEO, and Janus structure multilayer can maximize the utilization efficiency of CEO in antimicrobial package. Moreover, the proposed film is composed of biodegradable and renewable materials, including CS and zein, which enhance its environmentally friendly properties.

In this work, a Janus structure multilayer antimicrobial packaging film is custom designed by layer-by-layer casting method to achieve an improvement in antimicrobial properties of films. The TA and CEO co-loaded Pickering emulsion incorporated with CS served as inner loading layer of multilayer film, while zein film functioned as the outer barrier layer. We comprehensively assessed the structural, mechanical, barrier, and functional properties of developed films, meanwhile, the sustainable release properties and release behavior were researched in detail. Furthermore, the potential of result films as high-performance antimicrobial film was investigated in preserving meat. This work provides an effective strategy for antimicrobial packaging through the controlled release of cinnamon essential oil, aiming to improve food preservation.

2. Materials and Methods

2.1. Materials

Zein (CAS#9010-66-6, from corn) and trichloroacetic acid (TCA) were obtained from Shanghai Aladdin Biochemical Technology Co., Ltd. (Shanghai, China). CS (CAS#9012-76-4, deacetylation degree > 90% viscosity 0.2 pa s), gelatine (CAS#9000-70-8, type A, bloom value of 300), and glycerol were procured from Macklin Bio-Tech Ltd. (Shanghai, China). TA was purchased from Yuanye Bio-Technology Co., Ltd. (Shanghai, China). CEO was purchased from Jiangxi Taicheng natural perfume Co., Ltd. (Ji'an, China). Plate count agar, yeast extract, and tryptone were procured from Beijing Land Bridge Technology Co., Ltd (Beijing, China). Other reagents (analytically pure) were purchased from Sinopharm Chemical Reagent Co., Ltd (Beijing, China). *P. paralactis* MN10, *A. pullicarnis* MN21, and *L. sakei* VMR17 were kindly supplied by Prof. Zhang's lab (Institute of Food Science and Technology, Beijing, China).

2.2. Preparation of co-loaded TA and CEO Pickering emulsion

The co-loaded TA and CEO Pickering emulsion was prepared according our previous procedure (Fan, Yang, Wang, Zhu, Wen, Li, et al., 2024). Briefly, zein (10 mg/mL) and TA (2 mg/mL) were dissolved in 70% (v/v) ethanol in water to form the zein and TA hybrid particle dispersion solution. Subsequently, CEO was added dropwise to the zein and TA hybrid particle dispersion solution at a ratio of 1:9 (v/v) and sheared with a high shear homogenizing emulsifier (HR-500, Shanghai Huxi Industry Co., Ltd, China) at 8000 rpm for 2 min. Finally, the co-loaded TA and CEO Pickering emulsion was obtained by adding an equal volume of ultrapure water to the CEO-zein and TA hybrid particle dispersion solution.

2.3. Fabrication of the zein/chitosan films with Janus structure (ZCPE) films

The ZCPE films were prepared with layer-by-layer assembly. Briefly, 5 wt% zein solution was prepared by dispersing zein power in 70% (v/v) acetic acid in water. Then, 0.3 wt% gelatine and 30% (w/w, based on the zein powder mass) were added to above zein solution to form the Z layer film forming solution. After stirring, the above solution (10 mL) was cast into a 90 mm diameter plastic plate and dried at 50℃ until a sticky film had formed (Z layer).

CS (1.0 g), gelatine (0.3 g), and glycerol (0.3 g) were mixed in 100 mL of 2% (v/v) acetic acid in water. Different concentrations of zein and TA hybrid particle stabilized Pickering emulsion (0%, 3%, 6%, and 9%, v/v) were added to the mixture and designed as CPEX film-forming solutions, where X is the concentration of the co-loaded TA and CEO Pickering emulsion. Twenty milliliters of CPEX film-forming solution were poured onto the Z layer and then dried 50℃ for 12 h. The prepared bilayer films were named as ZCPE0, ZCPE3, ZCPE6, and ZCPE9. Before further measurement, all films were conditioned at 55% relative humidity for 72 h.

2.4. Characterization of the ZCPE films

Morphology and structure. The films were observed with an SU 1510 scanning electron microscope (SEM, HITACHI, Japan) at 10.0 kV. Before observation, film cross sections were brittle-fracturing with liquid nitrogen, then fixed on aluminium stubs and coated with a layer of thick gold (< 10 nm) under a vacuum. Fourier-transform infrared (FT-IR) spectra were recorded on a Tensor 27 FTIR spectrophotometer (Bruker, Germany). The films were scanned 64 times from 4000 to 400 cm-1 at a resolution of 4 cm-1. The X-ray diffraction (XRD) patterns of the films were recorded using an Ultima Ⅳ with Cu Kα radiation (Rigaku, Tokyo, Japan).

Thermal stability. The thermal stability of films was assessed with simultaneous thermogravimetry by using Pyris Diamond TG thermogravimetric analyzer (PerkinElmer Inc., New Castle, DE, USA). The sample was heated at a rate of 10℃ /min in the range of 30-500℃ under nitrogen atmosphere.

Color and optical properties. The color parameters of the films were determined using a CM-600d colorimeter (Konica Minolta, Tokyo, Japan). The lightness (L*), redness (a*), yellowness (b*), and total color difference (ΔE) were recorded. The whiteness index (WI) was calculated according to the following Eq. (4.2.1):

$$WI\ (\%) = 100-[(100-L^*)^2+(a^*)^2+(b^*)^2)]^{1/2} \qquad (4.2.1)$$

The transmittance of the films was measured using an 6000PC ultraviolet-visible (UV-Vis) spectrophotometer (Shanghai Metash Instruments Co., Ltd., Shanghai, China) in the range of 200-800 nm. Before measurements, the film samples were cut into 40×10 mm strips.

Thickness and mechanical properties. The thickness of the films was measured using an MDC-25SX micrometer calliper (Mitutoyo Corporation, Kawasaki, Japan). The TA-XTPlus Texture Analyzer (Stable Micro System Co., Ltd., UK) was employed to measure the tensile strength (TS) and elongation at break (EAB) of the films. Briefly, the films were cut into rectangle strips (10×70 mm) and fixed between the two clamps with an initial distance of 40 mm; the tested stretching speed was 50 mm/min.

Water contact angle (WCA). The WCA of the films was assessed with a SZ-CAMC32 contact angle analyzer (Shanghai Xuanjun Instrument Co., LTD, China). Briefly, a drop of ultrapure water (5 μL) was dropped on the fixed film surface, and the droplet images were captured by digital camera.

Water content, swelling and solubility. The water content, swelling rate, and water solubility of the films were determined according to the procedure described by Zhang et al. (2022) with a slight modification. The films (20×20 mm) were initially weighed (m_0) and then dried at 105℃ for 24 h before being weighed again (m_1). The dried films were exposed to 30 mL ultrapure for 24 h and weighed (m_2) without residual water on the surface. Then, the films were completely dried at 105℃ for 24 h and weighed again (m_3). The water content, swelling rate and water solubility were calculated as follows Eqs (4.2.2), (4.2.3) and (4.2.4):

$$\text{Water content (\%)} = \frac{m0-m1}{mo} \times 100 \quad (4.\ 2.\ 2)$$

$$\text{Swelling rate (\%)} = \frac{m2-m1}{m1} \times 100 \quad (4.\ 2.\ 3)$$

$$\text{Water solubility (\%)} = \frac{m1-m3}{m1} \times 100 \quad (4.\ 2.\ 4)$$

Water vapor and oxygen barrier properties. The water vapor permeability (WVP) and oxygen permeability (OP) of the films were measured according to the methods described by Dong et al. (2024) with slight modifications. In brief, the films were cut into 20×20 mm strips and sealed on top of centrifuge tubes (50 mL vertical) with 20.0 ± 0.5 g anhydrous silica gels. Then, the samples were incubated in a desiccator with saturated NaCl solution (75% ± 2% relative humidity) at 25℃ for 48 h. WVP was calculated with the following Eq. (4. 2. 5):

$$\text{WVP } (10^{-10}\ \text{g/m s Pa}) = \frac{\triangle m \times e}{t \times A \times \triangle p} \quad (4.\ 2.\ 5)$$

where Δm (g) is the gain in weight of the centrifuge tube; e is the thickness of the film (m); t is the incubation time (s); A (m^2) is the area of the centrifuge tube; and Δp (Pa) is the saturation vapor pressure of water.

To measure OP, the films were cut into 20 × 20 mm strips and sealed on top of centrifuge tubes (50 mL vertical) with 20.0 ± 0.5 g deoxidizer.

OP was calculated with the following Eq. (4. 2. 6):

$$\text{OP } (10^{-5}\ \text{g/m}^2\ \text{s}) = \frac{\triangle m}{t \times A \triangle p} \quad (4.\ 2.\ 6)$$

where Δm (g) is the gain in weight of the centrifuge tube; t is the incubation time (s); A (m2) is the area of the centrifuge tube; and Δp (Pa) is the saturation vapor pressure of water.

2.5. Antimicrobial activity of the ZCPE films

The antimicrobial activity of the films against *P. paralactis* MN10, *A. pullicarnis* MN21, and *L. sakei* VMR17 was evaluated based on the method described by literature (Ma, Xing, Zhao, Zhang, Xin, Liu, et al., 2023). In brief, the films were cut into 20 × 20 mm squares and placed in 6-well plates. One hundred microliters of bacterial solution (approximately 106 colony-forming units, CFU/mL) were added to the loading side of the films and cultured at 30℃ for 2 h. Then, 9.9 mL of lysogeny broth (LB) medium was added to each well, followed by further culturing under the same conditions. One hundred microliters of the bacterial suspension were spread uniformly on an LB agar plate and uniformly and incubated at 30 ℃ for 24 h. Sterile filter paper was used as the control group. The antimicrobial ratio was calculated with the following Eq. (4. 2. 7):

$$\text{Antimicrobial ratio (\%)} = (S_1\text{-}S_2)/S_1 \times 100 \quad (4.\ 2.\ 7)$$

where S_1 and S_2 are the bacterial colony counting for the control and film groups, respectively.

2.6. Antioxidant activity of ZCPE films

The antioxidant activity of films was determined by DPPH (BC4755, Solarbio) and ABTS (BC4775, Solarbio) radical scavenging activity. The measurement and calculation process were carried out in strict accordance with the manufacturer's instructions.

2.7. Release behavior of the ZCPE films

The release behavior of the films was monitored according to the previous studies (L. Wang, et al., 2023) with slight modifications. ZCPE9 films were cut into 20 × 20 mm squares and securely fixed within a connector. Phosphate-buffered solution (PBS, pH 7.0) was added to both sides of the connector, ensuring that only the portion of the film exposed through the connector cavity was in direct contact with the PBS. This setup allowed independent monitoring of the release behavior from the Z layer and the CPE9 layer of the ZCPE9 film. The tests were conducted under constant temperature (4°C) and humidity conditions (50% relative humidity). At specific time intervals, 200 μL of PBS was withdrawn, and its absorbance at 287 nm was measured using a spectrophotometer. The withdrawn PBS was replaced with fresh PBS to maintain consistent test conditions. The cumulative release of CEO was calculated, and a CEO release kinetic curve was constructed based on these measurements.

The release mechanism of the ZCPE films was evaluated by using Korsmeyer-Peppas model (Rojas, Misic, Zizovic, Dicastillo, Velásquez, Rajewska, et al., 2024), which is expressed as following Eq. (4. 2. 8):

$$Mt/M\infty = k\,t^{n} \qquad (4.\ 2.\ 8)$$

where $Mt/M\infty$ represents the fraction of CEO released at given time t, k is release velocity constant, and n is the diffusional exponent, which indicates the type of release mechanism.

2.8. Application of the ZCPE films for meat preservation

Fresh chilled meat was purchased from a local supermarket (Haidian, Beijing, China). The meat was cut into 15.0 ± 0.5 g pieces and wrapped with a commercial polyethylene (PE) film, the ZCPE0 film, or the ZCPE9 film, unwrapped meat served as the control group. All samples were processed in a sterile environment and stored at 4.0 ± 0.5℃ for 15 days.

2.8.1. Color

The color parameters of meat were monitored using a CM-600d colorimeter (Konica Minolta, Tokyo, Japan). L*, a*, and b* were recorded at three different locations on the surface of meat.

2.8.2. Total viable count (TVC)

The TVC of meat was measured according to literature with a slight modification (Gu, Li, Chen, Li, Xiao, Zhang, et al., 2023). Briefly, 10.0 g ± 0.5 g of meat was placed in 90 mL of sterile saline (0.9% [v/v] NaCl) solution in aseptic bags. It was

subjected to extraction with a JN-400i sterile equaliser mixer (Ningbo Jiangnan Instrument Factory, Ningbo, China). The extract was diluted 10-fold with sterile 0.9% (v/v) NaCl solution. Finally, 100 μL of the diluted extract was spread on plate count agar and incubated at 37 °C for 48 h.

2.8.3. Total volatile basic nitrogen (TVB-N)

The TVB-N of meat was measured by using an auto-Kjeldahl device (K9840, Hanon Instruments, Jinan, China). Before measurements, 6.0 ± 0.2 g of meat was added to 30 mL of 2% (w/v) TCA and homogenised. Ten milliliters of the meat-TCA mixture supernatant and 5 mL of 1% (w/v) magnesium oxide solution were added to the distillation tube. After distillation, the receiving bottle of liquid was titrated using 0.01 M HCl. The TVB-N of meat was calculated using the Eq. (4. 2. 9):

$$\text{TVB-N (mg/100 g)} = \frac{(V1-V2)\times 0.01\times 14}{m\times(V/V0)} \times 100 \qquad (4.\ 2.\ 9)$$

where V_1 is the volume of consumed 0.01 M HCl solution (mL), V_2 is the volume of consumed 0.01 M HCl solution (mL) in the blank group, m is the weight of meat (g), V is the volume of the used filter (mL), and V_0 is the total volume of filtrate (mL).

2.9. Statistical analysis

The experiments were performed in triplicate with individually prepared films. The results are expressed as the mean ± standard deviation. The data were analyzed using SPSS Statistics 26.0 (IBM Corp., Armonk, New York, USA). Analysis of variance (ANOVA) followed by Duncan's multiple tests was used to evaluate the significance of the differences in means. $P < 0.05$ was considered to be statistically significant.

3. Results and discussion

3.1. Fabrication and characterization of the ZCPE films

We fabricated the ZCPE films by using LBL assembly. First, we cast the zein based film forming solution to form the first layer. We uniformly incorporated the co-loaded TA and CEO Pickering emulsion into CS to form the loading layer film forming solution. When we cast above mixture on the first layer, there was weak adhesion due to differences in hydrophobicity between zein and the CS emulsion mixture. To solve this problem, we introduced gelatine into the zein solution and the CS-emulsion mixture as an "adhesive". The zein–gelatine film formed the Z layer and the CS–gelatine–emulsion film formed the loading layer. Finally, we prepared the ZCPE films by casting the precursor solution of the loading layer onto the Z layer. As anticipated, these two layers showed satisfactory interfacial compatibility.

3.1.1. Morphology of the ZCPE films

We investigated the microstructure of the ZCPE films by using a scanning electron microscope. As presented in Figure 4-1A, the surface of Z layer appeared smooth for ZCPE9 and other ZCPE films. However, compared with the ZCPE0 film, the surface of the loading layer of the ZCPE9 was rough, perhaps due to the aggregation of co-loaded TA and CEO Pickering emulsion caused by drying stress during the film formation.

The similar aggregation was observed in sodium alginate films containing ginger essential oil-loaded Pickering emulsion (Y. Zhang, Pu, Jiang, Chen, Shen, Zhang, et al., 2024). The ZCPE0 and ZCPE9 film cross-sections showed the seamless combination of the Z and loading layers, reflecting the good interfacial compatibility between these two layers. Additionally, we noted porous in the ZCPE9 loading layer, primarily related to CEO evaporation during film formation.

3.1.2. Structure and thermal properties of the ZCPE films

The intermolecular interactions between co-loaded TA and CEO Pickering emulsion embedded in the loading layer was evaluated by using FT-IR spectry. As presented in Figure 4-1 B1, the broad peaks in the range of 3300-3000 cm^{-1} are attributable to the O-H and N-H stretching vibrations (Fan, Wang, Wen, Li, Fang, Richel, et al., 2023). The characteristic band was shifted from 3230 to 3236 cm^{-1} as the amount of co-loaded TA and CEO Pickering emulsion increased, implying weaker hydrogen bonds between co-loaded TA and CEO Pickering emulsion and CS. In addition, the intermolecular interactions of the layer to layer were also characterized (Figure 4-1 B2). Compared with the CPEX layer, the characteristic peak at 3300-3000 cm^{-1} showed a significant shifted when combined with the Z layer. These results indicate the strong hydrogen bonding between the loading layer and Z layers, providing compelling evidence of the interfacial compatibility of the ZCPE films. Additionally, the others distinctive peaks were observed at 2900-2800 cm^{-1}, near 1700 cm^{-1}, and near 1550 cm^{-1}, belonging to the stretching of =C-H, amide I, and amide II, respectively. Although there were some degrees of strengthening, weakening, and shifting in the ZCPE films, these changes only involved non-covalent interactions, such as hydrogen bonds and electrostatic interaction, demonstrating the fabrication process did not significantly change the chemical structure of these films. After assessing the interactions present in the ZCPE films, we investigated the crystal structure using XRD. As shown in Figure 4-1 C1, we recorded two typical characteristic peaks at 2θ of approximately 9° and 20.0°, assigned to hydrated crystal and regular lattice, respectively. We observed these peaks for all single CPEX layers, suggesting the crystal structure of the loading layer was maintained after incorporating of co-loaded TA and CEO Pickering emulsion. However, the intensity of the corresponding peak at 2θ around 20.0° was decreased as the concentration of co-loaded TA and CEO Pickering emulsion increased, this phenomenon might be attributed to hydrogen bonding between the emulsion and CS. We also investigated the crystallinity of the ZCPE films from the side of Z layer (Figure 4-1 C2). Notably, the main XRD peaks from this side are wider and weaker than the single CPEX layer, implying that the crystal structure tends to be amorphous due to the strong interaction between the Z and CPEX layer. Generally, materials with lower crystallinity show good elongation in mechanical properties (Y. Sun, Liu, Zhang, Wang, & Li, 2020), which we confirmed in section 3.1.4.

The thermal stability is critical for potential secondary processing and overall material stability of films, which could be assessed by thermogravimetric analysis. The temperature-dependent thermogravimetric and corresponding differential thermogravimetric curves can be observed in Figure 4-1 D1 and D2, respectively. The

weight of the ZCPE films decreased as the temperature increased, with three distinct steps. The first stage appeared at 80-120°C, which could be attributed to the evaporation of water and volatile substances in the films. In this stage, all ZCPE films behaved similarly. The second stage occurred from 120 to 250°C; it may be related to the degradation of CS and glycerol. The third stage was at 250-380°C, corresponding to the decomposition of the polymeric backbone alongside carbon. The films containing co-loaded TA and CEO Pickering emulsion had a higher degradation temperature, indicating an improvement in their thermal stability. This result could be explained by the interaction and the higher compatibility between the film components. Collectively, these results imply enhanced thermal stability of the ZCPE films due to the addition of co-loaded TA and CEO Pickering emulsion.

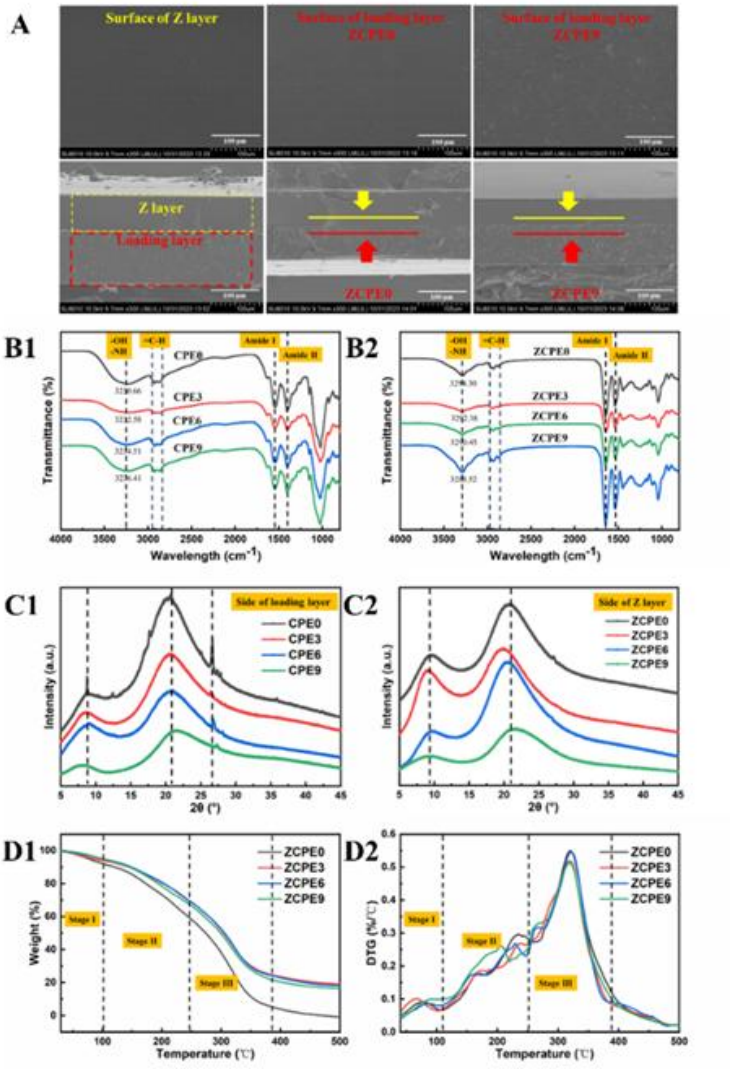

Figure 4-1 (A) SEM images of ZCPE films, including surface and cross-sectional of films. (B1, B2) FTIR spectra of loading layer and ZCPE films. (C1, C2) XRD patterns of ZCPE films, measured from loading layer and Z layer, respectively. (D1) TG curves and (D2) DTG curves of ZCPE films.

3.1.3. Optical properties of the ZCPE films

The color parameter of the ZCPE films is summarized in Table 4-1. L^* decreased significantly with the addition of co-loaded TA and CEO Pickering emulsion ($P < 0.05$). a^* and b^* increased from 0.58 to 6.63 and from 40.03 to 56.62, respectively. As the content of co-loaded TA and CEO Pickering emulsion increased, the color saturation deepened. We measured the visual chromatic aberration as ΔE, which increased. The higher ΔE and the lower WI of the ZCPE films are consistent with the appearance of the ZCPE films. To clarify the optical properties of the films, we measured their UV-Vis transmittance spectra (Figure 4-2A). Light transmittance decreased gradually as the amount of co-loaded TA and CEO Pickering emulsion increased, this phenomenon that could be attributed to the abundant unsaturated chromophile bonds in CEO. In particular, the ZCPE films blocked almost 100% of UV light (200-400 nm). The opacity of the films (Table 4-1) correlated positively with the emulsion content. Compared with the ZCPE0 film, the opacity of the ZCPE9 film increased by 73.31%. These results indicate an enhanced UV barrier capability of the ZCPE films.

Table 4-1 Colorimetric parameters of ZCPEX films.

Film	*L**	*a**	*b**	ΔE	WI (%)	Opacity
ZCPE0	78.03±0.52^{a}	0.58±0.24^{d}	40.03±1.69^{c}	53.12±1.45^{d}	54.33±1.67^{a}	2.66±0.01^{d}
ZCPE3	77.01±0.22^{a}	1.92±0.03^{c}	51.16±0.62^{b}	61.94±0.34^{c}	43.88±0.48^{b}	3.00±0.04^{c}
ZCPE6	74.50±0.78^{b}	3.83±0.92^{b}	53.72±1.18^{b}	65.61±1.42^{b}	40.40±1.42^{b}	3.75±0.01^{b}
ZCPE9	71.40±0.72^{c}	6.63±0.29^{a}	56.62±0.74^{a}	69.85±0.12^{a}	36.21±0.40^{c}	4.61±0.03^{a}

The values were shown as mean±standard deviation (SD). Different letters represent significant differences.

3.1.4. Mechanical properties of the ZCPE films

We determined the TS and EAB to evaluate the mechanical properties of the ZCPE films (Figure 4-2B). The TS and EAB of the ZCPE0 films were 21.32 MPa and 3.34%, respectively. After loading the emulsion, the TS of the ZCPE9 film decreased slightly to 19.05 MPa, which might be due to the fact that emulsion droplets disturbed the continuity of the film's interior (Q.-R. Liu, Wang, Qi, Huang, & Xiao, 2019). This is similar to the results reported by Xu et al.(Xue, Zhu, Sun, Yang, Wu, & Li, 2023), who prepared konjac glucomannan films with oregano essential oil- loaded Pickering emulsion. The EAB of the ZCPE films increased, especially for the ZCPE9 film. This change could be explained by the replacement of strong interactions between polymers with weak interactions between oil and polymer (Fasihi, Noshirvani, & Hashemi, 2023), suggesting the plasticization of co-loaded TA and CEO Pickering emulsion increased the flexibility and deformability of films. Specifically, as the content of the Pickering emulsion increases, there is a replacement of strong polymer-polymer interactions with weaker oil-polymer interfacial interactions. This leads to a reduction in the cohesive strength of the matrix, resulting in a slight decrease in TS. At the same time, the presence of the emulsion droplets acts as stress concentrators, which improve the film's ability to deform under applied stress, thereby increasing EAB. Some researchers have reported that the addition of essential oil loaded emulsion can negatively impact the mechanical properties of films (Xu, He, Wei, Duan, Yu, Li, et al., 2023; Y. Zhang, et al., 2024). Therefore, future research on emulsion-containing films could focus on strategies to enhance their mechanical performance while maintaining other functional properties. However, we recognize that the balance between strength and flexibility will depend on the specific requirements of the application.

3.1.5. Barrier properties of the ZCPE films

The barrier properties of food packaging materials are critical for maintaining the food's quality. Here, we evaluated the barrier properties of the ZCPE films to water and oxygen. As shown in Figure 4-2 C, the WVP of ZCPE0 film was 8.34×10^{-11} g/ (Pa s m), it decreased to 7.85×10^{-11} g/ (Pa s m) for the ZCPE9 film, suggesting that the addition of co-loaded TA and CEO Pickering emulsion improved the water vapor barrier performance. The essential oil loaded emulsion increases the tortuosity of the water molecule diffusion path, which could enhance the water barrier properties of films (Fan, et al., 2023). However, OP of the ZCPE films increased from 6.76 to 11.02 g/ (Pa s m) (Figure 4-2D), indicating decreased oxygen barrier performance. Liu et al. (S. Liu, Jiang, Zhang, Gao, Jiang, Waterhouse, et al., 2024)attributed this negative effect in oxygen barrier performance to the evaporation of essential oil during the film-forming drying process. These results show that the presence of essential oil loaded emulsion may alter a film's barrier performance.

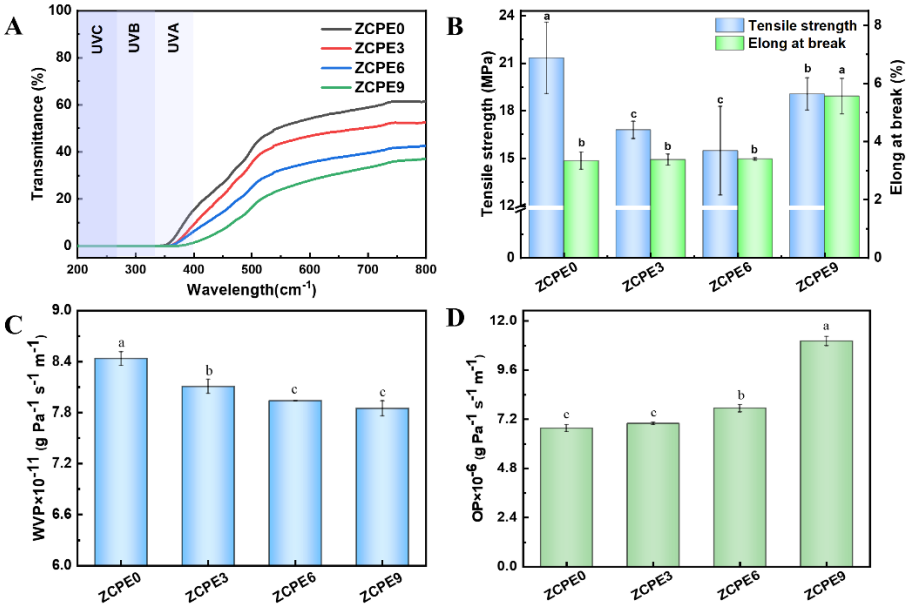

Figure 4-2 (A) UV-vis transmission spectra of ZCPE films, (B) mechanical properties, (C) water barrier property and (D) oxygen barrier property of ZCPE films.

3.1.6. Water sensitivity of the ZCPE films

The water sensitivity of films (especially those biobased polymers films) is intended to evaluate the material's susceptibility to water interaction, which is relevant to its potential application in food packaging where exposure to moisture can affect material performance (Duan, Yang, Wu, Wang, Liu, & Liu, 2022). The water content of the ZCPE films ranged from 23.60% to ~24.01% (Figure 4-3A), with no significant difference between the films ($P > 0.05$). Noticeably, the Z layer had a lower water content than the loading layer, indicating that the Z layer is responsible for the low water permeability of the ZCPE films. A high-water content of a film could lead to a negative effect on TS and water barrier properties (Aguirre-Loredo, Rodríguez-Hernández, Morales-Sánchez, Gómez-Aldapa, & Velazquez, 2016). The water solubility could predict the stability of films in application. As shown in Figure 4-3B, the water solubility of the ZCPE films decreased with the addition of co-loaded TA and CEO Pickering emulsion. For practical applications, reducing the water solubility of films could expand their application range in foods with a high moisture content (W. Zhang, Jiang, Rhim, Cao, & Jiang, 2022). Figure 4-3C shows the swelling rate of the ZCPE films. The swelling rate of CPEX layer (47.61% ~ 51.71%) was lower than the swelling rate of the Z layer (162.52%), indicating the sustained and stable release rate of active substances from the CPEX layer. The lower swelling rate of the CPEX layer provides a more controlled and gradual release of antimicrobial agents, even as humidity fluctuates. This stability is advantageous in real-world applications, where

humidity levels can vary during storage and transport. Of note, the swelling rate was not significantly different between the ZCPE films ($P > 0.05$). The swelling rate of ZCPE films was about 65%, which is close to the swelling rate of CPEX layer. This phenomenon could be attributed to a large number of hydroxyl group are involved into the assembly of ZCPE films, resulting in the reduction of binding sites for water molecules (Qiao, Lu, Chen, Liu, Li, & Zhang, 2023). To further evaluated the water sensitivity of ZCPE films, we measured the WCA of each side of the films (Figure 4-3D). The WCA of the Z layer barely changed (about 45°), while the WCA of the loading layer decreased as the proportion of emulsion increased. Surprisingly, the WCA of the Z layer was lower than the predicted WCA, perhaps due to hydrophilic groups of zein that face outward during the film drying process, as has been observed in gelatine-zein bilayer film (Easdani, Ahammed, Saqib, Liu, & Zhong, 2024).

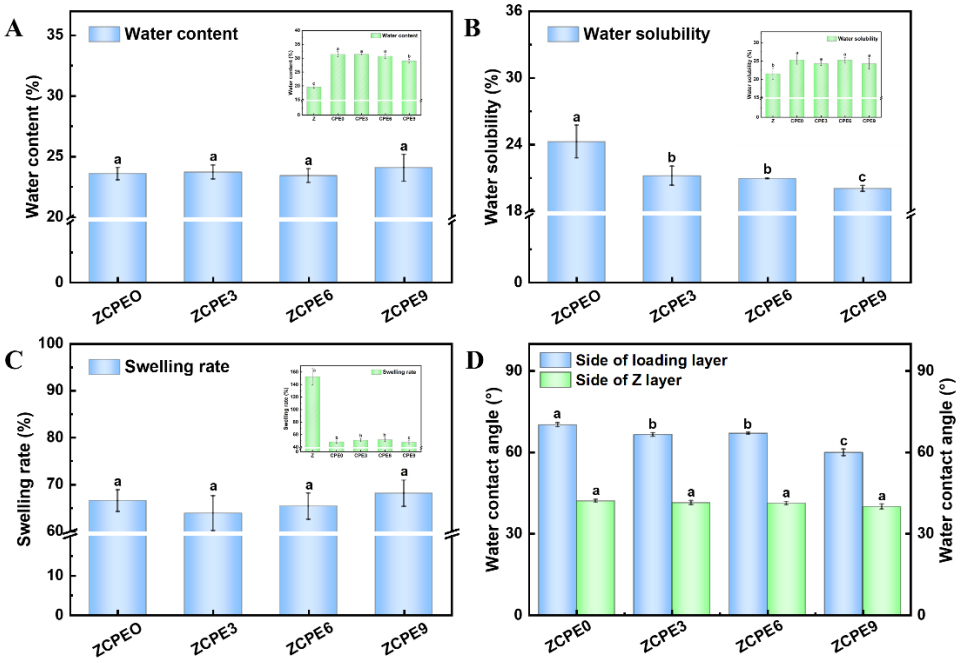

Figure 4-3(A) Water content, (B) water solubility, (C) swelling rate, and (D) water contact angle of ZCPE films.

3.2. The antimicrobial and antioxidant properties of the ZCPE films

3.2.1. Antimicrobial activity

Microorganism proliferation accelerates the spoilage of meat (Shao, Chen, Wang, Zhang, Xu, & Wang, 2021). We evaluated the antimicrobial activity of the ZCPE

films against bacteria related to meat spoilage: *P.paralactis* MN10, *A.pullicarnis* MN21, and *L.sakei* VMR17 (Figure 4-4A). Visible dense colony units formed on the agar plates of control group, whereas there were scarcely any colony units on the agar plates of the ZCPE film groups, except for the ZCPE0 film. The antimicrobial ratio of ZCPE9 against *P.paralactis* MN10, *A.pullicarnis* MN21, and *L.sakei* VMR17 was > 99% (Figure 4-4B). The *P. paralactis* MN10 and *A. pullicarnis* MN21 were the main genera found in our previous work of screening bacteria in meat, and these two strain with the highest spoilage ability in vitro respectively (Wen, Zhang, Morton, Wang, Chai, Li, et al., 2024). *L. sakei* VMR17 serves as a representative of gram-positive bacteria with spoilage potential in meat products. By focusing on these representative strains, we aimed to demonstrate the potential applicability of ZCPE films in mitigating spoilage and extending the shelf life of meat products. The excellent antimicrobial activity observed can be attributed to the release of CEO from the ZCPE films. CEO demonstrates strong antibacterial properties due to its rich composition of bioactive compounds, particularly cinnamaldehyde, which serves as its primary active component. Cinnamaldehyde interacts with the lipid bilayer of bacterial cell membranes, increasing their permeability. This disruption results in the leakage of intracellular contents, such as ions and proteins, ultimately leading to bacterial cell death (Fan, et al., 2023; W. Zhang, Ezati, Khan, Assadpour, Rhim, & Jafari, 2023). These results indicate that the ZCPE films have satisfactory antimicrobial properties and potential to maintain the quality of packaged food.

3.2.2. Antioxidant activity

The antioxidant activity of films is another critical factor for functional food packaging. The DPPH and ABTS assays are effective methods for assessing the ability of antioxidants to neutralize stable free radicals. These assays align well with the characteristics of essential oils in our film, particularly due to their effectiveness in non-polar systems. Moreover, the combination of DPPH and ABTS assays provides a comprehensive evaluation of the antioxidant capacity of natural compounds within film matrices, ensuring reliable and robust analysis (Miao, Gu, Shi, Zhang, Yu, Xiao, et al., 2024; Yang, Zhang, & Cai, 2024). Both the DPPH and ABTS radical scavenging activity of the ZCPE films was increased significantly ($P < 0.05$), from 28.01% to 74.30% for DPPH radical scavenging activity, and from 17.93% to 93.80% for ABTS radical scavenging activity (Figure 4-4C). In addition, we noted an emulsion concentration dependent effect of antioxidant activity. The antioxidant activity of the ZCPE films is due to the TA and CEO. TA has abundant hydroxyl groups, that provide good hydrogen donating capacity and promote DPPH and ABTS radical scavenging (Figure 4-4D) (W. Zhang, Roy, Ezati, Yang, & Rhim, 2023). A large number of terpenoids and aldehydes endow CEO with good antioxidant activity. Hence, the co-loaded TA and CEO Pickering emulsion enhances antioxidant activity due to the synergistic effects of TA and CEO (Fan, et al., 2024).

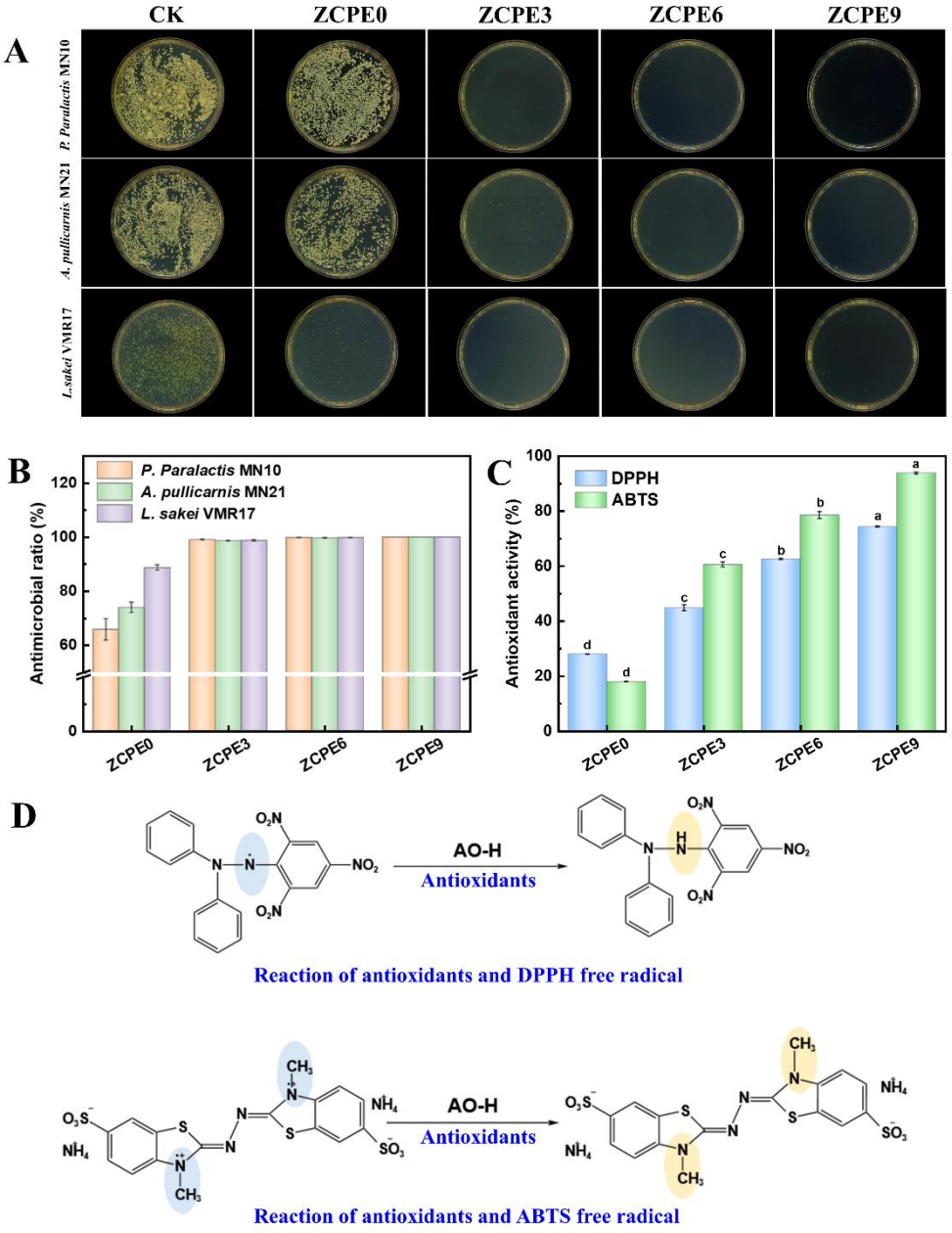

Figure 4-4 (A) Colony forming units of *P.paralactis* MN10, *A.pullicarnis* MN21, *L.sakei* VMR17 after cultivation with ZCPE films. (B) Antimicrobial ratio of ZCPE films against *P.paralactis* MN10, *A.pullicarnis* MN21, *L.sakei* VMR17. (C) Antioxidant activity of ZCPE films and (D) reaction of antioxidants and DPPH, ABTS free radical.

3.3. Release mechanism of the ZCPE films

3.3.1. Release kinetics

To investigate the release properties of CEO from ZCPE films, we subjected the ZCPE9 film to migration assays using PBS as a common food simulated medium at 4℃. As shown in Figure 4-5A, the ZCPE9 film had obvious controlled release characteristics, showing burst release behavior for initial 1-2 days and followed by sustained release for 3-7 days. It is worth noting that much more CEO was released from loading layer (CPE9 layer) than the Z layer, implying the blocking effect of Z layer regarding active substance release. This characteristic might be related to the high swelling rate of the Z layer. We prepared the blend film by mixing the loading layer (CPE9 layer) and Z layer film-forming solutions together and then casting. The release characteristics of blend film was shown in Figure 4-6. The release patterns of CEO from both sides of the blended film were similar. However, the amount of CEO released from the loading layer of the blended film was lower than the amount of CEO released from the loading layer of the ZCPE9 film. The important contribution of the ZCPE9 films in controlling active release was highlighted by contrasting with the blend film. The loading layer functions as the inner layer for sustained release of active substances, while the Z layer serves as a barrier to minimize the release of active substances into the environment. The efficiency of antimicrobial packaging could be improved by reducing the waste of active substances.

3.3.2. Diffusion release mechanism

We further evaluated the release mechanism of CEO from the ZCPE9 film by fitting the release profile with mathematical models. The zero-order, first-order, Higuchi, and Korsmeyer–Peppas kinetic models were used to analyse the release behaviour of CEO from the ZCPE9 loading layer (Yu, Li, Ma, Wang, Zhu, & Wang, 2023). The related parameters are shown in Figure 4-5B. Based on the regression coefficients obtained from models, the Korsmeyer–Peppas model demonstrated the highest reliability to fit the experimental release data of CEO from the loading layer of ZCPE9. Therefore, we applied the Korsmeyer–Peppas model to explore the release mechanism of CEO from the ZCPE9 film (Figure 4-5C). The n parameter in the Korsmeyer–Peppas model represents the active substance release type: $n < 0.5$ for quasi-Fickian diffusion, $n = 0.5$ for Fickian diffusion, and $n > 0.5$ for anomalous transport (Rojas, et al., 2024). The n value of the ZCPE9 Korsmeyer–Peppas model was < 0.5, indicating that CEO release from the ZCPE film follows a quasi-Fickian diffusion process.

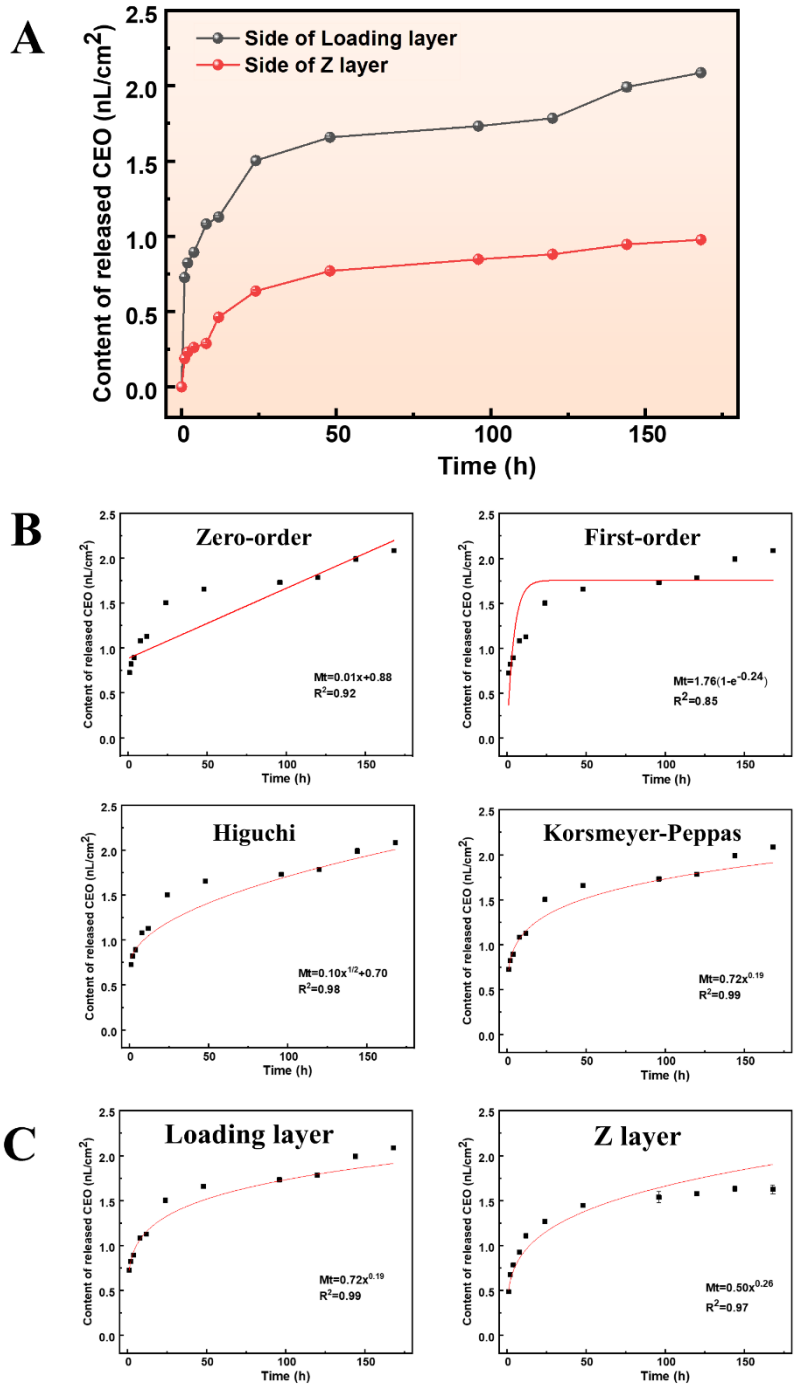

Figure 4-5 (A) Time-dependent release curve of ZCPE9 film. (B) Analysis of CEO release kinetics from loading layer of ZCPE9 by zero-order, first-order, Higuchi and Korsmeyer-

Peppas kinetic model. (C) Kinetic fitted results of CEO release from different side of ZCPE9 under Korsmeyer-Peppas model.

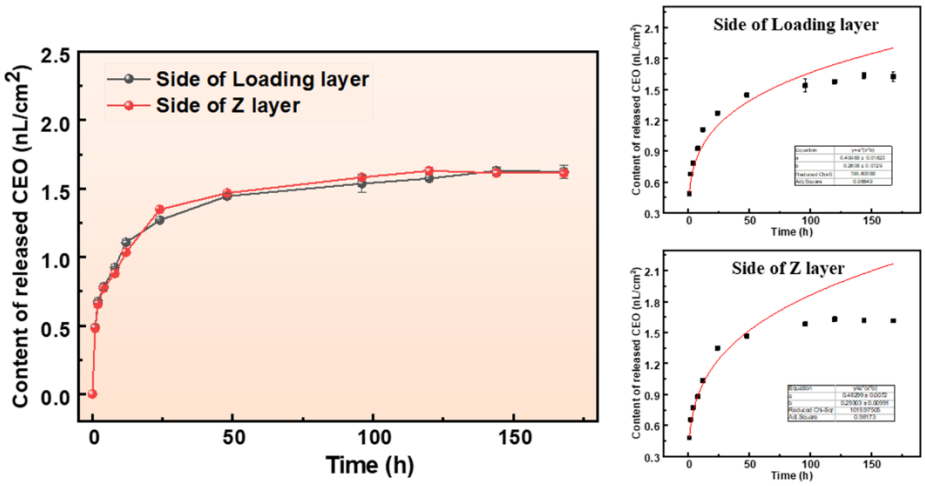

Figure 4-6 The release characteristics of blend film. (A) Time-dependent release curve of blend film. (B) Analysis of CEO release kinetics from two sides by Korsmeyer-Peppas kinetic model.

3.4. Application of ZCPE films in preserving meat

The ZCPE9 film was selected for practical applications in meat preservation. based on its optimal combination of mechanical properties, barrier performance, and antimicrobial and antioxidant activities.

Meat color, an important quality attribute that influences purchasing decisions, is indeed one of the most critical parameters for freshness evaluation (Faustman, Sun, Mancini, & Suman, 2010; Purslow, Warner, Clarke, & Hughes, 2020). Studies have demonstrated a direct correlation between meat color and its freshness and quality (Joo, Kim, Hwang, & Ryu, 2013; Suman & Joseph, 2013). The brightness and redness result of meat are presented in Figure 4-7A and Figure 4-6B, respectively. L^* showed a downward trend, meaning that the meat gradually became darker. a^* showed an upward trend, except for the PE film group. The opposite result of the PE film group was due to the mucus and white colonies on the surface of the meat, consistent with a previous study (Zheng, Tang, Yang, Ran, & Li, 2023).

Meat spoilage is highly correlated with bacterial proliferation. We assessed the spoilage degree of packaged meat by determining the TVC. As shown in the Figure. 4-7C, the TVC increased in each group during the storage period. On day 6, the TVC of the control group and PE film group was 6.01 and 6.09 lg CFU/g, respectively, exceeding the limit (6.00 lg CFU/g) stipulated by the People's Republic of China. The TVC of fresh meat was 2.94 lg CFU/g and increased up to 5.89 lg CFU/g in the ZCPE0 group on day 15, consistently remaining below the limit value throughout the preservation process. This outcome could be attributed to the CS in the ZCPE0 film,

retarding bacterial proliferation. The TVC of the ZCPE9 group increased slowly, to a maximum of 4.45 lg CFU/g on day 15, suggesting the sustained release of antimicrobial substances.

TVB-N is main product of protein degradation and can reflect the freshness of meat. As displayed in Figure 4-7D, the initial TVB-N of fresh meat was 5.45 mg/100 g, slightly lower than previous studies (Zheng, Tang, Yang, Ran, & Li, 2023). TVB-N increased in all groups during storage, probably due to bacteria-mediated breakdown. On day 9, TVB-N was 16.03 and 15.04 mg/100 g for the control and PE film groups, exceeding the limit of 15 mg/100g according to Chinese Standard GB 2707-2016, suggesting the inedibility of the meat. By contrast, TVB-N of the ZCPE9 group (15.41 mg/100 g) was much lower than control and PE groups on day 15, but it still which slightly exceeded the limitation. In conclusion, the ZCPE9 film could extend the shelf life of fresh meat by inhibiting the growth of microorganisms and decelerating the bacteria-induced protein degradation.

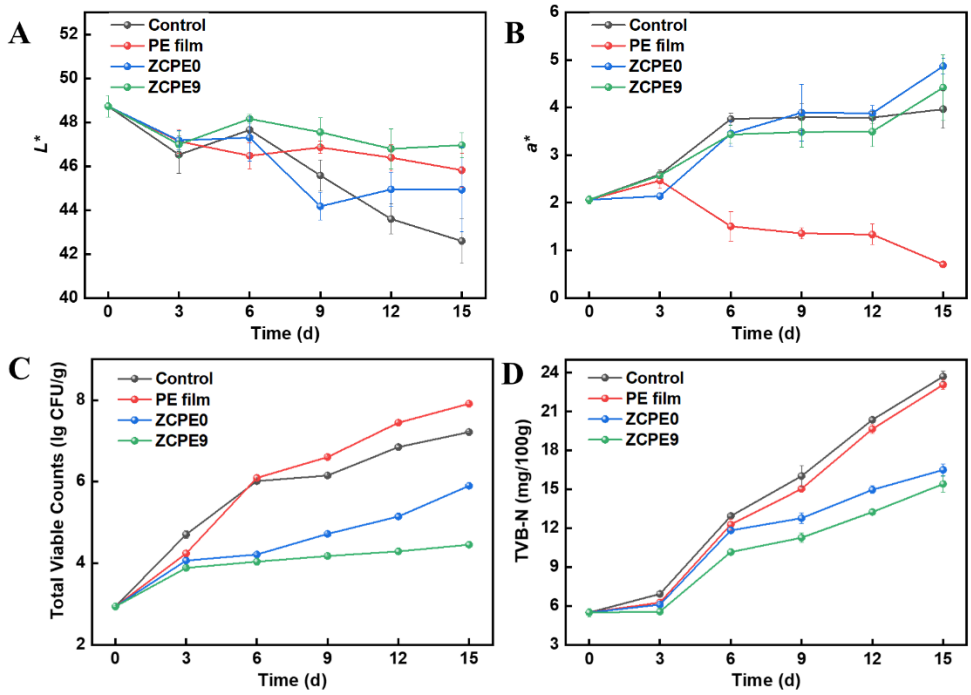

Figure 4-7 (A) L*, (B) a*, (C) total viable counts, and (D) total volatile basic nitrogen value of meat samples wrapped with PE films, ZCPE0 films and ZCPE9 films.

4. Conclusions

In this work, we successfully fabricated a zein/CS film with the Janus structure and incorporated co-loaded TA and CEO Pickering emulsion. The constructed films possessed good interfacial compatibility, enhanced thermal stability, and excellent barrier and UV resistance properties. In addition, the ZCPE films provided excellent functional performance in antimicrobial activity against *P. paralactis* MN10, *A. pullicarnis* MN21, and *L. sakei* VMR17; the antimicrobial ratio of the ZCPE9 film was almost 100%. The DPPH and ABTS radical scavenging activities increased from 28.01% to 74.30% and from 17.93% to 93.83%, respectively. The release behavior of CEO from ZCPE9 film showed obvious sustained controlled release characteristics and followed a quasi-Fickian diffusion process. Moreover, for practical meat preservation, compared to control group, the TVC and TVB-N in the ZCPE9 group were decreased by 2.76 lg CFU/g and 35.01%, respectively, during 15 days of storage. Overall, the current work provides a promising alternative for high-performance and eco-friendly antimicrobial packaging, addressing the growing need for sustainable solutions in the food industry.

5. References

Aguirre-Loredo, R. Y., Rodríguez-Hernández, A. I., Morales-Sánchez, E., Gómez-Aldapa, C. A., & Velazquez, G. (2016). Effect of equilibrium moisture content on barrier, mechanical and thermal properties of chitosan films. Food Chemistry, 196, 560-566.

Asgher, M., Qamar, S. A., Bilal, M., & Iqbal, H. M. N. (2020). Bio-based active food packaging materials: Sustainable alternative to conventional petrochemical-based packaging materials. Food Research International, 137, 109625.

Chang, H., Xu, J., Macqueen, L. A., Aytac, Z., Peters, M. M., Zimmerman, J. F., Xu, T., Demokritou, P., & Parker, K. K. (2022). High-throughput coating with biodegradable antimicrobial pullulan fibres extends shelf life and reduces weight loss in an avocado model. Nature Food, 3(6), 428-436.

Cheng, Y., Cai, X., Zhang, X., Zhao, Y., Song, R., Xu, Y., & Gao, H. (2024). Applications in Pickering emulsions of enhancing preservation properties: Current trends and future prospects in active food packaging coatings and films. Trends in Food Science & Technology, 151, 104643.

Duan, A., Yang, J., Wu, L., Wang, T., Liu, Q., & Liu, Y. (2022). Preparation, physicochemical and application evaluation of raspberry anthocyanin and curcumin based on chitosan/starch/gelatin film. International Journal of Biological Macromolecules, 220, 147-158.

Easdani, M., Ahammed, S., Saqib, M. N., Liu, F., & Zhong, F. (2024). Engineering biodegradable controlled gelatin-zein bilayer film with improved mechanical strength and flexibility. Food Hydrocolloids, 148, 109430.

Ezzaky, Y., Elmoslih, A., Silva, B. N., Bonilla-Luque, O. M., Possas, A., Valero, A., Cadavez, V., Gonzales-Barron, U., & Achemchem, F. (2023). In vitro antimicrobial activity of extracts and essential oils of Cinnamomum, Salvia, and

Mentha spp. against foodborne pathogens: A meta-analysis study. Comprehensive Reviews in Food Science and Food Safety, 22(6), 4516-4536.

Fan, S., Wang, D., Wen, X., Li, X., Fang, F., Richel, A., Xiao, N., Fauconnier, M.-L., Hou, C., & Zhang, D. (2023). Incorporation of cinnamon essential oil-loaded Pickering emulsion for improving antimicrobial properties and control release of chitosan/gelatin films. Food Hydrocolloids, 138, 108438.

Fan, S., Yang, Q., Wang, D., Zhu, C., Wen, X., Li, X., Richel, A., Fauconnier, M.-L., Yang, W., Hou, C., & Zhang, D. (2024). Zein and tannic acid hybrid particles improving physical stability, controlled release properties, and antimicrobial activity of cinnamon essential oil loaded Pickering emulsions. Food Chemistry, 446, 138512.

Fasihi, H., Noshirvani, N., & Hashemi, M. (2023). Novel bioactive films integrated with Pickering emulsion of ginger essential oil for food packaging application. Food Bioscience, 51, 102269.

Faustman, C., Sun, Q., Mancini, R., & Suman, S. P. (2010). Myoglobin and lipid oxidation interactions: Mechanistic bases and control. Meat Science, 86(1), 86-94.

Gu, M., Li, C., Chen, L., Li, S., Xiao, N., Zhang, D., & Zheng, X. (2023). Insight from untargeted metabolomics: Revealing the potential marker compounds changes in refrigerated pork based on random forests machine learning algorithm. Food Chemistry, 424, 136341.

Hassoun, A., Boukid, F., Ozogul, F., Aït-Kaddour, A., Soriano, J. M., Lorenzo, J. M., Perestrelo, R., Galanakis, C. M., Bono, G., Bouyahya, A., Bhat, Z., Smaoui, S., Jambrak, A. R., & Câmara, J. S. (2023). Creating new opportunities for sustainable food packaging through dimensions of industry 4.0: New insights into the food waste perspective. Trends in Food Science & Technology, 142, 104238.

Joo, S. T., Kim, G. D., Hwang, Y. H., & Ryu, Y. C. (2013). Control of fresh meat quality through manipulation of muscle fiber characteristics. Meat Science, 95(4), 828-836.

Liu, Q.-R., Wang, W., Qi, J., Huang, Q., & Xiao, J. (2019). Oregano essential oil loaded soybean polysaccharide films: Effect of Pickering type immobilization on physical and antimicrobial properties. Food Hydrocolloids, 87, 165-172.

Liu, S., Jiang, X., Zhang, M., Gao, X., Jiang, R., Waterhouse, G. I. N., & Fan, H. (2024). Porous carbon nitride-chitosan/zein bilayer functional films with efficient photocatalytic antibacterial activity and tunable water barrier performance for food packaging. Food Bioscience, 61, 104748.

Lucas-González, R., Yilmaz, B., Mousavi Khaneghah, A., Hano, C., Shariati, M. A., Bangar, S. P., Goksen, G., Dhama, K., & Lorenzo, J. M. (2023). Cinnamon: An antimicrobial ingredient for active packaging. Food Packaging and Shelf Life, 35, 101026.

Ma, Z., Xing, Z., Zhao, Y., Zhang, H., Xin, Q., Liu, J., Qin, M., Ding, C., & Li, J. (2023). Lotus leaf inspired sustainable and multifunctional Janus film for food packaging. Chemical Engineering Journal, 457, 141279.

Malekjani, N., Karimi, R., Assadpour, E., & Jafari, S. M. Control of release in active packaging/coating for food products; approaches, mechanisms, profiles, and modeling. Critical Reviews in Food Science and Nutrition, 1-23.

Miao, W., Gu, R., Shi, X., Zhang, J., Yu, L., Xiao, H., & Li, C. (2024). Indicative bacterial cellulose films incorporated with curcumin-embedded Pickering emulsions: Preparation, antibacterial performance, and mechanism. Chemical Engineering Journal, 495, 153284.

Priyadarshi, R., Roy, S., Ghosh, T., Biswas, D., & Rhim, J.-W. (2022). Antimicrobial nanofillers reinforced biopolymer composite films for active food packaging applications - A review. Sustainable Materials and Technologies, 32, e00353.

Purslow, P. P., Warner, R. D., Clarke, F. M., & Hughes, J. M. (2020). Variations in meat colour due to factors other than myoglobin chemistry; a synthesis of recent findings (invited review). Meat Science, 159, 107941.

Qiao, D., Lu, J., Chen, Z., Liu, X., Li, M., & Zhang, B. (2023). Zein inclusion changes the rheological, hydrophobic and mechanical properties of agar/konjac glucomannan based system. Food Hydrocolloids, 137, 108365.

Qu, W., Wang, W., Zhang, C., Chen, X., Wang, J., Xue, W., Zhu, J., & Wu, H. (2023). Development of composite film based on polyvinyl alcohol with binary nanoreinforcements for active packaging of fresh-cut apples. Chemical Engineering Journal, 477, 146862.

Rojas, A., Misic, D., Zizovic, I., Dicastillo, C. L. d., Velásquez, E., Rajewska, A., Rozas, B., Catalán, L., Vidal, C. P., Guarda, A., & Galotto, M. J. (2024). Supercritical fluid and cocrystallization technologies for designing antimicrobial food packaging PLA nanocomposite foams loaded with eugenol cocrystals with prolonged release. Chemical Engineering Journal, 481, 148407.

Shao, L., Chen, S., Wang, H., Zhang, J., Xu, X., & Wang, H. (2021). Advances in understanding the predominance, phenotypes, and mechanisms of bacteria related to meat spoilage. Trends in Food Science & Technology, 118, 822-832.

Snyder, A. B., Martin, N., & Wiedmann, M. (2024). Microbial food spoilage: impact, causative agents and control strategies. Nature Reviews Microbiology, 22(9), 528-542.

Suman, S. P., & Joseph, P. (2013). Myoglobin chemistry and meat color. Annual review of food science and technology, 4(1), 79-99.

Sun, J., Leng, X., Zang, J., & Zhao, G. (2024). Bio-based antibacterial food packaging films and coatings containing cinnamaldehyde: A review. Critical Reviews in Food Science and Nutrition, 64(1), 140-152.

Sun, Y., Liu, Z., Zhang, L., Wang, X., & Li, L. (2020). Effects of plasticizer type and concentration on rheological, physico-mechanical and structural properties of chitosan/zein film. International Journal of Biological Macromolecules, 143, 334-340.

Tavassoli, M., Khezerlou, A., Punia Bangar, S., Bakhshizadeh, M., Haghi, P. B., Moghaddam, T. N., & Ehsani, A. (2023). Functionality developments of Pickering

emulsion in food packaging: Principles, applications, and future perspectives. Trends in Food Science & Technology, 132, 171-187.

Tian, B., Liu, J., Yang, W., & Wan, J.-B. (2023). Biopolymer Food Packaging Films Incorporated with Essential Oils. Journal of Agricultural and Food Chemistry, 71(3), 1325-1347.

Wang, L., Yuan, M., Sun, E., Wu, J., Lv, A., Zhang, X., Guo, J., Zhu, Y., Guo, H., Li, X., & Wang, K. (2023). Antibacterial food packaging capable of sustained and unidirectional release carvacrol/thymol nanoemulsions for pork preservation. Food Hydrocolloids, 145, 109169.

Wang, T., & Su, E. (2024). Electrospinning meets food packaging: A promising pathway towards novel opportunities in food preservation. Food Packaging and Shelf Life, 41, 101234.

Wen, X., Zhang, D., Morton, J. D., Wang, S., Chai, X., Li, X., Yang, Q., Li, J., Yang, W., & Hou, C. (2024). Contribution of mono- and co-culture of Pseudomonas paralactis, Acinetobacter MN21 and Stenotrophomonas maltophilia to the spoilage of chill-stored lamb. Food Research International, 186, 114313.

Xu, J., He, M., Wei, C., Duan, M., Yu, S., Li, D., Zhong, W., Tong, C., Pang, J., & Wu, C. (2023). Konjac glucomannan films with Pickering emulsion stabilized by TEMPO-oxidized chitin nanocrystal for active food packaging. Food Hydrocolloids, 139, 108539.

Xue, W., Zhu, J., Sun, P., Yang, F., Wu, H., & Li, W. (2023). Permeability of biodegradable film comprising biopolymers derived from marine origin for food packaging application: A review. Trends in Food Science & Technology, 136, 295-307.

Yadav, P., Silvenius, F., Katajajuuri, J.-M., & Leinonen, I. (2024). Life cycle assessment of reusable plastic food packaging. Journal of Cleaner Production, 448, 141529.

Yang, Z., Zhang, D., & Cai, J. (2024). Robust design of starch composite nanofibrous films for active food packaging: Towards improved mechanical, antioxidant, and antibacterial properties. International Journal of Biological Macromolecules, 260, 129329.

Yao, Q.-b., Huang, F., Lu, Y.-h., Huang, J.-m., Ali, M., Jia, X.-Z., Zeng, X.-A., & Huang, Y.-y. (2024). Polysaccharide-based food packaging and intelligent packaging applications: A comprehensive review. Trends in Food Science & Technology, 147, 104390.

Yu, X., Li, X., Ma, S., Wang, Y., Zhu, W., & Wang, H. (2023). Biomass-Based, Interface Tunable, and Dual-Responsive Pickering Emulsions for Smart Release of Pesticides. Advanced Functional Materials, 33(27), 2214911.

Zhang, W., Ezati, P., Khan, A., Assadpour, E., Rhim, J.-W., & Jafari, S. M. (2023). Encapsulation and delivery systems of cinnamon essential oil for food preservation applications. Advances in Colloid and Interface Science, 318, 102965.

Zhang, W., Jiang, H., Rhim, J.-W., Cao, J., & Jiang, W. (2022). Effective strategies of sustained release and retention enhancement of essential oils in active food packaging films/coatings. Food Chemistry, 367, 130671.

Zhang, W., Roy, S., Ezati, P., Yang, D.-P., & Rhim, J.-W. (2023). Tannic acid: A green crosslinker for biopolymer-based food packaging films. Trends in Food Science & Technology, 136, 11-23.

Zhang, Y., Pu, Y., Jiang, H., Chen, L., Shen, C., Zhang, W., Cao, J., & Jiang, W. (2024). Improved sustained-release properties of ginger essential oil in a Pickering emulsion system incorporated in sodium alginate film and delayed postharvest senescence of mango fruits. Food Chemistry, 435, 137534.

Zhao, Q., Fan, L., Li, J., & Zhong, S. (2024). Pickering emulsions stabilized by biopolymer-based nanoparticles or hybrid particles for the development of food packaging films: A review. Food Hydrocolloids, 146, 109185.

Zheng, T., Tang, P., Yang, C., Ran, R., & Li, G. (2023). Development of active packaging films based on collagen/gallic acid-grafted chitosan incorporating with ε-polylysine for pork preservation. Food Hydrocolloids, 140, 108590.

Summary

In this work, a Janus structure multilayer antimicrobial packaging film is custom designed by layer-by-layer casting method, in which CEO-loaded PEs (prepared in chapter III) incorporated with CS served as inner loading layer of multilayer film, while zein film functioned as the outer barrier layer. The asymmetric multilayer structure is designed to regulate CEO release directionally, favoring inward diffusion toward the food surface, while maintaining a sustained release profile. These findings validated the hypothesis that regulating the CEO release behavior through PE integration and multilayer structuring could not only enhance antimicrobial efficacy but also significantly improve meat preservation performance. The successful extension of pork shelf life demonstrated the application potential of this strategy for perishable food packaging, aligning with the overarching goal of this dissertation to develop sustainable and functional controlled-release antimicrobial materials.

Chapter 5

Quercetin nanocrystals reinforced chitosan/polyvinyl alcohol/cinnamon essential oil-loaded Pickering emulsion film with enhanced mechanical and controlled-release antimicrobial properties for meat preservation

Short overview

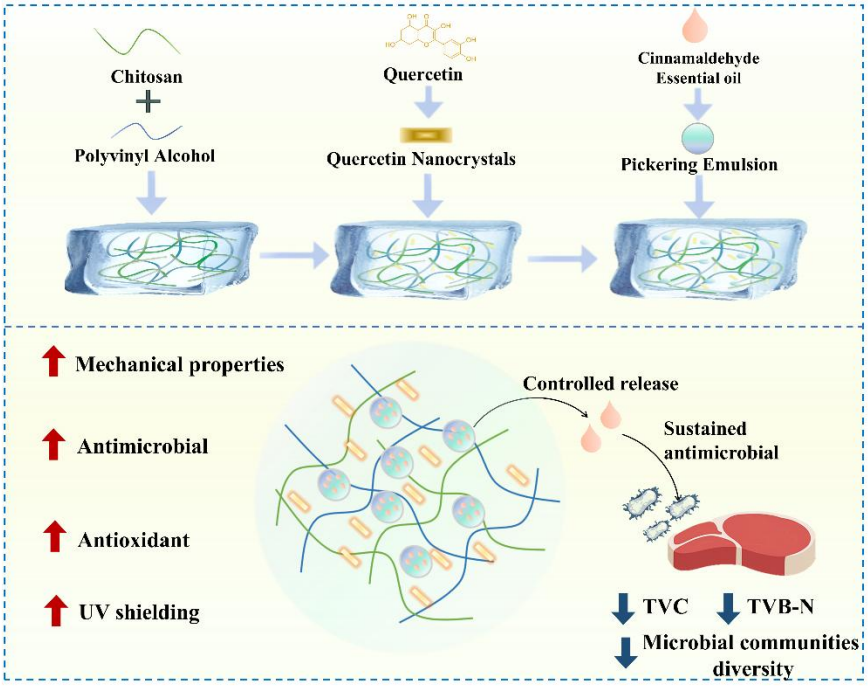

Graphical abstract: Quercetin nanocrystals reinforced chitosan/polyvinyl alcohol/cinnamon essential oil-loaded Pickering emulsion film with enhanced mechanical and controlled-release antimicrobial properties for meat preservation

The research content presented herein has been submitted to ***Food Packaging and Shelf Life*** and are presently under peer review for potential publication.

Abstract

Despite extensive efforts in developing bio-based active packaging, most current films still suffer from poor release kinetics of active ingredients. This study presents an innovative strategy to improve the controlled release performance of antimicrobial packaging film by incorporating cinnamon essential oil (CEO)-loaded Pickering emulsions as carriers and quercetin nanocrystals (QNs) as nanofillers into chitosan/polyvinyl alcohol (CS/PVA) composite film (PCE@QNs). Notably, the PCE@QNs film exhibited enhanced mechanical performance, with a tensile strength of 39.09 ± 0.46 MPa. This improvement was attributed to the strengthened internal hydrogen bonding network between QNs, CEO-loaded PE, and the CS/PVA matrix, as evidenced by FTIR, XRD, and TG analyses. Furthermore, PCE@QNs demonstrated remarkable antimicrobial activity (99.99% inhibition against food spoilage bacteria) and significantly enhanced antioxidant capacity (approximately five-fold increase). The incorporation of QNs effectively modulated the CEO release behavior, exhibiting a Fickian diffusion mechanism, thereby enhancing the potential for long-term antimicrobial efficacy. The controlled release antimicrobial characteristics of PCE@QNs render it highly effective for fresh meat preservation, extending shelf life to 11 days at 4°C. This work provides a promising strategy for designing controlled-release systems, contributing to the development of antimicrobial packaging films.

Keywords: Antimicrobial packaging; Chitosan/polyvinyl alcohol; Quercetin nanocrystals; Pickering emulsion; Meat preservation

1. Introduction

The spoilage of food caused by microbial activity presents critical concerns for both environmental sustainability and global food security. According to the Food and Agriculture Organization (FAO) of the United Nations, approximately one-third of all food produced globally is lost or wasted each year, of which an estimated 20% to 25% is attributed to microbial spoilage (Mather, Gilmour, Reid, & French, 2024; Parfitt, Croker, & Brockhaus, 2021). Fresh meat offers an ecosystem with high water content and nutrient availability for diverse microorganisms, which can then grow during storage. This microbial growth not only accelerates the deterioration of physicochemical and sensory qualities but also significantly increases the risk of foodborne illnesses. Consequently, the development of effective preservation strategies that suppress microbial proliferation while preserving the freshness and safety of fresh meat products has emerged as a critical focus within the food industry.

Antimicrobial packaging has been developed as an effective strategy to inhibit the growth of foodborne pathogens and spoilage microorganism in fresh meat products by incorporating active agents into packaging materials (Du, Sun, Chong, Yang, Zhu, & Wen, 2023; W. Zhang, Ezati, Khan, Assadpour, Rhim, & Jafari, 2023). Cinnamon essential oil (CEO), as a plant-derived active compound, exhibits potent antimicrobial properties and diverse bioactivities. It has been widely explored as an active agent in antimicrobial packaging to effectively inhibit the growth and proliferation of spoilage microorganisms in fresh meat. However, CEO is usually highly volatile and sensitive to various environmental factors, the direct incorporation of CEO into packaging materials often suffers from burst release and poor release kinetics, which limits antibacterial persistence and efficacy (Chang et al., 2022; Rojas, Misic et al., 2024). To improve the retention of CEO within CS/PVA composite film, CEO can be encapsulated within oil-in-water (O/W) Pickering emulsions (PEs) and subsequently incorporated into the packaging film (Cheng et al., 2024; Ji & Wang, 2025).However, although the incorporation of CEO-loaded PEs enables the protection of CEO, it also introduces hydrophobic phases and particle-laden interfaces into the film matrix (Fan, Yang, Zhu, Li, Richel, Fauconnier, et al., 2024). These structural disruptions can compromise the film's compactness and continuity, resulting in diminished mechanical performance (Wang, Yang, Liu, Zhou, Fu, Gu, et al., 2024). Moreover, CEO may diffuse more rapidly along structural defects, undermining the intended sustained-release function. These adverse effects significantly limit the practical application of CEO-loaded PEs in the field of food packaging. Given these challenges, reinforcing CEO-loaded PEs-based films with nanofillers represents a promising strategy to enhance film performance and modulate CEO release profiles of antimicrobial packaging systems.

Quercetin nanocrystals (QNs) are formed through the self-assembly of quercetin molecules into nanoscale crystalline particles with ultrafine particle size and high specific surface area. It is reported that these nanocrystals can be uniformly dispersed within the polymer matrix and establish strong intermolecular interactions with polymer chains, thereby enhancing the structural uniformity and compactness of the

film (Li et al., 2023). In addition, QNs exhibit potent antioxidant and antimicrobial properties (Guo, Luo, Wu, Zhang, Chen, Li, et al., 2024), making them particularly attractive as green multifunctional nanofillers for active food packaging systems. Despite their promising functionalities, the application of QNs in active packaging systems has been scarcely reported. In particular, their potential synergy with PEs for modulating the release behavior of CEO remains unexplored. We hypothesized that the uniform dispersion of QNs would restrict polymer chain mobility and reinforce the matrix through their rigid crystalline structure and high aspect ratio, thereby stabilizing the network architecture of CEO-loaded PEs-based films, enhancing mechanical and ultimately facilitating sustained release of CEO.

In this work, a CEO-loaded PEs/chitosan (CS) /polyvinyl alcohol (PVA) composite film reinforced with QNs (referred to PCE@QNs) was fabricated via a stepwise assembly method (Scheme 1). The effects of incorporating QNs and CEO-loaded PEs on the physicochemical properties of the CS/PVA composites film, including mechanical, optical, barrier, antimicrobial and antioxidant properties were systematically evaluated. Furthermore, the preservation efficacy of PCE@QNs for fresh meat was investigated, and potential preservation mechanisms were analyzed based on microbial community dynamics. To the best of our knowledge, this is the first research to employ green nanofillers QNs to achieve both improvement in mechanical properties of CEO-loaded PEs-based films and sustained release of CEO. This work provides a new approach to engineering sustainable and high-performance antimicrobial packaging films with enhanced controlled release, offering potential applications in extending the shelf life of perishable foods.

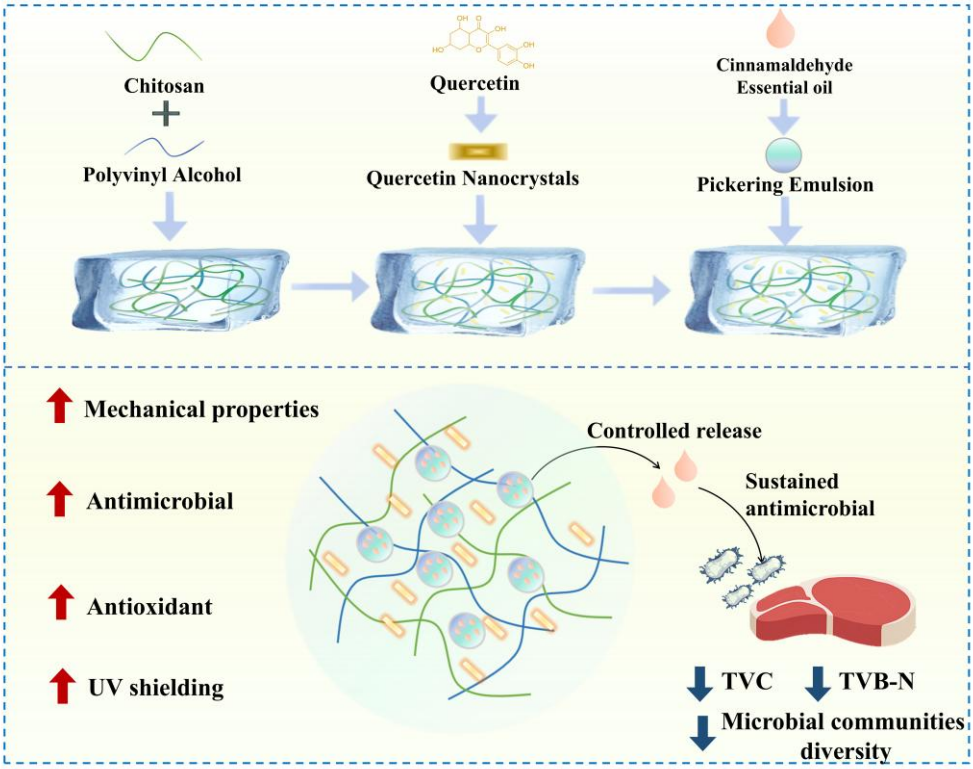

Figure 5-1 Schematic illustration for synthesis of quercetin nanocrystals enhanced chitosan/polyvinyl alcohol/CEO-loaded Pickering emulsion composite films (PCE@QNs) based on stepwise assembly method.

2. Experimental section

2.1. Materials

Quercetin (97%) was procured from Shanghai yuanye Bio-Technology Co., LTD., PVA (Mw31000-50000, alcoholysis degree 98-99%), CS (deacetylation degree ⩾ 95%) and glycerol were obtained from Shanghai Macklin Biochemical Technology Co., LTD. 1,1-diphenyl-2-picrylhydrazyl (DPPH, 97%), 2,2'-Azinobis- (3-ethylbenzthiazoline-6- sulphonate) (ABTS) were procured from Shanghai yuanye Bio-Technology Co., LTD. *P. paralactis* MN10, *A. pullicarnis* MN21, and *L. sakei* VMR17 were sourced from Prof. Zhang's lab (Institute of Food Science and Technology, Beijing, China). Lysogeny broth (LB) was purchased from Beijing Land Bridge Technology Co., LTD. Ethanol absolute, acetic acid and other chemical reagents were supplied by Beijing Sinopharm Chemical Reagent Co., Ltd., the reagents used in this work were all analytical grade unless explicitly stated otherwise.

2.2. Preparation of QNs

QNs were prepared using ultrasonic-assisted antisolvent crystallization method, following the procedure described in literature (Li, et al., 2023) with some modifications. QNs were prepared using ultrasonic-assisted antisolvent crystallization method, following the procedure described in literature (Li et al., 2023) with some modifications. First, a quercetin solution (20 mg/mL) was prepared by dissolving quercetin powder in anhydrous ethanol. The quercetin solution was then added dropwise to nine times its volume of pre-chilled ultrapure water, with the assistance of ultrasonic (power: 45 W). The quercetin nanocrystal suspension (2 mg/mL) was obtained by facilitating crystallization in an ice bath. QNs subjected to ultrasonic treatment for 30, 60 or 120 min were labeled QNs-30 min, QNs-60 min and QNs-120 min, respectively.

2.3. Characterization of QNs

2.3.1. Particle size and Zeta potential

The Particle size and Zeta potential of QNs in solution were measured using Zetasizer Nano ZS (Malvern Instruments Inc., Malvern, UK). Before measurement, the QNs suspension was diluter 10-fold with ultrapure water.

2.3.2. Microscopic morphology and structure

The microtopography of QNs was observed by Scanning electron microscope (SEM, SU 1510 Hitachi, Japan) and Transmission electron microscope (TEM, H 7500, Hitachi, Japan), respectively. The infrared spectra of QNs were determined using Tensor 27 FTIR spectroscopy (Bruker, Germany) at the range of 400-4000 cm-1. The XRD patterns of QNs were recorded using Ultima Ⅳ X-ray diffractometer (Rigaku, Japan). The UV-vis and fluorescence spectra of QNs were recorded using UV-6000PC (Shanghai Metash Instruments Co., Ltd., Shanghai, China) and F-2500 spectrofluorometer (Hitachi, Japan), respectively.

2.3.3. Antimicrobial and antioxidant activities

The spoilage bacteria of *P. paralactis* MN10, *A. pullicarnis* MN21, and *L. sakei* VMR17 were stored in our lab and selected as test strains for antimicrobial experiments of QNs. A 100 μL bacterial suspension (approximately 10^6 CFU/mL) was added into 1 mL QNs suspension and co-incubated for 12 h at 30℃. Subsequently, 100 μL resulting mixture was diluted and spread onto LB agar plates, followed by incubation at 30 ℃ for 12 h, after which the plates were photographed. For antioxidant test, 10 μL QNs suspension was mixed with 190 μL DPPH work solution (0.1 mM DPPH-ethanol solution) and 190 μL ABTS work solution (7.4 mM ABTS-water solution and 2.6 mM $K_2S_2O_8$-water solution), respectively. After reaction in dark (30 min for DPPH mixed solution, 6 min for ABTS mixed solution), the UV-vis spectra of different system were recorded at 400-800 nm.

2.4. Preparation of PCE@QNs

The PCE@QNs were fabricated using a step-by-step assembly method. CS power was dissolved in acetic acid aqueous solution (2%, v/v) at 50 ℃ and PVA power was

dissolved in ultrapure water at 90 ℃, respectively. After complete dissolution, the 1.5 wt% CS solution was mixed with an isovolumetric 2 wt% PVA solution. Then, 30 wt % (based on the solid weight) glycerol was added to form film-forming solution. The PE loaded with CEO were prepared as our previously described methods (Fan, Yang, Wang, et al., 2024; Fan, Yang, Zhu, et al., 2024). Subsequently, 10% (v/v) of QNs-60 min QNs suspension and 10% (v/v) CEO-loaded PEs were blended into CS/ PVA film-forming solution, respectively. After stirred for 2 h, 20 mL mixture was cast into a 90 mm Petri dish and dried at 50°C for 12 h, resulting in films named PC@QNs and PCE, respectively. To obtain PCE@QNs films, 10% (v/v) of QNs-60 min QNs suspension and 10% CEO loaded PEs were blended into CS/PVA film-forming solution, simultaneously. Before further characterization, all films were equilibrated in a 50% relative humidity environment for 48 h.

2.5. Characterization of PCE@QNs

2.5.1. Microscopic morphology and structure

The microstructures of the films including surface and cross-sectional were examined using a SEM (SU 1510 Hitachi, Japan). The cross-sectional parts of films were obtained under liquid nitrogen embrittlement. Microscopic morphology and structure. Infrared spectroscopy (Tensor 27, Bruker, Germany) was utilized to record the chemical structure and potential interactions of films. X-ray diffractometer (Ultima Ⅳ, Rigaku, Japan) was employed to determine the XRD pattern of the films at 5-60° . Thermogravimetric analyzer (Pyris Diamond, New Castle, USA) was employed to monitoring thermal degradation of films. The film samples were heated at a rate of 10℃/min in the range of 30-500℃ under nitrogen atmosphere.

2.5.2. Physicomechanical properties

The mechanical properties of films including tensile strength (TS) and elongation at break (EAB) were tested according to our previous procedure (Fan, et al., 2023). Film samples with uniform thickness and smooth surfaces were selected for measurement.

Water sensitivity. The water contact angle (WCA) of films was tested using SZ-CAMC32 contact angle analyzer (Shanghai Xuanjun Instrument Co., LTD, China). For the water content, swelling rate and water solubility evaluations, films (20×20 mm) were initially weighed (m_0) and then dried at 105℃ for 24 h before being weighed again (m_1). The dried films were exposed to 30 mL ultrapure for 24 h and weighed (m_2) without residual water on the surface. Then, the films were completely dried at 105℃ for 24 h and weighed again (m_3). The water content, swelling rate and water solubility were calculated as Eqs. (5.2.1), (5.2.2) and (5.2.3):

$$\text{Water content (\%)} = (m_0-m_1)/m_0\times100 \quad (5.2.1)$$

$$\text{Swelling rate (\%)} = (m_2-m_1)/m_1\times100 \quad (5.2.2)$$

$$\text{Water solubility (\%)} = (m_1-m_3)/m_1\times100 \quad (5.2.3)$$

The water vapor permeability (WVP) of the films was measured according to the methods described by Dong et al. (2024) with slight modifications. In brief, the films were cut into 20×20 mm strips and sealed on top of centrifuge tubes (50 mL vertical)

with 20.0 ± 0.5 g anhydrous silica gels. Then, the samples were incubated in a desiccator with saturated NaCl solution (75% ± 2% relative humidity) at 25℃ for 48 h. WVP was calculated with the following Eq. (5.2.4):

$$\text{WVP } (10^{-12}\text{ g/m s Pa}) = \frac{\Delta m \times e}{t \times A \times \Delta p} \qquad (5.2.4)$$

where Δm (g) is the gain in weight of the centrifuge tube; e is the thickness of the film (m); t is the incubation time (s); A (m^2) is the area of the centrifuge tube; and Δp (Pa) is the saturation vapor pressure of water. Nine parallels were used for each film.

2.5.3. Optical and ammonia response properties

A UV-visible spectrophotometer (UV-6000PC, Metash, China) was employed to record the UV shielding properties and optical properties through a previously reported method (Jiang, Zhao, Li, Chen, Mo, & Liu, 2024). The transparency of films was calculated according to the following Eq. (5.2.5):

$$\text{Transparency} = -(\log T_{600})/x \qquad (5.2.5)$$

Where T_{600} is the transmittance at 600 nm, and x represents the film thickness (mm).

The ammonia sensitivity was evaluated with the reference to the method of Wang et al. (2024) with some modifications. In brief, films were exposed to 1 mL ammonia solution (30%, v/v) in a sealed Petri dish for 30 min. The visible color change of films was recorded by a smartphone.

2.5.4. Antimicrobial and antioxidant properties

The antimicrobial activity of films was evaluated against *P. paralactis* MN10, *A. pullicarnis* MN21, and *L. sakei* VMR17 based on the method described by Ma et al. (2023). The antioxidant capacity of films was determined according to the produce of literature (Qin, Zou, Hou, Wu, Loy, & Lin, 2024) with some modifications. A 100 μL bacteria solution (approximately 10^6 CFU/mL) was dripped on surface of film (20 × 20 mm) and culture at 30°C for 2 h, then 9.9 mL LB liquid medium was added for further 2 h culturation. A 100 μL above suspension was evenly spread onto an LB agar plate and incubated at 30°C for 24 hours. The antimicrobial activity was calculated using the following Eq. (5.2.6):

$$\text{Antimicrobial activity } (\%) = \frac{S1-S2}{S1} \times 100 \qquad (5.2.6)$$

where S_1 and S_2 are the bacterial colony counting for the control and film groups, respectively.

The antioxidant capacity of films was determined according to the produce of literature (Qin et al., 2024) with some modifications. 0.2 g of film sample was soaked in 5 mL of 95% ethanol solution for 12 h. A 10 μL of above solution was mixed with 190 μL ABTS work solution (Equal proportion of 7.4 mM ABTS-water solution and 2.6 mM K2S2O8-water solution were reacted in the dark for 12 h), after incubated in darkness for 30 min, the absorbance of mixture was determined at 734 nm. The ABTS radical scavenging activity was calculated with the following Eq. (5.2.7):

$$\text{ABTS radical scavenging activity } (\%) = \left(1 - \frac{A1-A0}{A}\right) \times 100 \qquad \text{Eq. (5.2.7)}$$

Where A_1 is the absorbance of the film sample group, A_0 is the absorbance of the blank group, A is the absorbance of the control group.

For DPPH radical scavenging, 10 μL of film sample solution was mixed with 190 μL DPPH solution (0.1 mM), and the absorbance of the mixture was determined at 517 nm. The DPPH radical scavenging activity was calculated with the following Eq. (5.2.8):

$$\text{DPPH radical scavenging activity (\%)} = (1 - \frac{A1 - A0}{A}) \times 100 \quad (5.2.8)$$

Where A_1 is the absorbance of the film sample group, A_0 is the absorbance of the blank group, A is the absorbance of the control group.

2.5.5. Release kinetics

The release behavior of films was evaluated according to the method described by Zhu et al (2025). A 50% ethanol and 95% ethanol solutions were selected as food simulants to represent semi-fatty and fatty foods, respectively. A 5×5 cm film was dipped into 20 mL food simulants for 120 h with slight continuous shaking at 25 °C. At the selected time points, 100 μL of the solution was taken to measure the absorbance at 287 nm. The concentration of CEO in the solution system was periodically quantified based on a previously established standard curve. To describe the mass transfer mechanism, the cumulative release profile data were fitted to various kinetic release models, including zero-order, first-order, Higuchi, and Ritger-Peppas models (Fan, Yang, Zhu, et al., 2024).

2.5.6. Biodegradability test

Biodegradability of films was tested referring to the method of literature (Yue, Wang, Zhou, You, Wang, & Wu, 2024). The film samples were buried in a plastic container with nutrient soil. The morphology of film samples was recorded every 7 days.

2.6. Application in meat preservation

2.6.1. Treatment of meat

Pork was selected as the model meat due to its high perishability and widespread consumption, making it suitable for evaluating the effectiveness of antimicrobial packaging. The fresh longissimus dorsi muscle of pork was used in the preservation experiment, which was purchased from Beijing Ershang Meat Food Group Co., LTD (Beijing, China) and transported to lab within sterile sampling bags. The fresh pork was cut into cuboids (50 ± 5 g) and placed in a Polypropylene package (3×3×6 cm) and covered with resulted film and Polyethylene film as a control. The packaged meat was storage in a refrigerator at 4℃.

2.6.2. Sensory evaluation

A sensory analysis group containing 8 trained panelists aged between 24-30 years, was employed to evaluated the quality of meat. The items of sensory evaluation involved overall acceptability, odor, appearance and texture, which were scored via 10-point scale. All assessments were conducted under controlled conditions following standard sensory evaluation protocols. The results were presented as the mean values; lower score indicated a decrease in the freshness of the meat.

2.6.3. Total viable count (TVC) and total volatile basic nitrogen analysis (TVB-N)

The TVC and TVB-N were determined strictly according to the China National Standards, GB4789.2-2016 and GB 5009.228-2016, respectively.

2.6.4. Microbial diversity analysis

The pork samples packaged with different films were taken in a sterile environment for microbial diversity analysis according to the procedure of wen et al. (2022). Total microbial DNA was extracted using the E.Z.N.A.® soil DNA Kit (Omega Bio-tek, Norcross, GA, USA) following manufacturer's instruction and checked by 1% agarose gel electrophoresis experiments. The V3-V4 region of the 16S rRNA were employed for PCR amplification. Afterward, the Majorbio Bio-pharm Technology Co., Ltd. (Shanghai, China) provided sequencing procedures of samples utilized the Illumina MiSeq platform. The raw sequencing data was processed using UPARSE (version 11) to cluster operational taxonomic units (OTUs) at 97% similarity level.

2.7. Statistical analysis

The experiments were conducted in triplicate unless otherwise specified, and the results were expressed as mean ± standard deviation (SD). The one-way analysis of variance (ANOVA) and Tukey's test were evaluated using SPSS 26.0 (SPSS Inc, Chicago, USA) under a 95% confidence interval.

3. Results and discussion

3.1. Preparation and characterization of the QNs

Quercetin's poor water solubility restricts its application in active packaging. A promising approach to address this limitation is the fabrication of aqueous QNs, which leverages the aggregation behavior through supramolecular interaction forces to enhance solubility and improve functional integration into packaging materials (Guo, et al., 2024; W. Zhao, Li, He, Li, Aryal, Fabiilli, et al., 2024). This study began with the preparation of QNs using an anti-solvent crystallization technique assisted by ultrasound. Figure 5-1A and B illustrate the particle size distribution and Zeta potential of the QNs. The ultrasonic treatment durations (30 min, 60 min, and 120 min) were varied as experimental factors. As the ultrasonic treatment time increased, the particle size of the QNs decreased, while the absolute value of the Zeta potential increased from -18.00±0.16 mV to -14.90±0.22 mV. Particle size and Zeta potential were the critical attributes of nanocrystals (Madane & Ranade, 2022). The larger particle size and lower absolute Zeta potential of QNs suggested that prolonged ultrasonic treatment negatively impacted their dispersion. Thus, the time scale of crystallization of QNs synthetic was 60 min for the following film-forming experiment. The SEM and TEM images (Figure 5-2C and D) revealed that QNs exhibited a monodispersed rod-like morphology, Li et al. (2023) also obtained similar results. The FTIR spectra of a series of QNs were investigated to determine the structure of quercetin after anti-solvent crystallization (Figure 5-2E). Compared to raw quercetin, the FTIR spectra of all QNs were almost similar. There were no changes of characteristic peaks had observed at 1640 cm^{-1}, 1530 cm^{-1} and 1384 cm^{-1}, which were attributed to carbonyl groups, aromatic rings and phenolic hydroxyl groups, respectively. This result indicated that the essential functional groups of

quercetin were preserved. In addition, the crystalline peaks presented in XRD patterns (Figure 5-2F) indicated the high crystalline structure, particularly correlative sharp characteristic peaks at 25.5° (Cao, Feng, Meng, Li, & Wang, 2020). These results confirm the successful preparation of QNs.

Figure 5-2G shows that the intensity of characteristic peak at 320-385 nm, B-ring cinnamoyl systems of quercetin molecules, had an increase. It could be explained as the weak molecular interactions during the preparation of QNs. It has been reported that quercetin exhibits an aggregation-induced emission (AIE) effect (He, Niu, Chen, Li, Liu, & Li, 2018), which is highly emissive in aggregated state.

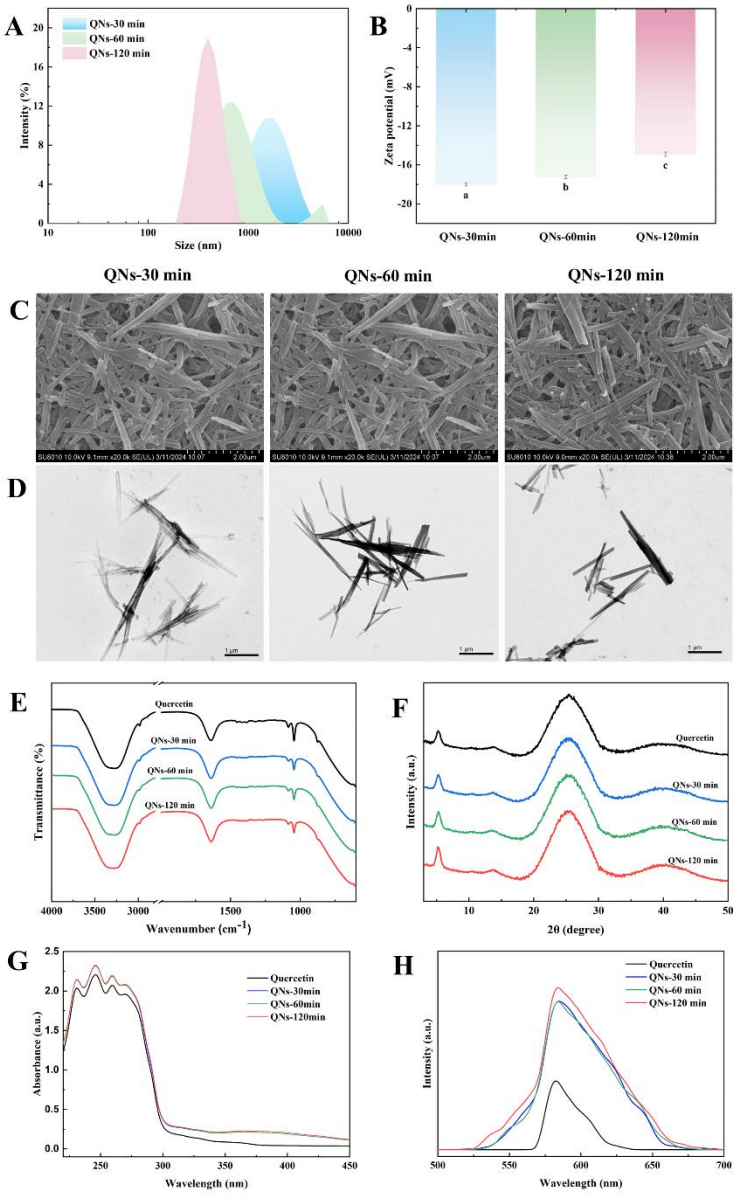

Figure 5-2 Characterization of the quercetin nanocrystals (QNs). Particle size distribution (A) and Zeta potential (B) of QNs in solution system. Morphology images of QNs observed by scanning electron microscope (C) and transmission electron microscope(D). FTIR spectra (E), XRD spectra (F), UV–vis absorption spectra (G) and fluorescence spectra (H) of QNs.

The enhanced keto emission (AIE fluorescence) of QNs has been confirmed in Figure 5-2h. In addition, the pH-responsive characteristics of QNs in aqueous solution

were investigated in both colorimetric and fluorescent modes (Figure 5-3A and B). The color under the natural light of QNs suspension changed from light yellow to deep orange as the pH value of the system increased. This was similar to the phenomenon observed by Jiang et al. (2024) in the raw quercetin system. Meanwhile, the fluorescence under λ=365 nm of QNs was enhanced. The molecular structure of quercetin contains multiple phenolic hydroxyl groups and carbonyl groups, these functional groups can interact with H^+ or OH^- in the system, leading to changes in the absorption spectrum (Figure 5-3C). This directly influences the color observed by our naked eye. This phenomenon of enhanced fluorescence emission could be attributed to undergo deprotonation of phenolic hydroxyl groups with increasing pH (Figure 5-3D-F), which restricted intramolecular motions (Zhou & Han, 2022).

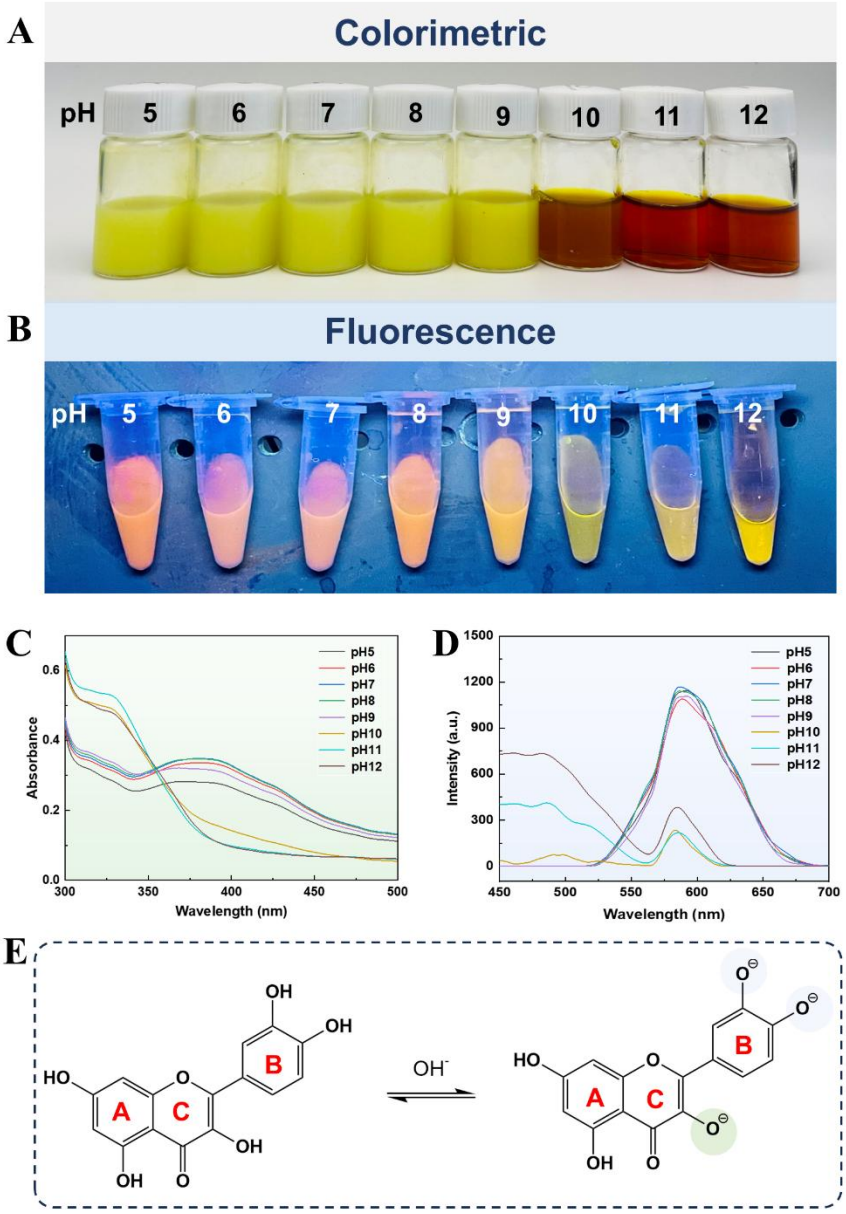

Figure 5-3 Colorimetric (A) and fluorescence (B) images, UV-vis (C) and fluorescence spectra (D) of QNs at different pH environments (5, 6, 7, 8, 9, 10, 11, 12).

3.2. Antimicrobial and antioxidant activity of the QNs

The antimicrobial activities of quercetin and QNs against spoilage bacteria were assessed using the agar-plate method. As shown in Figure 5-4A, compared to the blank group, the number of colonies on the plates treated with quercetin was significantly reduced, indicating a clear inhibitory effect of quercetin on all three tested bacterial strains. Meanwhile, it was observed interestingly that there was almost no colony growth on the plates of QNs treated groups, including groups of QNs-30 min, QNs-60 min and QNs-120 min, which could be attributed to the strong attachment and high barrier permeation capable of the QNs (Guo, et al., 2024; Lai, Schlich, Pireddu, Fadda, & Sinico, 2019). In addition, ABTS and DPPH free radical scavenging assay was employed to evaluate the antioxidant activity of the QNs. Activated ABTS+ free radical exhibited characteristic absorption peaks at 734 nm. The presence of antioxidants (quercetin and QNs) suppressed the formation of ABTS+, leading to a decrease in absorbance at the characteristic peak (Figure 5-4B). The disappearance of characteristic absorption peak at 517 nm represented that DPPH free radical was scavenged and converted into a covalent structure (Figure 5-4C). This observation indicated the potent antioxidant effects of QNs.

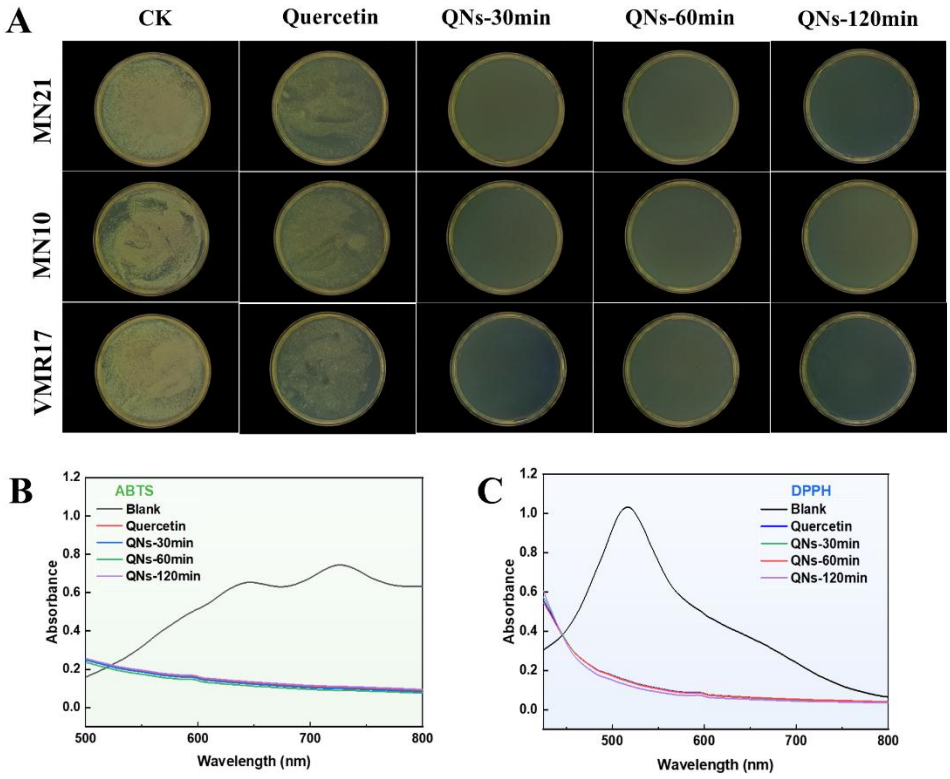

Figure 5-4 Antimicrobial properties of quercetin nanocrystals (QNs) against spoilage bacteria *P. paralactis* MN10, *A. pullicarnis* MN21, and *L. sakei* VMR17 (A). Antioxidant activities of QNs, the abilities to scavenge ABTS radical (B) and DPPH radical (C).

3.3. Preparation and structural characterization of the PCE@QNs

In this work, the multifunctionality of the film was highlighted and developed. Specifically, the biodegradable composite polymer CS/PVA served as the film base matrix, functionalized with nanostructured QNs and CEO-loaded PE through a stepwise assembly method (Figure 5-5A). The microstructure of the films including surface and cross section was observed using SEM (Figure 5-5B). The surface of pure CS/PVA composite film (PC) was smooth and uniform, whereas the surfaces of CS/PVA composite films containing QNs (PC@QNs), CS/PVA composite films containing CEO-loaded PE (PCE), and CS/PVA composite films functionalized with nanostructured QNs and CEO-loaded PE (PCE@QNs) exhibited varying degrees of particle protrusions. A layered structure was observed in the cross-section of the PC@QNs, which may be related to the self-assembly of molecules arranged in parallel. At the same time, the addition of QNs kept the order of molecules, which made the arrangement more compact. However, some aggregations were observed in the cross section of the PCE@QNs, which could be explained that the QNs adsorb onto the surface of the PE droplets. The FTIR spectra of films were depicted in Figure 5-5C to investigate the structural change of films. An obviously strengthened of characteristic absorption peak of PC@QNs was occurred around 3300 cm^{-1}, attribute to the absorption of the phenolic hydroxyl group of QNs molecules. Furthermore, the characteristic peak at this wavenumber became broadened with the addition of CEO-loaded PE, indicating that more hydrogen bonds were formed. The overlapping vibration frequencies of these hydrogen bonds, which involved both strong and weak hydrogen bonds, resulted in a broader absorption peak. X-ray diffractometer was employed to evolute the crystal structure of films and results were presented in Figure 5-5D. All films exhibited obvious characteristic peaks at $2\theta=19.9°$, attributed to the semi-crystalline PVA. This characteristic peak of PC@QNs was enhanced, it might be related to the increased of preferred orientation after doping with QNs. However, the opposite result was observed after the incorporation of the CEO-loaded PE. The decrease in crystallinity could enhance the flexibility of molecule chain, which was beneficial for packaging applications (Huie Jiang, Zhao, Li, Chen, Mo, & Liu, 2024). The thermodynamic stability of films was measured using the TG and DTG curves (Figure 5-5E and F). The weight loss occurred in four main stages, PC, PC@QNs, PCE and PCE@QNs showed a quite similar trend. The mass loss of initial stage (about 35-130°C) and second stage (about 130-245°C) involved moisture volatilization and degradation of glycerol in the film, respectively. Thermally degraded occurred in 245-360°C was mainly related to the deterioration of CS and PVA molecular chains. Finally, the residual mass at 550°C indicated the simultaneous decomposition of CS, PVA, QNs and other substances.

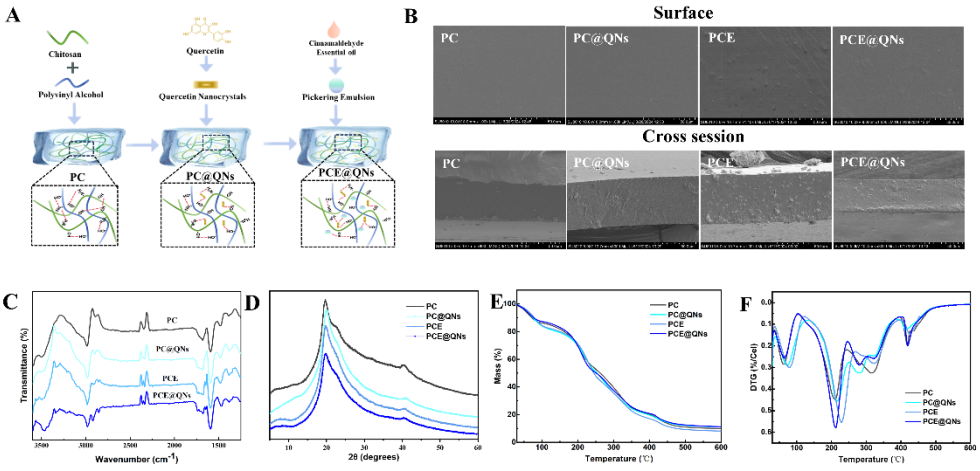

Figure 5-5 Schematic illustration of quercetin nanocrystals enhanced chitosan/polyvinyl alcohol/CEO-loaded Pickering emulsion composite films (PCE@QNs) based on stepwise assembly method (A). Characterization of the PCE@QNs; scanning electron microscopy (SEM) images of films, including surface and cross-section morphologies (B) FTIR spectra (C), XRD spectra (D), thermogravimetric curve of films (E) and derivative thermogravimetric curve of films (F).

3.4. Physicomechanical characterization of the PCE@QNs

Mechanical property is a critical indicator for evaluating the applicability of food packaging materials. Here, the effects of varying amounts of QNs and PE on the mechanical properties of film were investigated. The TS and EAB of neat PC film were 30.92±0.84 MPa and 113.71±2.17%, respectively. With the content of QNs increased, TS values showed a gradual increase trend (Figure 5-6A), PCE1@QNs2 film showed the maximum value was 39.09±0.46 MPa, and the TS value was no statistically significant differences with PCE1@QNs3. A similar result was observed by Li et al. (2023) in flavanols nanocrystals enhanced PVA/carrageenan films. However, increasing the PE content resulted in a decrease in both TS and EAB (Figure 5-6B), which could be explained that the integrity of the film was disrupted by higher emulsion additions (Almasi, Azizi, & Amjadi, 2020; J.-D. Wang, Yang, Liu, Zhou, Fu, Gu, et al., 2024). This negative impact on the mechanical properties could be mitigated by enhancing the high density of the polymer network. In this work, QNs and CS/PVA molecules formed a compact structure through extensive hydrogen bond cross-linking (Figure 5-6C), which reduced the slippage and displacement between molecular chains. The improved TS of films emphasized the great value in application of QNs as nanofillers. It is important to highlight that the mechanical properties of the films developed in this study significantly surpass those of other emulsion films loaded with essential oil (X. Chen, Lan, & Xie, 2024; Fan, et al., 2023; Xia, et al.,

2023; Xu, Jia, Li, Sun, Cai, Wu, et al., 2024; Yu, Gong, Wang, Wang, Liu, Huang, et al., 2024) (Figure 5-6D).

The assessment of water sensitivity is crucial for evaluating the stability and reliability of packaging materials in practical applications. Water sensitivity was evaluated by testing WC, WS, SR and WCA of films, part of the results was displayed in Table 5-1. The MC values of PCE was measured at 23.81±0.39%, significantly lower than that of pure PC (28.46 ± 0.55%). This reduction can be attributed to the incorporation of CEO-loaded PE, which diminishes the moisture absorption of PC due to the inherently hydrophobic properties of CEO. However, no significant changes in the WC values of PCE@QNs were observed. PCE@QNs films exhibited the lowest WS value of 18.47 ± 1.00% (Table 5.1) and SR value of 49.20 ± 1.60% (Figure 5-6E), indicating that the synergistic interaction of QNs and CEO-loaded PE not only enhanced the film's resistance to water dissolution but also strengthened the structural stability of the films in aqueous environments (D. Wang, Fan, Li, Chen, Wen, Xu, et al., 2024). Additionally, the observed increase in the WCA results (Figure 5-6F) further substantiates the aforementioned perspective, indicating that the specific interactions between QNs and CEO-loaded PE could influence the surface characteristics of PCE@QNs.

Table 5-1 Water content (WC), water solubility (WS) and transparency of quercetin nanocrystals enhanced chitosan/polyvinyl alcohol/CEO loaded Pickering emulsion composite films (PCE@QNs).

	WC (%)	WS (%)	Transparency
PC	28.46±0.55^{a}	24.65±0.93^{a}	1.98±0.01^{c}
PC@QNs	22.43±0.39^{b}	19.99±0.66^{b}	2.90±0.02^{b}
PCE	23.81±0.96^{b}	19.67±0.77^{b}	3.22±0.06^{a}
PCE@QNs	21.88±1.05^{b}	18.47±1.00^{b}	3.30±0.03^{a}

The values were shown as mean±standard deviation (SD). Different letters represent significant differences.

Water vapor permeability (WVP) of packaging film was the dominant factor in preventing moisture damage (Huang, Ren, Zhong, Olah, Li, Baer, et al., 2023). The WVP of PCE@QNs films was found to be significantly lower than that of PC, but no observable difference between PC@QNs and PCE (Figure 5-6G), indicating the improvement in water vapor barrier properties of films. QNs effectively fill the material's pores via nanoscale dimensions, thereby reducing the diffusion pathways for water vapor. Concurrently, the CEO-loaded PE impedes water vapor penetration through the hydrophobic nature of CEO. These mechanisms synergistically form a dense physical barrier, significantly enhancing the water vapor barrier properties of film.

Overall, the observed improvements in water sensitivity demonstrated the potential of films for applications requiring enhanced moisture resistance.

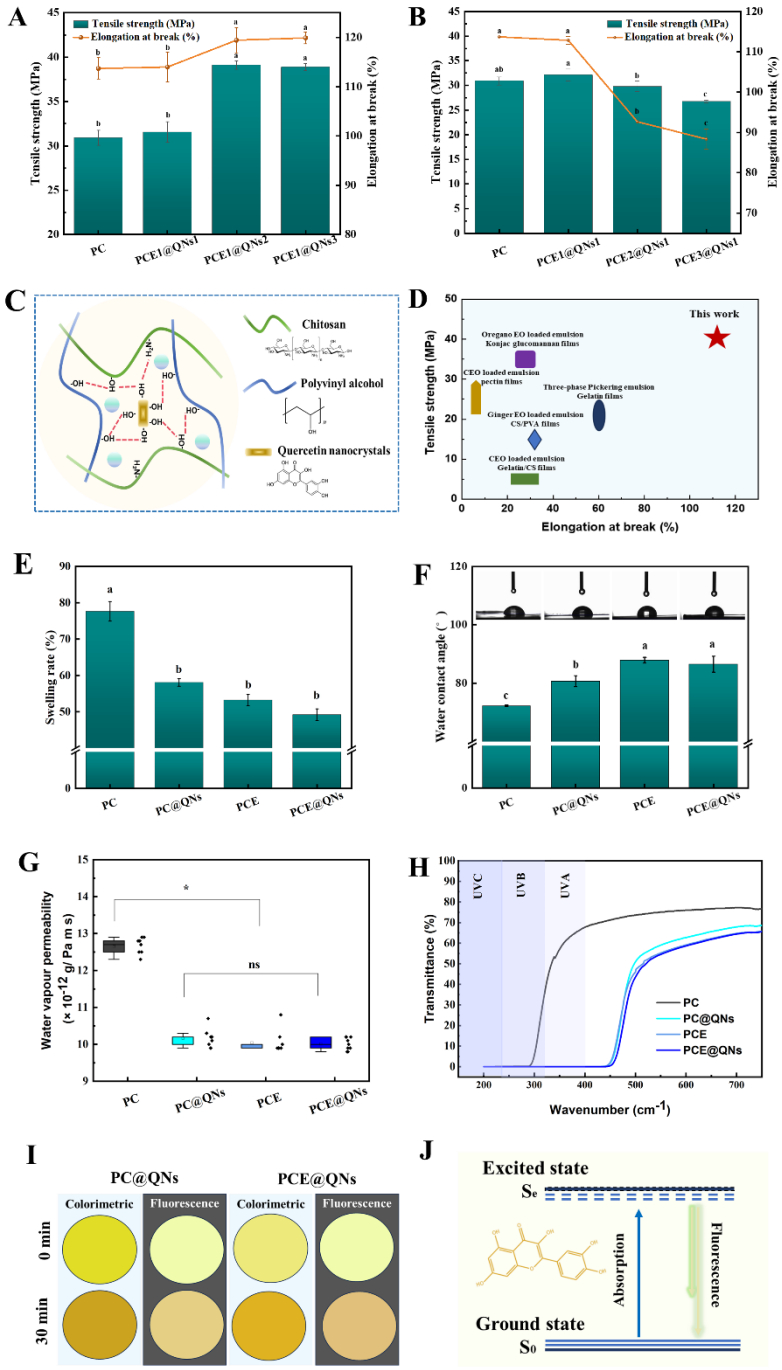

Figure 5-6 Mechanical properties of the quercetin nanocrystals enhanced chitosan/polyvinyl alcohol/CEO loaded-Pickering emulsion composite films (PCE@QNs),

tensile strength and elongation at break of films with different QNs concentrations (A) and CEO-loaded Pickering emulsion addition levels (B). The 5%, 10%, and 15% (v/v) addition level of QNs were labeled as Q1, Q2, and Q3; the 5%, 10%, and 15% (v/v) addition level of CEO-loaded Pickering emulsion were labeled as E1, E2, and E3. Schematic diagram of the internal cross-linking structure of PCE@QNs (C). Comparison of the mechanical properties for PCE@QNs compared with other essential oils loaded Pickering emulsion films (D). Water sensitivity of PCE@QNs, swelling rate (E), water contact angle (F) and water vapor permeability (G). Optical properties of PCE@QNs assessed by measuring their transmittance across a wavelength range of 200 to 800 nm (H). Colorimetric and fluorescence dual-mode response of PCE@QNs to volatile ammonia (I) and mechanism of fluorescence in PCE@QNs (J).

The optical properties of films were assessed by measuring their transmittance across a wavelength range of 200 to 800 nm (Fan, Yang, Zhu, Li, Richel, Fauconnier, et al., 2024). Transparency quantifies the extent to which the human eye (sensitive to 600 nm light) perceives the clarity of a film (Huie, et al., 2023). Although the transparency of PCE@QNs was higher than that of PC and PC@QNs (Table 5-1), it still had excellent optical acceptability. Figure 5-6h depicted the UV-shielding properties of films intuitively. UVA (320–400 nm) and UVB (280–320 nm) irradiation had negative effects on food, particularly those with high fat content (Y. Zhang & Jiang, 2023). The barrier of the PCE@QNs to ultraviolet light (280–400 nm) was almost 100 %, indicating a strong UV-shielding capacity of PCE@QNs. This can be mainly attributed to the UV absorption ability of quercetin and reductive aldehyde group of CEOs. The results of optical properties showed that the PCE@QNs had significant protective effects on food when used as UV protection packaging film.

3.5. Dual-mode response of volatile ammonia

Biogenic amines are commonly produced during protein degradation in the meat spoilage process, leading to the formation of an alkaline environment within the food packaging (Gu, Li, Chen, Li, Xiao, Zhang, et al., 2023). The response of PCE@QNs film to alkaline environment was investigated using volatile ammonia to simulate the release of biogenic amines compounds and evaluate the application potential of intelligent packaging. As shown in Figure 5-6I, the PCE@QNs films undergo obvious changes from light yellow to tawny with an increase in the exposure time. In addition, a noticeable change in fluorescence color was observed. Figure 5-6J illustrated the fluorescence mechanism of PCE@QNs, the intramolecular electronic energy level of quercetin transition from the ground state (S0) to the unstable excited singlet state (Se) under the promotion of UV light, the energy was released, manifesting as a yellow-green fluorescence due to the excited state intramolecular proton transfer (ESIPT) process, and this fluorescence phenomenon becomes more pronounced in its aggregated state (QNs) (Tong, Shi, Tong, Shi, Ali, & Guo, 2021). It should be noted that only slight differences in colorimetric and fluorescence color changes between PC@QNs and PCE@QNs, confirmed that the Pickering emulsion has minimal impact on the color changes of films. This result indicated that PCE@QNs has a high

sensitivity to volatile ammonia response in both colorimetric and fluorescent modes and considerate as an excellent candidate for intelligent packaging applications.

3.6. Antimicrobial and antioxidant activity of the PCE@QNs

The rapid proliferation of spoilage microorganisms is a primary factor contributing to the reduced shelf life of food. The antibacterial effectiveness of prepared films was tested against representative spoilage bacteria of *A. pullicarnis* MN21 (Gram-negative), *P. paralactis* MN10 (Gram-negative) and *L. sakei* VMR17 (Gram-positive). As shown in Figure 5-7A, it was observed that no colony-forming units on the agar plates of MN10, MN21, and VMR17 after treatment with the PCE@QNs film, indicating the excellent in vitro antibacterial performance of PCE@QNs film. Subsequently, the inhibition capacity of the films was calculated (Figure 5-7B). The antimicrobial efficacy of both PCE and PCE@QNs against the three tested bacterial strains was observed to approach 100%, demonstrating the superior antimicrobial properties of PCE@QNs. This remarkable performance is predominantly ascribed to the potent inhibitory effects exerted by cinnamaldehyde present in CEO. As shown in Figure 5-7C, when the hydrophobic CEO broke through the barrier of PE and leaked from the PCE@QNs film, active molecules, such as cinnamaldehyde, were the first to disrupt the integrity of bacterial cell walls and membranes. Subsequently, the synthesis of nucleic acids, proteins, and other cellular metabolic processes in bacteria was disrupted, ultimately leading to cell death. It has been reported that Gram-positive bacteria are more sensitive to cinnamaldehyde than Gram-negative bacteria, owing to differences in their cell envelope structures (Lucas-González, Yilmaz, Mousavi Khaneghah, Hano, Shariati, Bangar, et al., 2023). However, in this work, there was no significant difference in the inhibitory effect of PCE@QNs film on two types bacterial strains. Oxidation is another reason that shortens the shelf life of food. As shown in Figure 5-7D and Figure 5-7E, the radical scavenging abilities against DPPH and ABTS of PCE@QNs were 73.65±1.26% and 90.75±1.58%, respectively. Consistent with our initial hypothesis, the recorded values significantly surpassed those of PC, demonstrating an approximate five-fold increase. This enhancement highlights the antioxidant capacity of PCE@QNs, attributable to synergistic effects between QNs and CEO. These desirable findings regarding the antimicrobial and antioxidant properties highlighted that PCE@QNs film has great potential for multifunctional active packaging.

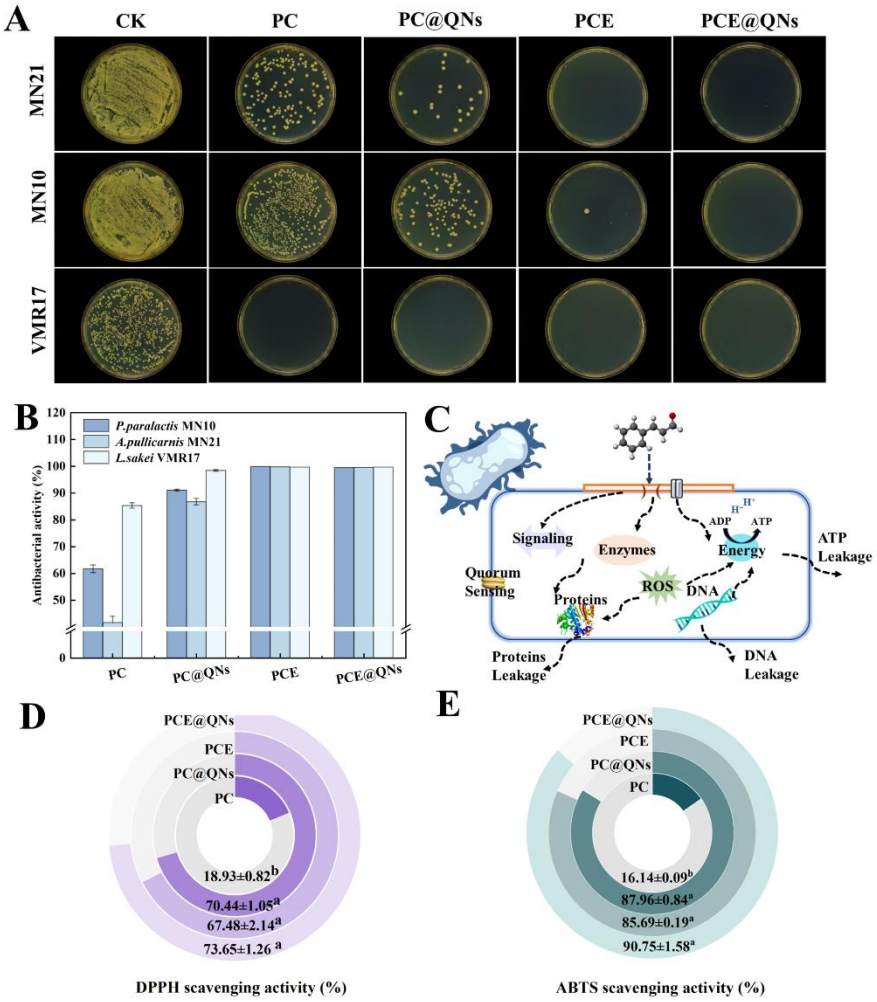

Figure 5-7 Antimicrobial properties of quercetin nanocrystals enhanced chitosan/polyvinyl alcohol/CEO-loaded Pickering emulsion composite films (PCE@QNs) against spoilage bacteria *P. paralactis* MN10, *A. pullicarnis* MN21, and *L. sakei* VMR17. Photographs of colony growth in LB agar plates (A) and ratio of antimicrobial activity (B) after treatment with different films. PCE@QNs exhibits antimicrobial mechanism through multiple pathways (C). DPPH scavenging activity (D) and ABTS scavenging activity (E) of PCE@QNs.

3.7. Release behavior and mechanism analysis

The release behavior of films was influenced by the composition and the structure of the films, and the type of food simulants (Zhu, et al., 2025). The films containing only CEO-loaded PEs (PCE) and those reinforced with QNs (PCE@QNs) were select

to monitor the release behavior of CEO in different food simulants over a 120-h period. As shown in Figure 5-8, the CEO was released from PCE and PCE@QNs films reaching final cumulative release percentages of 76.52% and 58.45% in 50% ethanol medium, and 85.50% and 85.16% in 95% ethanol medium, respectively. All the films exhibited a similar CEO release profile characterized by a sustained release behavior. This could be attributed to the encapsulation of the PEs, which effectively modulated the gradual release of CEO over time. These results are consistent with our previous findings, where similar sustained release behavior was observed in chitosan/gelatin films containing CEO-loaded PEs (Fan, et al., 2023). Notably, in 50% ethanol medium, the cumulative release rate of CEO from PCE@QNs films was significantly lower than that from PCE films. This reduction can be attributed to the incorporation of QNs, which increased the density of the polymer crosslinking network and strengthened interfacial interactions within the matrix. These structural changes created additional diffusion barriers, thereby enhancing CEO retention and improving the controlled release performance of the PCE@QNs system. However, this advantage was not evident in 95% ethanol aqueous medium, possibly due to the high hydrophobicity of quercetin as a natural polyphenol. The excessive ethanol content may have led to partial dissolution of QNs from the film matrix, resulting in a looser PCE@QNs structure and consequently weakening its ability to sustain the release of CEO. The CEO release data were fitted to four kinetic models (Table 2), and the correlation coefficients (R^2) indicated that the Korsmeyer-Peppas model best described the release profiles of both PCE and PCE@QNs films, suggesting a diffusion-controlled release mechanism. For the PCE@QNs film, the Korsmeyer-Peppas model yielded an n value of 0.002 and 0.15, indicating a Fickian diffusion process. This result suggests that the release rate of CEO in PCE@QNs is primarily governed by the diffusion of the active substance through the matrix, with the mass transfer driving force originating from the concentration gradient of the CEO.

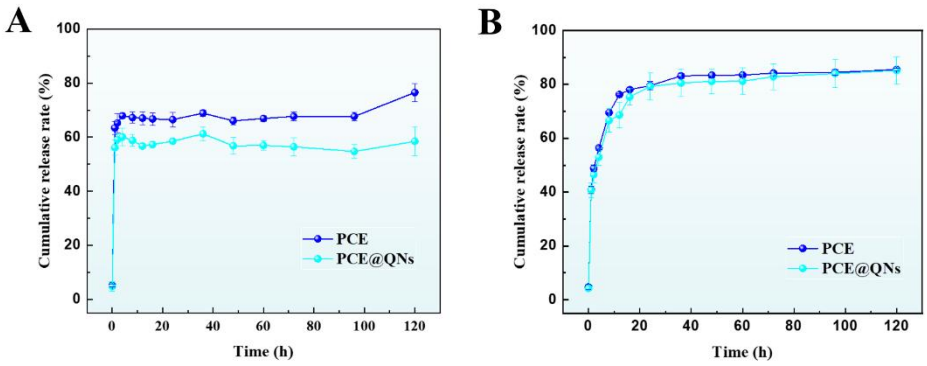

Figure 5-8 The release kinetics profiles of CEO in 50% ethanol (f) and 95% ethanol (g) for films containing only CEO-loaded Pickering emulsion (PCE) and films reinforced with quercetin nanocrystal-enhanced (PCE@QNs).

Table 5-2 Kinetic release model fitting for CEO release at different food simulants.

Fitting Model	Formula	Sample	Ethanol (%)	Fit value		R^2
				k	n	
Zero order	$M_t/M_\infty=kt$	PCE	50	0.60	-	0.31
			95	0.23	-	0.55
		PCE@QNs	50	0.14	-	0.06
			95	0.95	-	0.47
First order	$M_t/M_\infty=1-e^{-kt}$	PCE	50	2.74	-	0.99
			95	0.23	-	0.94
		PCE@QNs	50	3.68	-	0.98
			95	0.49	-	0.96
Higuchi	$M_t/M_\infty=kt^{1/2}$	PCE	50		-	
			95	0.45	-	0.55
		PCE@QNs	50		-	
			95	1.89	-	0.47
Korsmeyer Peppas	$M_t/M_\infty=kt^n$	PCE	50	66.58	0.005	0.99
			95	57.49	0.10	0.98
		PCE@QNs	50	58.07	0.002	0.98
			95	44.27	0.15	0.98

Note: M_t represents the cumulative release amount at time t, M_∞ represents the cumulative release amount at infinite time, Mt/M∞ represents the cumulative release percentage at time t. The best fitting result is determined based on the highest correlation coefficient (R).

3.8. Environmental sustainability assessment

The biodegradability of films is of significant importance to environmental sustainability. The soil burial experiment was used to assess the sustainability of films with the polyethylene film as control. Figure 5-9 presented the morphological changes of the films during the period of soil burial. Examination of the figure reveals that the PCE@QNs films undergo nearly complete degradation, primarily attributable to the activity of small animals and fungi in the soil. In contrast, the polyethylene film remains structurally intact after 28 days without degradation (Gui, Xiao, Zou, Zhang, Fu, Liu, et al., 2024). Petroleum-based food packaging plastics commonly require hundreds and even thousands of years to completely degrade (Chamas, Moon, Zheng, Qiu, Tabassum, Jang, et al., 2020). The mild condition and fast speed make PCE@QNs a highly environmentally friendly material for food packaging.

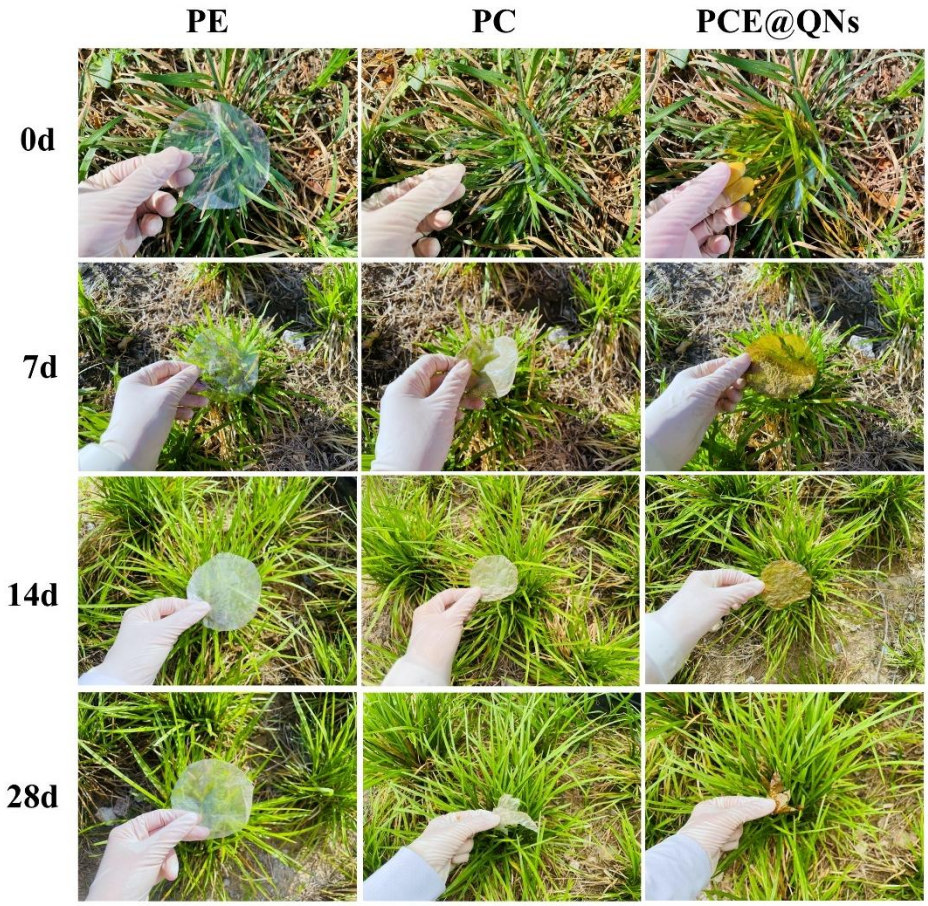

Figure 5-9 The biodegradability of PCE@QNs film assessed by soil burial experiment.

3.9. Application in meat preservation

To evaluate the actual application effect of prepared films, the meat was cut into appropriate sizes and placed in polypropylene containers, covered by polyethylene (CK group), PC, PC@QNs and PCE@QNs film, respectively. And the packaged meat was storage at 4 °C for 11 days.

3.9.1. Sensory evaluation and physiochemical properties

For consumers, the sensory changes in meat are the most direct evaluation of shelf life and quality. As illustrated in Figure 5-10A, initially, all meat samples exhibited bright red color, clear grain and firm texture, with no visible differences between the treatment groups. As the storage time extended, the meat sample packaged by PCE@QNs film showed steady red color and rigid form while the meat of CK group trended to pale and softened. The sensory evaluation panel scored the meat samples of different treatment groups from aspects of overall acceptability, appearance, texture

and odor (Figure 5-10B). On the seventh day of storage, due to the meat samples appeared pale and sticky surface, accompanied by a strong foul odor, the staff assigned lower scores (less than four points) to the CK group samples, deeming them unacceptable. However, the overall acceptability of meat samples of PCE@QNs group was higher than that of other groups during the storage period, which still received a score of 6 at the end of the storage period, suggesting that PCE@QNs contributes to the extended shelf life of meat.

During the spoilage process, the proteins of meat decomposed by enzymes and microorganisms, resulting in the production and accumulation of amines and alkaline nitrogenous substances. The freshness of meat theoretically positively correlated in the value of TVB-N. As shown in Figure 5-10C, the TVB-N value at 0 d was 6.24±0.42 mg/100g and exhibited a rising trend during the cold storage period in all groups. The TVB-N value of CK group was 15.61±0.26 mg/100g on the seventh day of storage, which exceeded the acceptability maximum limit by Chinese Standard GB 2707-2016 (15 mg/100g), while the TVB-N value of PCE@QNs group was 13.82 ±0.30 mg/100g on the eleventh day of storage. In addition, the TVB-N values of PCE@QNs group were consistently remained lower than that of the other groups during the storage period. TVC value was also reflect the freshness of meat. As shown in Figure 5-10D, the starting value of TVC of meat was 2.80±0.16 log CFU/g, increasing to 7.72±0.01 log CFU/g and 6.63±0.05 log CFU/g of CK group and PCE@QNs group till the end of storage, respectively. It was considered unacceptable of meat due to microbial spoilage while the TVC value exceeds 7 log CFU/g (L. Zhang, Yu, Xu, Jiang, Xia, & Yu, 2023). These results suggested that the PCE@QNs film could effectively extend the shelf life of meat.

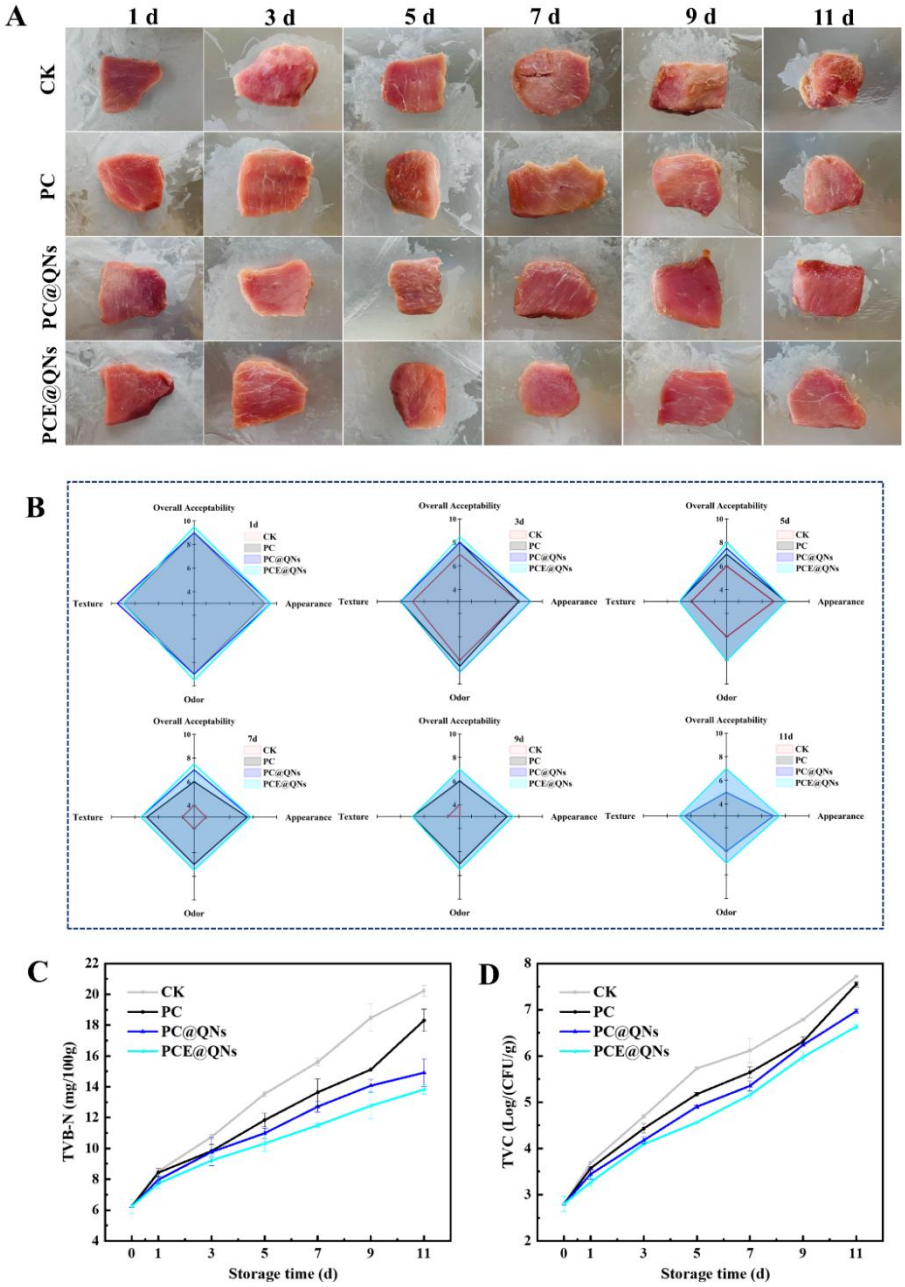

Figure 5-10 Preservation performances of the quercetin nanocrystals enhanced chitosan/polyvinyl alcohol/CEO-loaded Pickering emulsion composite films (PCE@QNs) on meat. Digital pictures (A), sensory score (B), TNB-N (C), and TVC (D) of meat samples during storage at 4 °C.

3.9.2. Microbial diversity changes

The diversity and richness of microbial communities are related to the spoilage process of meat, which could be investigated by 16S rRNA high-throughput gene amplicon sequencing method (Wen, et al., 2022). Based on the physiochemical results, key time points were designated as representative, including 0d, 1d, 3d, 9d and 11d. OTUs served as an important foundation for diversity and community structure analysis, as shown in Figure 5-11A, the OTUs of samples of PCE@QNs group was 1334, which was lower than that of other film treated group, indicating fewer microorganism species in samples of PCE@QNs group. Based on the OTUs results, Table 5-3 showed the alpha diversity index of meat samples, it was observed that all samples had good coverage (>99.98%), reflecting the sequencing data could sufficient coverage of all species present in the samples. Shannon and Simpson index represented species diversity and richness, respectively (Y. Zhao, Meng, Shao, Dai, Li, & Jia, 2022). According to the value listed in Table 5-3, the Shannon index of samples of the PCE@QNs group decreased with increasing storage time while the Simpson index trend to increasing, suggesting a diminution of bacterial richness and diversity. This result was highly consistent with Wang et al. (2022), treating meat with thyme essential oil nanoemulsions. In addition, the decline in Chao1 and ACE indices typically indicated a reduction in species richness within the samples (Table 5-3). These outcomes underscore that meat samples packaged by PCE@QNs profoundly influence the microbial community complexity. Figure 5-11B showed the bacterial community structure of samples at the phylum level. *Proteobacteria* (58.99%), *Firmicutes* (10.67%), *Bacteroidota* (9.52%), *Actinobacteria* (9.26%) and *Acidobacteriota* (2.32%) were the predominant bacterial phyla in the fresh sample (0 d). As the storage time increasing, despite initial differences in bacterial community composition, *Proteobacteria*, a common dominant spoilage bacteria strain in most freshly prepared meat (Y. Zhao, Meng, Shao, Dai, Li, & Jia, 2022), gradually became the dominant phyla, accounting for more than 90% of the bacterial community structure. However, *Proteobacteria* accounted significantly lower proportion ($P < 0.05$) in sample of PCE@QNs group at the end of storage (9 d, 11 d), indicating that the PCE@QNs films could continuously inhibit the growth of *Proteobacteria* in meat. This result was highly consistent with previous study (H. Zhang, Liang, Li, & Kang, 2020), the long inhibition effect on the microbial growth of meat was attribute to the slow-release of antibacterial substances in PCE@QNs. Bacterial genus heatmap (Figure 5-11C) and PCoA (Figure 5-11D) portrayed the dynamic bacterial shifts. Clustering analysis of heatmap showed that the microflora composition of PCE@QNs group on first storage day was basically similar to that of fresh samples (0 d), emphasizing the effective of PCE@QNs in the initial stage of storage. According to the PCoA analysis, PCoA1 and PCoA2 accounted for 68.54% and 13.35% of the total variance, respectively. Together, these two principal coordinates explained 81.89% of the overall variability in the microbial community data, effectively capturing the differences among the samples. The results indicated that microbial community succession was significantly influenced by different packaging treatments. The CK group showed a highly dispersed distribution and the greatest shift along the PCoA1

axis, reflecting rapid microbial succession and severe spoilage. In contrast, samples from the PCE@QNs group clustered more closely to the day 0 samples and exhibited a more compact distribution, suggesting that this treatment most effectively inhibited microbial changes and preserved a community structure similar to the initial state, thereby demonstrating superior preservation potential. ANOSIM analysis was used to further evaluate the significance of grouping. Figure 5-11E showed that the difference between each film treatment group was more significant than the difference within the same treatment group on Phylum level, indicating the statistical results are meaningful (Y. Chen, Lin, Yang, Cui, Chisoro, Yang, et al., 2024). Notably, the result of Beta diversity difference analysis based on Kruskal-Wallis H test (Figure 5-10F) showed that the distance value of PCE@QNs group decreased more significantly during storage, indicating a deeper level in the loss of diversity and individuality in the microbial community.

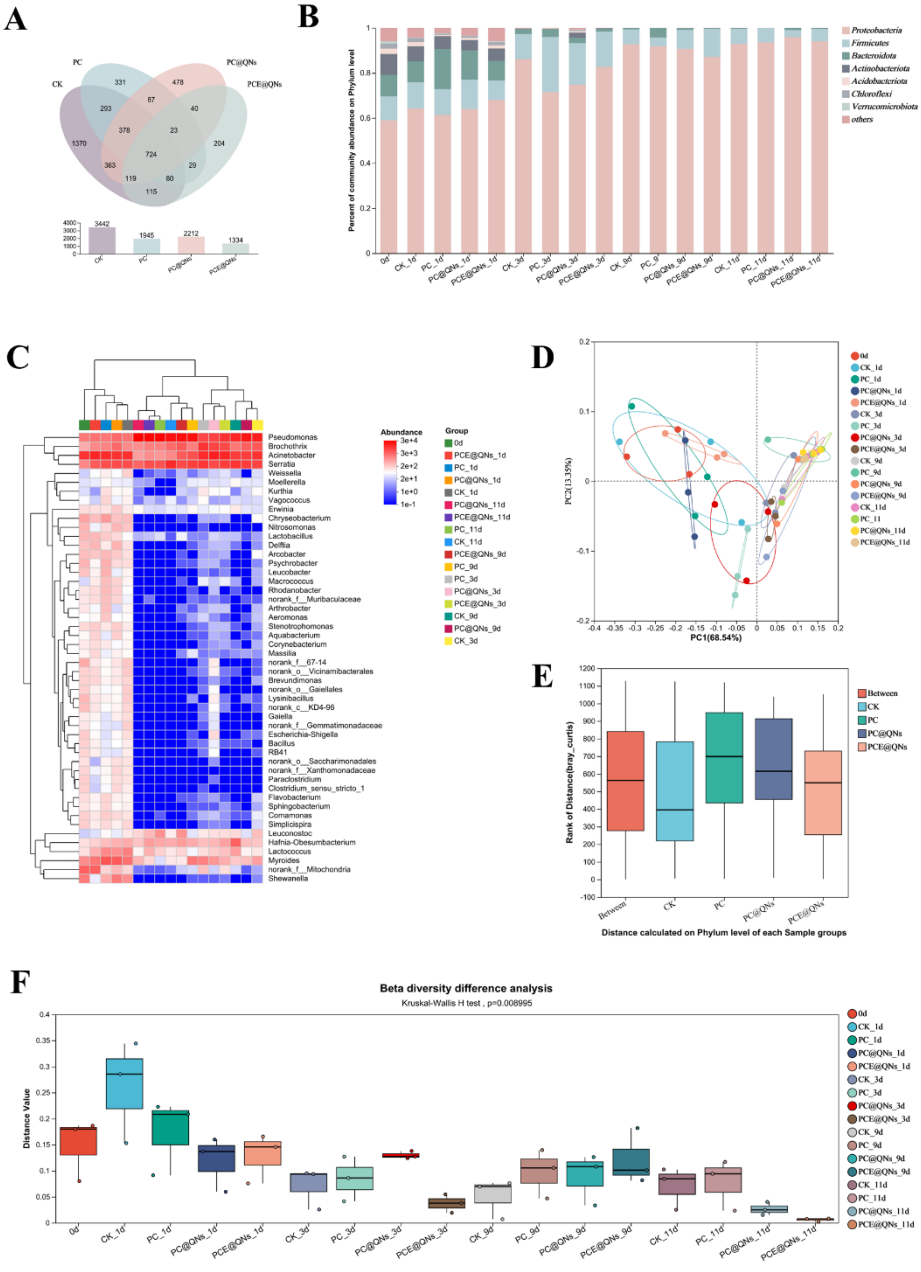

Figure 5-11 Microbial communities' diversity of packaged meat during storage. The Venn diagrams of OTU richness distribution (A), bar charts (B) and heatmap (C) of the top 50

abundant genera displaying relative abundance of microbes on phylum level. Principal coordinate analysis (D), ANOSIM analysis (E) and Beta diversity difference analysis (F) on phylum level.

Table 5-3 Comparison of alpha diversity estimation of the 16S rRNA gene libraries of packaged meat with different film.

Sample	Day	Shannon	Simpson	ACE	Chao	Coverage (%)
CK	0	1.48±0.23	0.39±0.08	30.36±0.02	27.11±3.62	100.00±0.00
	1	1.25±0.26	0.46±0.15	30.55±4.71	26.83±1.03	100.00±0.00
	3	0.47±0.07	0.76±0.06	16.09±3.02	14.92±2.20	100.00±0.00
	9	0.28±0.07	0.87±0.05	15.63±3.27	10.67±2.49	100.00±0.00
	11	0.25±0.11	0.87±0.07	13.00±0.00	5.83±1.93	100.00±0.00
PC	0	1.48±0.23	0.39±0.08	30.36±0.02	27.11±3.62	100.00±0.00
	1	1.19±0.16	0.44±0.07	28.80±3.14	28.33±2.62	100.00±0.00
	3	0.73±0.02	0.58±0.03	20.29±2.01	18.50±3.54	100.00±0.00
	9	0.31±0.18	0.85±0.10	8.28±2.95	7.00±1.63	100.00±0.00
	11	0.23±0.05	0.88±0.03	5.25±1.12	5.00±0.82	100.00±0.00
PC@QNs	0	1.48±0.23	0.39±0.08	30.36±0.02	27.11±3.62	100.00±0.00
	1	1.20±0.13	0.45±0.01	28.27±1.43	28.33±2.05	100.00±0.00
	3	0.78±0.24	0.60±0.08	13.57±4.00	16.44±3.61	100.00±0.00
	9	0.32±0.11	0.83±0.08	7.89±2.89	6.17±2.39	100.00±0.00
	11	0.19±0.07	0.92±0.03	4.50±0.50	4.33±0.47	100.00±0.00
PCE@QNs	0	1.48±0.23	0.39±0.08	30.36±0.02	27.11±3.62	100.00±0.00
	1	1.32±0.20	0.46±0.09	30.74±3.74	29.00±2.00	100.00±0.00
	3	0.53±0.03	0.71±0.02	12.28±2.75	10.89±3.19	100.00±0.00
	9	0.38±0.15	0.79±0.11	9.71±0.15	9.66±0.15	100.00±0.00
	11	0.25±0.00	0.88±0.00	4.50±0.50	4.50±0.50	100.00±0.00

The values were shown as mean±standard deviation (SD).

3.9.3. Preservation mechanism

During meat storage, the CEO encapsulate within the PEs and release onto the surface of meat from PCE@QNs. The incorporation of QNs enhances the compactness of PCE@QNs, forming a stronger diffusion barrier that enables slow and sustained release of CEO, which effectively inhibiting the growth of spoilage microorganisms on the meat surface, delaying the microbial spoilage process and extending shelf life of meat. Simultaneously, the strong antioxidant capacity of the PCE@QNs, that attributable to the synergistic effect of QNs and CEO, helps mitigate lipid oxidation, thereby preserving the color and quality of the meat. In addition, the multi-layered barrier structure of PCE@QNs created by QNs nanofiller and hydrophobicity CEO-loaded PE effectively mitigated quality degradation induced by water vapor and ultraviolet radiation during storage.

4. Conclusions

In this study, a controlled release active packaging film was developed by integrating QNs and CEO-loaded PEs into a CS/PVA composite film, and successfully applied for meat preservation. FTIR result showed that the internal structure of PCE@QNs was preserved through hydrogen bonding interactions among QNs, the CEO-loaded PE, and the CS/PVA polymer chains. And XRD, and TG showed that QNs improved the stability of the film. Mechanical properties characterizations confirmed that the incorporation of QNs significantly enhanced TS and EAB of PCE@QNs, exceeding other essential oil-loaded PEs based films. Additionally, PCE@QNs showed excellent water vapor barrier and UV-blocking properties. Furthermore, PCE@QNs exhibited desirable antimicrobial and antioxidant activities due to the synergistic effect between QNs and the CEO-loaded PEs. The PCE@QNs exhibited sustained release performance with a release duration of up to 120 hours, predominantly governed by typical Fickian diffusion. The biodegradability and environmental friendliness of the films were also evaluated and verified. Additionally, through the sustained release of CEO, PCE@QNs reduced microbial diversity successfully extended the shelf life of fresh pork to 11 days at 4°C. Overall, this work proposed an innovative and sustainable approach to designing antimicrobial packaging films, showing potential for food preservation.

5. References

Almasi, H., Azizi, S., & Amjadi, S. (2020). Development and characterization of pectin films activated by nanoemulsion and Pickering emulsion stabilized marjoram (Origanum majorana L.) essential oil. Food Hydrocolloids, 99, 105338.

Cao, L., Feng, H., Meng, F., Li, J., & Wang, L. (2020). Fabrication of a high tensile and antioxidative film via a green strategy of self-growing needle-like quercetin crystals in cassia gum for lipid preservation. Journal of Cleaner Production, 266, 121885.

Chamas, A., Moon, H., Zheng, J., Qiu, Y., Tabassum, T., Jang, J. H., Abu-Omar, M., Scott, S. L., & Suh, S. (2020). Degradation Rates of Plastics in the Environment. ACS Sustainable Chemistry & Engineering, 8(9), 3494-3511.

Chang, H., Xu, J., Macqueen, L. A., Aytac, Z., Peters, M. M., Zimmerman, J. F., Xu, T., Demokritou, P., & Parker, K. K. (2022). High-throughput coating with biodegradable antimicrobial pullulan fibres extends shelf life and reduces weight loss in an avocado model. Nature Food, 3(6), 428-436.

Chen, X., Lan, W., & Xie, J. (2024). Characterization of active films based on chitosan/polyvinyl alcohol integrated with ginger essential oil-loaded bacterial cellulose and application in sea bass (Lateolabrax japonicas) packaging. Food Chemistry, 441, 138343.

Chen, Y., Lin, H., Yang, Y., Cui, L., Chisoro, P., Yang, C., Wu, G., Li, Q., Li, J., Zhang, C., & Li, X. (2024). Exploring the role of static magnetic field in supercooling storage from the viewpoint of meat quality and microbial community. Food Research International, 195, 114884.

Cheng, Y., Cai, X., Zhang, X., Zhao, Y., Song, R., Xu, Y., & Gao, H. (2024). Applications in Pickering emulsions of enhancing preservation properties: Current trends and future prospects in active food packaging coatings and films. Trends in Food Science & Technology, 151, 104643.

Du, H., Sun, X., Chong, X., Yang, M., Zhu, Z., & Wen, Y. (2023). A review on smart active packaging systems for food preservation: Applications and future trends. Trends in Food Science & Technology, 141, 104200.

Fan, S., Wang, D., Wen, X., Li, X., Fang, F., Richel, A., Xiao, N., Fauconnier, M.-L., Hou, C., & Zhang, D. (2023). Incorporation of cinnamon essential oil-loaded Pickering emulsion for improving antimicrobial properties and control release of chitosan/gelatin films. Food Hydrocolloids, 138, 108438.

Fan, S., Yang, Q., Wang, D., Zhu, C., Wen, X., Li, X., Richel, A., Fauconnier, M.-L., Yang, W., Hou, C., & Zhang, D. (2024). Zein and tannic acid hybrid particles improving physical stability, controlled release properties, and antimicrobial activity of cinnamon essential oil loaded Pickering emulsions. Food Chemistry, 446, 138512.

Fan, S., Yang, Q., Zhu, C., Li, X., Richel, A., Fauconnier, M.-L., Fang, F., Zhang, D., & Hou, C. (2024). Zein/chitosan Janus film incorporated with tannic acid and cinnamon essential oil co-loaded Pickering emulsion for sustained controlled release and pork preservation. International Journal of Biological Macromolecules, 138429.

Gu, M., Li, C., Su, Y., Chen, L., Li, S., Li, X., Zheng, X., & Zhang, D. (2023). Novel insights from protein degradation: Deciphering the dynamic evolution of biogenic amines as a quality indicator in pork during storage. Food Research International, 167, 112684.

Gui, T., Xiao, L.-P., Zou, S.-L., Zhang, Y., Fu, X., Liu, C.-H., & Sun, R.-C. (2024). Tough and biodegradable C-lignin cross-linked polyvinyl alcohol supramolecular composite films with closed-looping recyclability. Chemical Engineering Journal, 491, 151748.

Guo, X., Luo, W., Wu, L., Zhang, L., Chen, Y., Li, T., Li, H., Zhang, W., Liu, Y., Zheng, J., & Wang, Y. (2024). Natural Products from Herbal Medicine Self-Assemble into Advanced Bioactive Materials. Advanced Science, 11(35), 2403388.

He, T., Niu, N., Chen, Z., Li, S., Liu, S., & Li, J. (2018). Novel Quercetin Aggregation-Induced Emission Luminogen (AIEgen) with Excited-State Intramolecular Proton Transfer for In Vivo Bioimaging. Advanced Functional Materials, 28(11), 1706196.

Huang, H.-D., Ren, P.-G., Zhong, G.-J., Olah, A., Li, Z.-M., Baer, E., & Zhu, L. (2023). Promising strategies and new opportunities for high barrier polymer packaging films. Progress in Polymer Science, 144, 101722.

Huie, J., Suqiu, Z., Haiyan, J., Zhijian, L., Lijuan, C., Nihao, L., & Xinhua, L. (2023). Microporous chitosan/polyvinyl alcohol based active packaging materials with

integrated gas-transmission, radiation-cooling, anti-microbial, and ultraviolet shielding features. Chemical Engineering Journal, 473, 145432.

Jiang, H., Zhao, S., Li, Z., Chen, L., Mo, H., & Liu, X. (2024). Swan-feathers inspired smart-responsive sustainable carboxymethyl cellulose/polyvinyl alcohol based food packaging film for robustly integrated Intelligent and Active Packaging. Nano Today, 56, 102272.

Kuai, L., Liu, F., Chiou, B.-S., Avena-Bustillos, R. J., McHugh, T. H., & Zhong, F. (2021). Controlled release of antioxidants from active food packaging: A review. Food Hydrocolloids, 120, 106992.

Lai, F., Schlich, M., Pireddu, R., Fadda, A. M., & Sinico, C. (2019). Nanocrystals as effective delivery systems of poorly water-soluble natural molecules. Current Medicinal Chemistry, 26(24), 4657-4680.

Li, F., Zhe, T., Ma, K., Zhang, Y., Li, R., Cao, Y., Li, M., & Wang, L. (2023). One stone two birds: Multifunctional flavonol nanocrystals enable food packaging to both preserve freshness and visually monitor freshness. Chemical Engineering Journal, 453, 139760.

Lucas-González, R., Yilmaz, B., Mousavi Khaneghah, A., Hano, C., Shariati, M. A., Bangar, S. P., Goksen, G., Dhama, K., & Lorenzo, J. M. (2023). Cinnamon: An antimicrobial ingredient for active packaging. Food Packaging and Shelf Life, 35, 101026.

Ma, Z., Xing, Z., Zhao, Y., Zhang, H., Xin, Q., Liu, J., Qin, M., Ding, C., & Li, J. (2023). Lotus leaf inspired sustainable and multifunctional Janus film for food packaging. Chemical Engineering Journal, 457, 141279.

Madane, K., & Ranade, V. V. (2022). Anti-solvent crystallization: Particle size distribution with different devices. Chemical Engineering Journal, 446, 137235.

Mather, A. E., Gilmour, M. W., Reid, S. W. J., & French, N. P. (2024). Foodborne bacterial pathogens: genome-based approaches for enduring and emerging threats in a complex and changing world. Nature Reviews Microbiology, 22(9), 543-555.

Miao, W., Gu, R., Shi, X., Zhang, J., Yu, L., Xiao, H., & Li, C. (2024). Indicative bacterial cellulose films incorporated with curcumin-embedded Pickering emulsions: Preparation, antibacterial performance, and mechanism. Chemical Engineering Journal, 495, 153284.

Parfitt, J., Croker, T., & Brockhaus, A. (2021). Global Food Loss and Waste in Primary Production: A Reassessment of Its Scale and Significance. Sustainability, 13(21), 12087.

Priyadarshi, R., Roy, S., Ghosh, T., Biswas, D., & Rhim, J.-W. (2022). Antimicrobial nanofillers reinforced biopolymer composite films for active food packaging applications - A review. Sustainable Materials and Technologies, 32, e00353.

Qin, W., Zou, L., Hou, Y., Wu, Z., Loy, D. A., & Lin, D. (2024). Characterization of novel anthocyanins film @ carbon quantum dot nanofiber intelligent active double-layer film, physicochemical properties and fresh-keeping monitoring in Ictalurus punctatus fish. Chemical Engineering Journal, 496, 154041.

Qu, W., Wang, W., Zhang, C., Chen, X., Wang, J., Xue, W., Zhu, J., & Wu, H. (2023). Development of composite film based on polyvinyl alcohol with binary nanoreinforcements for active packaging of fresh-cut apples. Chemical Engineering Journal, 477, 146862.

Rojas, A., Misic, D., Zizovic, I., Dicastillo, C. L. d., Velásquez, E., Rajewska, A., Rozas, B., Catalán, L., Vidal, C. P., Guarda, A., & Galotto, M. J. (2024). Supercritical fluid and cocrystallization technologies for designing antimicrobial food packaging PLA nanocomposite foams loaded with eugenol cocrystals with prolonged release. Chemical Engineering Journal, 481, 148407.

Tong, C., Shi, F., Tong, X., Shi, S., Ali, I., & Guo, Y. (2021). Shining natural flavonols in sensing and bioimaging. TrAC Trends in Analytical Chemistry, 137, 116222.

Uysal-Unalan, I., Sogut, E., Realini, C. E., Cakmak, H., Oz, E., Espinosa, E., Morcillo-Martín, R., Oz, F., Nurmi, M., Cerqueira, M. A., Perera, K. Y., Ayhan, Z., Arserim-Ucar, D. K., Kanakaki, C., Chrysochou, P., Marcos, B., & Corredig, M. (2024). Bioplastic packaging for fresh meat and fish: Current status and future direction on mitigating food and packaging waste. Trends in Food Science & Technology, 152, 104660.

Wang, D., Fan, S., Li, X., Chen, L., Wen, X., Xu, Y., Zhu, C., Hou, C., & Zhang, D. (2024). Carboxymethyl chitosan/polyvinyl alcohol hydrogel films by incorporating MSNs as ε-PL carrier with pH-responsive controlled release and antibacterial properties. Food Packaging and Shelf Life, 46, 101360.

Wang, J.-D., Yang, S.-L., Liu, G.-S., Zhou, Q., Fu, L.-N., Gu, Q., Cai, Z.-H., Zhang, S., & Fu, Y.-J. (2024). A degradable multi-functional packaging based on chitosan/silk fibroin via incorporating cellulose nanocrystals-stabilized cinnamon essential oil pickering emulsion. Food Hydrocolloids, 153, 109978.

Wang, L., Liu, T., Liu, L., Liu, Y., & Wu, X. (2022). Impacts of chitosan nanoemulsions with thymol or thyme essential oil on volatile compounds and microbial diversity of refrigerated pork meat. Meat Science, 185, 108706.

Wang, W., Liu, X., Guo, F., Yu, Y., Lu, J., Li, Y., Cheng, Q., Peng, J., & Yu, G. (2024). Biodegradable cellulose/curcumin films with Janus structure for food packaging and freshness monitoring. Carbohydrate Polymers, 324, 121516.

Wen, X., Zhang, D., Li, X., Ding, T., Liang, C., Zheng, X., Yang, W., & Hou, C. (2022). Dynamic changes of bacteria and screening of potential spoilage markers of lamb in aerobic and vacuum packaging. Food Microbiology, 104, 103996.

Xia, J., Sun, X., Jia, P., Li, L., Xu, K., Cao, Y., Lü, X., & Wang, L. (2023). Multifunctional sustainable films of bacterial cellulose nanocrystal-based, three-phase pickering nanoemulsions: A promising active food packaging for cheese. Chemical Engineering Journal, 466, 143295.

Xu, J., He, M., Wei, C., Duan, M., Yu, S., Li, D., Zhong, W., Tong, C., Pang, J., & Wu, C. (2023). Konjac glucomannan films with Pickering emulsion stabilized by TEMPO-oxidized chitin nanocrystal for active food packaging. Food Hydrocolloids, 139, 108539.

Yu, Y., Gong, M., Wang, S., Wang, X., Liu, Y., Huang, D., Guan, H., Liu, H., Chen, Y., Jiang, Y., & Li, D. (2024). Pectin-based cinnamon essential oil Pickering emulsion film with two-sided differential wettability: A major role in the spatial distribution of microdroplets. International Journal of Biological Macromolecules, 277, 133727.

Yue, C., Wang, M., Zhou, Z., You, Y., Wang, G., & Wu, D. (2024). Cellulose-based intelligent packaging films with antibacterial, UV-blocking, and biodegradable properties for shrimp freshness monitoring. Chemical Engineering Journal, 488, 150975.

Zhang, H., Liang, Y., Li, X., & Kang, H. (2020). Effect of chitosan-gelatin coating containing nano-encapsulated tarragon essential oil on the preservation of pork slices. Meat Science, 166, 108137.

Zhang, L., Yu, D., Xu, Y., Jiang, Q., Xia, W., & Yu, D. (2023). Changes in quality and microbial diversity of refrigerated carp fillets treated by chitosan/zein bilayer film with curcumin/nisin-loaded pectin nanoparticles. Food Bioscience, 54, 102941.

Zhang, W., Ezati, P., Khan, A., Assadpour, E., Rhim, J.-W., & Jafari, S. M. (2023). Encapsulation and delivery systems of cinnamon essential oil for food preservation applications. Advances in Colloid and Interface Science, 318, 102965.

Zhang, W., Jiang, H., Rhim, J.-W., Cao, J., & Jiang, W. (2022). Effective strategies of sustained release and retention enhancement of essential oils in active food packaging films/coatings. Food Chemistry, 367, 130671.

Zhang, W., Khan, A., Ezati, P., Priyadarshi, R., Sani, M. A., Rathod, N. B., Goksen, G., & Rhim, J.-W. (2024). Advances in sustainable food packaging applications of chitosan/polyvinyl alcohol blend films. Food Chemistry, 443, 138506.

Zhang, Y., & Jiang, W. (2023). Effective strategies to enhance ultraviolet barrier ability in biodegradable polymer-based films/coatings for fruit and vegetable packaging. Trends in Food Science & Technology, 139, 104139.

Zhao, W., Li, Q., He, P., Li, C., Aryal, M., Fabiilli, M. L., & Xiao, H. (2024). Charge balanced aggregation: A universal approach to aqueous organic nanocrystals. Journal of Controlled Release, 375, 552-573.

Zhao, Y., Meng, Z., Shao, L., Dai, R., Li, X., & Jia, F. (2022). Employment of cold atmospheric plasma in chilled chicken breasts and the analysis of microbial diversity after the shelf-life storage. Food Research International, 162, 111934.

Zhou, P., & Han, K. (2022). ESIPT-based AIE luminogens: Design strategies, applications, and mechanisms. Aggregate, 3(5), e160.

Zhu, C., Yang, Q., Tian, M., Yang, W., Min, C., Fan, S., Wang, D., Li, X., Zhang, D., & Hou, C. (2025). Sustainable nanofiber films based on polylactic acid/modified cellulose nanocrystals containing various types of polyphenols, exhibiting antioxidant activity and high stability. Food Chemistry, 477, 143514.

Summary

In this study, a nanoparticle reinforcement strategy was successfully developed to construct CEO-loaded Pickering emulsion (PE)-based active films with improved structural integrity and controlled release performance. The physicochemical properties of the resulting CS/PVA films embedded with CEO-loaded PEs and quercetin nanocrystals (QNs) were systematically evaluated, including their mechanical strength, barrier properties, optical characteristics, antimicrobial activity, and antioxidant capacity. Compared with the multilayer Janus film strategy discussed in the previous chapter, the nanoparticle-reinforced approach offers an alternative and complementary pathway for achieving tunable CEO release and enhanced preservation performance. The results demonstrate that this strategy not only enables effective modulation of CEO diffusion but also translates interfacial and structural advantages into tangible improvements in fresh meat preservation. These findings further support the overall objective of developing tunable, controlled-release active packaging systems.

Chapter 6

General discussion, conclusion and perspectives

1. General discussion

In recent years, increasing concerns regarding food safety and preservation have accelerated the development of active packaging materials. Among them, controlled-release antimicrobial packaging has emerged as a promising strategy to prolong the shelf life of perishable foods by ensuring the sustained and effective delivery of bioactive agents (Almasi, Jahanbakhsh Oskouie, & Saleh, 2021; Chen, Chen, Xu, & Yam, 2019). However, conventional antimicrobial packaging systems often suffer from issues such as burst release, poor stability of active compounds, and limited long-term efficacy (Chang, Xu, Macqueen, Aytac, Peters, Zimmerman, et al., 2022; W. Zhang, Jiang, Rhim, Cao, & Jiang, 2022).

To address these challenges, this thesis proposes a novel packaging platform based on Pickering emulsions (PEs), in which essential oils (EOs) are stably encapsulated and released in a controlled manner. Unlike traditional emulsions stabilized by synthetic surfactants, PEs utilize solid particles as stabilizers, providing higher stability, reduced toxicity, and enhanced interfacial adsorption capacity (Cheng, Cai, Zhang, Zhao, Song, Xu, et al., 2024). These advantages make PEs particularly attractive for food packaging applications. Recent studies have demonstrated that PEs can effectively reduce EOs volatility, protect active components from oxidation, and prolong antimicrobial action (Cahyana, Putri, Solihah, Lutfi, Alqurashi, & Marta, 2022; Ji & Wang, 2025). However, their integration into film-forming systems, especially for achieving tunable release kinetics and strong antimicrobial performance under real storage conditions, remains insufficiently explored.

Throughout this thesis, a EOs loaded PE delivery manner (Chapter III) and two PEs-based film systems (Chapter IV and Chapter V) were designed and evaluated for their physicochemical properties, antimicrobial performance, and release behavior.

To effectively encapsulate cinnamon essential oil (CEO) in Pickering emulsions (PEs) for improved stability and sustained release, Chapter III employed a zein-tannic acid (ZT) complex-based interfacial engineering strategy. The thesis research starts with fabrication and optimization of CEO-loaded PEs stabilized by regulating mode of ZT hybrid particles, focusing on interfacial stability, CEO-loading capacity, and sustained-release behavior. Among the formulations, ZT5 formed the most compact and viscoelastic interfacial film, which not only improved the physical stability of the emulsions but also regulated CEO diffusion, enabling a sustained antimicrobial release profile. This approach highlights the effectiveness of interfacial engineering in designing robust PE-based delivery systems for long-term food preservation applications.

To effectively incorporate CEO-loaded Pickering emulsions (ZTC) into biodegradable packaging films and regulate CEO release behavior, Chapter IV designed a Janus structured zein/chitosan bilayer film via a layer-by-layer casting approach. The inner loading layer was composed of chitosan embedded with ZTC, while the outer barrier layer consisted of zein. This bilayer architecture enabled unidirectional and sustained release of the active compounds toward the food surface. Moreover, the release mechanism followed a quasi-Fickian diffusion model,

indicating that both diffusion and matrix relaxation played roles in controlling CEO migration. This structural design not only enhanced release efficiency and directionality but also maintained strong antimicrobial (>99%) and antioxidant performance of the film. These results demonstrate the effectiveness of integrating interfacial and architectural strategies to achieve controlled release of CEO in biodegradable packaging systems.

In parellel, CEO-loaded Pickering emulsions (ZTC) were effectively incorporated into a biodegradable chitosan/polyvinyl alcohol (CS/PVA) matrix through a rational structural design strategy that also included quercetin nanocrystals (QNs) as nanofillers. This design led to the formation of a robust and densely hydrogen-bonded network between QNs, CEO-loaded PEs, and the CS/PVA matrix. Such architecture not only enhanced the mechanical strength of the film (tensile strength of 39.09 ± 0.46 MPa) but also significantly influenced the CEO release behavior. These structural features contributed to a sustained release of CEO, enabling long-term antimicrobial efficacy (99.99% inhibition) and enhanced antioxidant performance (approximately five-fold increase). The film extended the shelf life of fresh meat to 11 days at 4 °C, demonstrating that rational design at the molecular and network levels is key to optimizing both mechanical and functional properties in biodegradable packaging systems.

By integrating the emulsion technology with biodegradable film matrices, a multifunctional packaging solution was developed with improved structural stability, prolonged antimicrobial activity, and potential applicability in meat preservation. Through a systematic investigation across multiple chapters, this work provides new insights into the PEs-based film, the mechanisms of sustained release, and the practical potential of such materials for active food packaging applications.

1.1. Development of EOs-loaded PEs: Toward improved controlled release performance

PEs provide a promising strategy to encapsulate and protect volatile EO compounds (Ji & Wang, 2025). The construction of PE-based controlled-release packaging systems relies heavily on the design of stable, efficient EO delivery carriers. However, their release behavior is critically governed by the nature of the stabilizing particles at the oil-water interface.

In chapter Ⅲ, we focused on the development of CEO-loaded PEs stabilized by zein-TA hybrid particles through interfacial engineering and optimization release behavior of PEs by regulating mode of zein-TA hybrid particles at the oil-water interface via pH-regulated self-assembly. This part aiming to enhance interfacial functionality and sustained release behavior of CEO-loaded PEs as a foundational step for film system integration.

Zein, the main storage protein in corn, is hydrophobic due to a high percentage of apolar amino acids, which has been studied as a stabilizer for PEs due to its structure and ability to self-organize (Souza, Ferreira, & Soares, 2022). However, zein particles failed to effectively stabilize the dispersed systems since they did not have adequate

interfacial properties (Xiao, Li, Xiong, Duan, Chen, Luo, et al., 2024). TA exhibits strong interactions with proteins and possesses antibacterial and antioxidant activities due to its abundant in hydroxyl groups (Hosseini, Moghaddam, Barner, Cometta, Hutmacher, & Medeiros Savi, 2025). Thus, zein-TA complexation was pursued to improve the stability of particle polymers in PE systems.

The interaction mode between zein and TA was effectively regulated by adjusting the reaction pH (pH 5, 7, and 9), consistent with prior studies on pH-dependent zein and ferulic acid binding (Q. Wang, Tang, Yang, Lei, Lei, Zhao, et al., 2022). The results demonstrated that the formation of ZT complexes with distinct physicochemical and interfacial properties. At pH 5, non-covalent interactions (hydrogen bonding and hydrophobic effects) dominated, leading to the formation of relatively large particles (293.5 nm). These complexes exhibited balanced hydrophobicity (contact angle ~74°), which was critical features for stabilizing oil-water interfaces (Low, Siva, Ho, Chan, & Tey, 2020). In contrast, under alkaline conditions (pH 9), covalent bonding became prominent (Xu, Wei, & Xue, 2023; X. Zhu, Chen, Hu, Han, Xu, Zhao, et al., 2021), but excessive unfolding and aggregation of zein may resulted in reduced interfacial integrity and poor emulsification behavior.

Our hypothesis that non-covalent interactions at pH 5 would optimize zein-TA assembly for interfacial applications was further validated. The ZT5 complex (formed at pH 5) showed the most balanced interfacial properties, as evidenced by its lower interfacial tension (11.31 mN/m), stronger interfacial viscoelasticity, and stable anchoring at the oil-water interface, leading to the formation of a thick and coherent PEs interfacial layer (Liu, Chen, Zhao, Guo, Wang, Feng, et al., 2023). This structural advantage aligns with the general design principle that dense interfacial networks prolong bioactive release by increasing diffusion path tortuosity (Liu, et al., 2023). Specifically, the CEO-loaded ZTC5 emulsion exhibited the smallest in Turbiscan Stability Index (TSI) compared to ZTC7 and ZTC9, encapsulation efficiency reached 86.83%, and the slowest CEO release rate among all tested systems. We attribute these outcomes to the dual roles of ZT5: proper wettability for anchors at interface and high viscoelasticity resisted droplet coalescence. These findings position ZTC5 as a promising candidate for controlled delivery of antimicrobial agents.

Notably, the antimicrobial activity of ZTCs was significantly enhanced, particularly in ZTC5, which showed the lowest MIC values (12.5 μL/mL) against both *P. paralactis* MN10 and *L. sakei* VMR17, two critical meat spoilage species (Wen, Zhang, Li, Ding, Liang, Zheng, et al., 2022). This enhancement could be attributed to the synergistic effect of CEO and TA as dual antimicrobial agents, combined with improved encapsulation and slow-release features that maintained antimicrobial activity over time.

Despite the promising results, this study has certain limitations that warrant further exploration. For example, the formulation of PEs was conducted using a fixed concentration of zein-TA complex particles. While this approach effectively revealed the influence of polyphenol–protein interaction modes on interfacial properties and release behavior, it did not fully account for the potential effects of varying particle concentrations.

In summary, this part of work lays a critical foundation for the further PEs-based controlled-release packaging film development. The interfacial structure and stability insights gained here provide not only a theoretical basis of PEs but also a material platform for the subsequent film formation.

1.2. Design and evaluation of multilayer active packaging films based on PEs: Toward unidirectional and sustained release

Active packaging systems incorporating EOs (such as CEO) have been widely investigated for their potent antimicrobial properties. However, current CEO-containing packaging films face critical challenges that hinder their practical application: i) the hydrophobicity of CEO renders it incompatible with bio-polymeric materials and the thermal sensitivity of CEO results in the inactivation of components during the film-forming process (W. Zhang, Ezati, Khan, Assadpour, Rhim, & Jafari, 2023); ii) blending CEO in bio-polymeric materials directly may result in a reduction of availability within the packaging cause of ‘burst effect’ (Malekjani, Karimi, Assadpour, & Jafari); iii) the CEO is released along both sides of packaging film, nearly half of the CEO was released into the surroundings (L. Wang, Yuan, Sun, Wu, Lv, Zhang, et al., 2023).

To overcome these limitations, the study of chapter IV proposes a novel approach by integrating CEO-loaded PEs (prepared in chapter III) into a biodegradable chitosan/zein Janus film system. The asymmetric multilayer structure is designed to regulate CEO release directionally, favoring inward diffusion toward the food surface, while maintaining a sustained release profile.

Chitosan, a naturally derived cationic polysaccharide, possesses excellent film-forming ability, high biocompatibility, intrinsic antimicrobial activity, and strong affinity for negatively charged colloidal particles (J. Wang & Zhuang, 2022). These features make chitosan an ideal matrix for incorporating and retaining CEO-loaded PEs. Zein, a hydrophobic prolamin protein from maize, was selected as the outer barrier layer due to its hydrophobic nature, which effective barrier against the outward diffusion of volatile compounds (L. Wang, et al., 2023).

The successful construction of a stable multilayer structure is crucial for achieving unidirectional and sustained release in active packaging films (W. Zhang, Jiang, Rhim, Cao, & Jiang, 2022). In this study, morphological characterization revealed that the incorporation of CEO-loaded PEs (CPE) into the chitosan layer, combined with the deposition of a zein barrier layer, led to the formation of well-organized Janus films with distinct and cohesive interfaces. FTIR results showed that non-covalent interactions (hydrogen bonding and electrostatic interactions) dominated the layer interfaces, promoting interfacial adhesion and stability (Fan, Wang, Wen, Li, Fang, Richel, et al., 2023). While the CEO-loaded PEs had a significant impact on chitosan film crystallinity and thermal stability, likely due to the disruption of the regular polymer chains by the emulsion droplets and the complex network (Y. Zhu, Su, Hu, Li, Xie, Zhang, et al., 2025). This structural loosening may contribute to enhanced diffusivity of CEO within the active layer, while the zein outer layer maintained a relatively more crystalline, dense structure, serving as an effective diffusion barrier.

The multilayer structural characteristics established in the Janus films, particularly the asymmetric interface and differential swelling behavior between the chitosan and zein layers, played a crucial role in regulating the release kinetics of CEO (Yang, Li, Li, Li, Shi, Huang, et al., 2024). The CEO release behavior of the ZCPE9 film demonstrated clear unidirectionality, significantly higher CEO release occurred through the inner (CPE) side, while the zein outer layer effectively suppressed diffusion. Additionally, the cumulative release of CEO from the loading layer side showed a sustained trend, with no significant burst release observed in the early stages. This behavior can be attributed to the dual regulation provided by the interfacial barrier effect of PEs structure and the physical diffusion resistance of multilayer film configuration (Yang, et al., 2024). In contrast, conventional blend films exhibited rapid and less controlled CEO release, confirming the superiority of the Janus structure design. Kinetic modeling analysis fitted the release data well to a quasi-Fickian diffusion mechanism ($n < 0.5$), indicating that CEO release was primarily governed by diffusion processes through the polymeric matrix and controlled by the multilayer architecture.

Functionally, the ZCPE films exhibited significantly enhanced antimicrobial activity compared to control films, achieving over 99% inhibition against representative spoilage bacteria (*P. paralactis* MN10, *A. pullicarnis* MN21, and *L. sakei* VMR17), which could be attributed to the controlled and prolonged release of CEO from the inner layer ensured a continuous supply of active compounds at effective concentrations around the food surface, and the presence of TA, provided synergistic antimicrobial effects through membrane disruption and oxidative stress mechanisms.

Finally, the enhanced antimicrobial activity of the ZCPE films was further validated through pork preservation tests. Compared to the control group, pork samples wrapped with ZCPE9 films showed significantly delayed microbial growth during refrigerated storage. The total viable counts (TVC) in the ZCPE9 group remained below the acceptable limit (<6 log CFU/g) for a notably longer duration. The total volatile basic nitrogen (TVB-N) content, an important marker of protein degradation and spoilage, increased at a slower rate in samples packaged with ZCPE films, indicating effective suppression of spoilage processes.

In summary, these results validated the hypothesis that regulating the CEO release behavior through PE integration and multilayer structuring could not only enhance antimicrobial efficacy but also significantly improve meat preservation performance. The successful extension of pork shelf life demonstrated the application potential of this strategy for perishable food packaging, aligning with the overarching goal of this dissertation to develop sustainable and functional controlled-release antimicrobial materials.

1.3. Development and modulation of nanoparticle-reinforced PEs-based active films: Toward enhanced structural integrity and controlled release

In our previous study, it was found that the release of CEO from CEO-loaded PE composite films was governed by a synergistic mechanism. The CEO molecules first diffused slowly through the emulsion droplet interfaces, then migrated through the cross-linked matrix network, and finally volatilized at the surface or entered the surrounding environment (Fan, et al., 2023). The concentration gradient of CEO across the film was the primary driving force for diffusion (Fan, Yang, Zhu, Li, Richel, Fauconnier, et al., 2024). While the multilayer Janus film strategy introduced earlier successfully achieved unidirectional and sustained release of CEO, challenges remained in further enhancing the structural stability and release modulation under different packaging scenarios.

Chitosan/polyvinyl alcohol (CS/PVA) composites offer excellent film-forming ability, mechanical strength, and biocompatibility. However, their intrinsic network density is often insufficient to precisely control the release of volatile active agents. We hypothesized that the introduction of nanoparticles could improve the cross-linking density of the polymer network, reduce the porosity within the matrix, and thereby further restrict the diffusion of EO. To validate this hypothesis, a nanoparticle-enhancement strategy was proposed during the development of functional controlled-release antimicrobial systems in this chapter. Specifically, CEO-loaded PEs were incorporated into a CS/PVA matrix, combined with quercetin nanocrystals (QNs) as functional fillers, aiming to regulate the microstructural compactness and controlled release characteristics of the films.

As evidenced by SEM, the incorporation of QNs and CEO-loaded PEs into the CS/PVA matrix resulting in a denser and more continuous internal structure compared to the control. Initially, this polymer network was primarily driven by strengthened hydrogen bonding interactions among CS and PVA (W. Zhang, Khan, Ezati, Priyadarshi, Sani, Rathod, et al., 2024). Upon the incorporation of QNs, the density of the hydrogen bond network increased, enhancing the cross-linked structure of the CS/PVA matrix (Lin, Zhang, Zhong, Chen, Chen, & Chen, 2025). Through physical entanglement and hydrogen bonding interactions, the polymer network effectively encapsulated the emulsion droplets within its pores, creating a spatial barrier that restricted droplet migration or coalescence (Y. Zhang, Pu, Jiang, Chen, Shen, Zhang, et al., 2024). XRD analysis suggested that while the incorporation of PEs slightly disrupted the crystallinity of the polymer matrix, the addition of QNs compensated for this disruption by promoting a more ordered molecular arrangement, contributing to overall structural reinforcement. Collectively, the nanoparticle filling strategy effectively reduced internal porosity, improved network stability, and laid a structure foundation for achieving more sustained and controlled CEO release.

The improvement in structural compactness also manifested in the reduced water sensitivity of the films. Compared to the control, the PCE@QNs films exhibited significantly lower swelling ratios and stronger hydrophobicity. This reduction can be

attributed to not only the hydrophobicity of CEO-loaded PEs and QNs but the denser polymer network, which limited water molecule penetration and minimized matrix expansion. Thus, the modulation of water affinity through microstructural reinforcement provided additional benefits for maintaining the functional performance of the active packaging films.

Antimicrobial assays demonstrated that films incorporated with CEO-loaded PEs (PCE) exhibited superior inhibition effects against representative spoilage bacteria (*P. paralactis* MN10, *A. pullicarnis* MN21, and *L. sakei* VMR17) compared to the blank CS/PVA films. The addition of QNs further improved antimicrobial activity, particularly in the PCE@QNs group, which showed the highest inhibition zones and bacteriostatic rates. This improvement can be attributed to the synergistic effect of sustained CEO release, and the potential bioactivity of QNs themselves. Antioxidant evaluations (DPPH and ABTS radical scavenging assays) revealed a consistent trend. Films containing CEO-loaded PEs and QNs displayed significantly higher free radical scavenging capacities than the control group. The continuous release of CEO, combined with the antioxidant nature of QNs, contributed to prolonged antioxidative protection, which is beneficial for maintaining food quality during storage.

The improved structural compactness and functional activity of the developed films were further validated through pork preservation experiments. Compared to the control group, pork samples wrapped with PCE and PCE@QNs films exhibited significantly delayed microbial growth during refrigerated storage. Particularly, the PCE@QNs group maintained total viable counts (TVC) below the acceptable limit (<6 log CFU/g) for a longer period, demonstrating effective spoilage inhibition. The films also contributed to slower protein degradation, as indicated by the lower total volatile basic nitrogen (TVB-N) values in the PCE@QNs group. This reduction in TVB-N reflects suppressed enzymatic and microbial decomposition activities, consistent with the enhanced antimicrobial and antioxidant performance of the films. Sensory evaluations further supported these findings, with pork samples packaged in PCE@QNs films showing better color, odor, and overall acceptability compared to those in the control group.

In summary, a nanoparticle reinforcement strategy was successfully developed to construct CEO-loaded PEs-based active films with enhanced structural integrity and controlled release behavior. Compared with the multilayer Janus film strategy explored in the previous chapter, the nanoparticle reinforcement approach provided an alternative and complementary pathway for achieving tunable controlled release and food preservation effects. In this chapter, the results confirm that the nanoparticle-reinforced CS/PVA films not only modulated CEO release but also translated their structural and functional advantages into tangible improvements in food preservation, aligning with the overarching objective of constructing tunable active packaging systems.

2. Conclusions

This dissertation systematically explored the design, construction, and modulation of controlled-release antimicrobial packaging systems based on CEO-loaded PEs,

aiming to address the challenges of inefficient release control and limited functional stability in traditional antimicrobial packaging materials.

Firstly, CEO-loaded PEs were developed and optimized by regulating the interaction modes of zein-TA complex particles under different pH conditions. The resulting zein-TA hybrid particles significantly enhanced the interfacial stability and enabled sustained release of CEO, establishing a robust delivery platform.

Based on optimized CEO-loaded PEs, two complementary film construction strategies were proposed. i) A multilayer Janus films were fabricated by incorporating the optimized CEO-loaded PEs into chitosan-based matrices, combined with a zein barrier layer, to achieve unidirectional and sustained release. ii) Nanoparticle-reinforced CS/PVA films were constructed by integrating CEO-loaded PEs with QNs, enhancing film compactness and further controlling release behavior. Both two strategies effectively improved CEO retention, antimicrobial activity and meat preservation efficacy.

Through systematic investigation, this research elucidated the structure-property-function relationships in PE-based packaging systems, providing theoretical insights into the role of interfacial engineering and microstructural modulation in regulating antimicrobial agents' release. The developed materials demonstrated significant potential for extending the shelf life of perishable foods, contributing to the advancement of sustainable, functional, and tunable active packaging technologies.

The findings of this dissertation offer a comprehensive foundation for future innovations in bio-based controlled-release systems and open new possibilities for the practical application of Pickering emulsion technologies in the food packaging field.

3. Perspectives

To further advance the development and application of PE-based active food packaging technologies, future research should focus on the following directions:

(i) Construction of multifunctional synergistic systems:

Exploring the multiphase interfacial properties of PEs to design composite carriers with dual or multiple functions. The aim is to achieve coordinated preservation effects by controlling the spatiotemporal distribution of various active compounds.

(ii) Development of stimuli-responsive precision delivery systems:

Engineering smart particles capable of responding to specific food spoilage microenvironmental cues, such as pH shifts, enzymatic activity, or metabolite accumulation. This can be achieved through chemical modifications, enabling intelligent, on-demand release of active ingredients to enhance preservation precision.

(iii) Structure-function integrated packaging development:

Overcoming the limitations of traditional film fabrication methods by integrating advanced manufacturing technologies such as microfluidic molding and 3D printing. These approaches can be used to develop innovative packaging formats, including controlled-release antimicrobial pads, smart hydrogel dressings, and porous cushioning materials, allowing precise spatial programming of active loading sites and dynamic release kinetics.

(iv) Analysis of migration behavior and safety risks:

Conducting comprehensive studies on the migration kinetics of active compounds from packaging matrices into food systems, while systematically evaluating their biological safety. Establishing a nanoparticle-bio interface interaction-based risk assessment framework is essential for ensuring the safe application of nanomaterials in food packaging across their entire lifecycle.

4. References

Almasi, H., Jahanbakhsh Oskouie, M., & Saleh, A. (2021). A review on techniques utilized for design of controlled release food active packaging. Critical Reviews in Food Science and Nutrition, 61(15), 2601-2621.

Cahyana, Y., Putri, Y. S. E., Solihah, D. S., Lutfi, F. S., Alqurashi, R. M., & Marta, H. (2022). Pickering Emulsions as Vehicles for Bioactive Compounds from Essential Oils. Molecules, 27(22), 7872.

Chang, H., Xu, J., Macqueen, L. A., Aytac, Z., Peters, M. M., Zimmerman, J. F., Xu, T., Demokritou, P., & Parker, K. K. (2022). High-throughput coating with biodegradable antimicrobial pullulan fibres extends shelf life and reduces weight loss in an avocado model. Nature Food, 3(6), 428-436.

Chen, X., Chen, M., Xu, C., & Yam, K. L. (2019). Critical review of controlled release packaging to improve food safety and quality. Critical Reviews in Food Science and Nutrition, 59(15), 2386-2399.

Cheng, Y., Cai, X., Zhang, X., Zhao, Y., Song, R., Xu, Y., & Gao, H. (2024). Applications in Pickering emulsions of enhancing preservation properties: Current trends and future prospects in active food packaging coatings and films. Trends in Food Science & Technology, 151.

Fan, S., Wang, D., Wen, X., Li, X., Fang, F., Richel, A., Xiao, N., Fauconnier, M.-L., Hou, C., & Zhang, D. (2023). Incorporation of cinnamon essential oil-loaded Pickering emulsion for improving antimicrobial properties and control release of chitosan/gelatin films. Food Hydrocolloids, 138, 108438.

Fan, S., Yang, Q., Zhu, C., Li, X., Richel, A., Fauconnier, M.-L., Fang, F., Zhang, D., & Hou, C. (2024). Zein/chitosan Janus film incorporated with tannic acid and cinnamon essential oil co-loaded Pickering emulsion for sustained controlled release and pork preservation. International Journal of Biological Macromolecules, 138429.

Hosseini, M., Moghaddam, L., Barner, L., Cometta, S., Hutmacher, D. W., & Medeiros Savi, F. (2025). The multifaceted role of tannic acid: From its extraction and structure to antibacterial properties and applications. Progress in Polymer Science, 160, 101908.

Ji, C., & Wang, Y. (2025). Recent advances in Pickering emulsions for inhibiting foodborne bacteria. Current Opinion in Food Science, 61, 101265.

Lin, B., Zhang, X., Zhong, Y., Chen, Y., Chen, X., & Chen, X. (2025). Preparation of vanillin nanoparticle/polyvinyl alcohol/chitosan film and its application in

preservation of large yellow croaker. International Journal of Biological Macromolecules, 287, 138440.

Liu, T., Chen, Y., Zhao, S., Guo, J., Wang, Y., Feng, L., Shan, Y., & Zheng, J. (2023). The sustained-release mechanism of citrus essential oil from cyclodextrin/cellulose-based Pickering emulsions. Food Hydrocolloids, 144, 109023.

Low, L. E., Siva, S. P., Ho, Y. K., Chan, E. S., & Tey, B. T. (2020). Recent advances of characterization techniques for the formation, physical properties and stability of Pickering emulsion. Advances in Colloid and Interface Science, 277, 102117.

Malekjani, N., Karimi, R., Assadpour, E., & Jafari, S. M. Control of release in active packaging/coating for food products; approaches, mechanisms, profiles, and modeling. Critical Reviews in Food Science and Nutrition, 1-23.

Souza, E. M. C., Ferreira, M. R. A., & Soares, L. A. L. (2022). Pickering emulsions stabilized by zein particles and their complexes and possibilities of use in the food industry: A review. Food Hydrocolloids, 131, 107781.

Wang, J., & Zhuang, S. (2022). Chitosan-based materials: Preparation, modification and application. Journal of Cleaner Production, 355, 131825.

Wang, L., Yuan, M., Sun, E., Wu, J., Lv, A., Zhang, X., Guo, J., Zhu, Y., Guo, H., Li, X., & Wang, K. (2023). Antibacterial food packaging capable of sustained and unidirectional release carvacrol/thymol nanoemulsions for pork preservation. Food Hydrocolloids, 145, 109169.

Wang, Q., Tang, Y., Yang, Y., Lei, L., Lei, X., Zhao, J., Zhang, Y., Li, L., Wang, Q., & Ming, J. (2022). The interaction mechanisms, and structural changes of the interaction between zein and ferulic acid under different pH conditions. Food Hydrocolloids, 124, 107251.

Wen, X., Zhang, D., Li, X., Ding, T., Liang, C., Zheng, X., Yang, W., & Hou, C. (2022). Dynamic changes of bacteria and screening of potential spoilage markers of lamb in aerobic and vacuum packaging. Food Microbiology, 104, 103996.

Xiao, M., Li, S., Xiong, L., Duan, J., Chen, X., Luo, X., Wang, D., Zou, L., Li, J., Hu, Y., & Zhang, J. (2024). Pickering emulsion gel of polyunsaturated fatty acid-rich oils stabilized by zein-tannic acid green nanoparticles for storage and oxidation stability enhancement. Journal of Colloid and Interface Science, 675, 646-659.

Xu, Y., Wei, Z., & Xue, C. (2023). Pickering emulsions stabilized by zein–gallic acid composite nanoparticles: Impact of covalent or non-covalent interactions on storage stability, lipid oxidation and digestibility. Food Chemistry, 408, 135254.

Yang, Z., Li, M., Li, Z., Li, Y., Shi, J., Huang, X., Sun, Y., Zhai, X., Zou, X., & Xiao, J. (2024). Incorporation of hawthorn pectin/β-cyclodextrin-stabilized Pickering emulsion and Titanium dioxide nanoparticles for improving the physical, biological, and release properties of guar gum/agar/sodium alginate-based bilayer films. Industrial Crops and Products, 212, 118302.

Zhang, W., Ezati, P., Khan, A., Assadpour, E., Rhim, J.-W., & Jafari, S. M. (2023). Encapsulation and delivery systems of cinnamon essential oil for food preservation applications. Advances in Colloid and Interface Science, 318, 102965.

Zhang, W., Jiang, H., Rhim, J.-W., Cao, J., & Jiang, W. (2022). Effective strategies of sustained release and retention enhancement of essential oils in active food packaging films/coatings. Food Chemistry, 367, 130671.

Zhang, W., Khan, A., Ezati, P., Priyadarshi, R., Sani, M. A., Rathod, N. B., Goksen, G., & Rhim, J.-W. (2024). Advances in sustainable food packaging applications of chitosan/polyvinyl alcohol blend films. Food Chemistry, 443, 138506.

Zhang, Y., Pu, Y., Jiang, H., Chen, L., Shen, C., Zhang, W., Cao, J., & Jiang, W. (2024). Improved sustained-release properties of ginger essential oil in a Pickering emulsion system incorporated in sodium alginate film and delayed postharvest senescence of mango fruits. Food Chemistry, 435, 137534.

Zhu, X., Chen, Y., Hu, Y., Han, Y., Xu, J., Zhao, Y., Chen, X., & Li, B. (2021). Tuning the molecular interactions between gliadin and tannic acid to prepare Pickering stabilizers with improved emulsifying properties. Food Hydrocolloids, 111, 106179.

Zhu, Y., Su, Y., Hu, L., Li, Z., Xie, T., Zhang, Y., Qiao, G., & Lu, F. (2025). pH-responsive zein/chitosan composite film containing cinnamon essential oil-loaded Pickering emulsion and black wolfberry anthocyanin: Physicochemical properties, and application in packing salmon. Food Chemistry, 479, 143815.

Chapter 7

Appendices

1. Appendix: List of Publications

1.1. Accepted publications (peer reviewed)

- **Fan, S**., Wang, D., Wen, X., Li, X., Fang, F., Richel, A., Xiao, N., Fauconnier, M.-L., Hou, C., & Zhang, D. (2023). Incorporation of cinnamon essential oil-loaded Pickering emulsion for improving antimicrobial properties and control release of chitosan/gelatin films. ***Food Hydrocolloids***, *138,* 108438.
- **Fan, S.**, Yang, Q., Wang, D., Zhu, C., Li, X., Richel, A., Fauconnier, M.-L., Yang, W., Hou, C., & Zhang, D. (2024). Zein and tannic acid hybrid particles improving physical stability, controlled release properties, and antimicrobial activity of cinnamon essential oil loaded Pickering emulsions. ***Food Chemistry***, *446,* 138512.
- **Fan, S.**, Yang, Q., Zhu, C., Li, X., Richel, A., Fauconnier, M.-L., Fang, F., Zhang, D., & Hou, C. (2024). Zein/chitosan Janus film incorporated with tannic acid and cinnamon essential oil co-loaded Pickering emulsion for sustained controlled release and pork preservation. ***International Journal of Biological Macromolecules***, *286,*138429.
- **Fan, S.,** Mu, H., Gao, H.*, Chen, H., Wu, W., Fang, X., Liu, R., & Niu, B. (2023). Preparation of PVA/PLA-based intelligent packaging to indicate the quality of shiitake mushrooms. ***Journal of Agriculture and Food Research,*** 12, 100589.
- Zhang Y.#, **Fan S.#,** Liu R., Chen H., Niu B., Chen H., Wu W., (2025). IoT technology as an effective strategy enhances food authentication for current fresh fruit supply chain. ***Future Postharvest and Food.***(Accpeted)

1.2. Authorized patent

- Hou, C., Zhang, D., **Fan, S.,** Yang, Q., Li, X., Fang, F. Chitosan/Zein Sustained-release Antibacterial Film with Janus Structure: Preparation and Application. ***Chinese Patent***, ZL 202410338810.1.

1.3. Submitted articles (under review)

- **Fan, S.,** Yang, Q., Zhu, C., Tian, M., Richel, A., Fauconnier, M.-L., Hou C., Zhang D., (2025). Reinforcement of Chitosan/ Polyvinyl alcohol Film by Quercetin Self-assembled Nanocrystals for Fresh Meat Preservation. (***Food Chemistry, revised***)
- **Fan, S.,** Yang, Q., Zhu, C., Richel, A., Fauconnier, M.-L., Tian, M., Wang, D., Li, X., Hou C., Zhang, D. Preparation of Quercetin Nanocrystals Enhanced Chitosan/Polyvinyl Alcohol/Cinnamon Essential Oil-Loaded Pickering Emulsion Film with Improved Mechanical and Controlled-Release Antimicrobial Properties for Meat Preservation. (***Food Packaging and Shelf Life, under review***)

1.4. Manuscript in preparation

- ***Fan, S.,*** Yang, Q., Zhu, C., Richel, A., Fauconnier, M.-L., Tian, M., Wang, D., Li, X., Hou C., Zhang, D. Enhancing Preservation Properties with Pickering Emulsions: Current Trends and Future Prospects for Active Food Packaging Coatings and Films.

(Preparation, aim to Trends in Food Science and Technology)

1.5. Contributed to the work

- Wang, D., **Fan, S.,** Li, X., Chen, L., Wen, X., Xu, Y., Zhu, C., Hou, C., & Zhang, D. (2024). Carboxymethyl chitosan/polyvinyl alcohol hydrogel films by incorporating MSNs as ε-PL carrier with pH-responsive controlled release and antibacterial properties. ***Food Packaging and Shelf Life,*** 46, 101360.
- Wang, D., Chen, J., Wen, X., **Fan, S.,** Zhu, C., Li, X., Fang, F., Yang, W., Fan, W., Zhang, D., & Hou, C. (2024). Self-assembled Chitosan/Polyvinyl alcohol hydrogel film incorporated with TiO_2 with excellent stability, mechanical and antibacterial properties for the preservation of chilled pork. ***Food Packaging and Shelf Life***, 45, 101328.
- Yang, Q., Zhang, X., Fan, W., Shao, L., Chen, L., Yang, W., **Fan, S.,** Zhu, C., Zhang, D., & Hou, C. (2025). Oxygen barrier multilayer films: Effects on the quality and microbial community of yak meat during super-chilled storage. ***Lwt-Food Science and Technonlgy,*** 221, 117605.
- Zhu, C., Yang, Q., Tian, M., Yang, W., Min, C., **Fan, S.,** Wang, D., Li, X., Zhang, D., & Hou, C. (2025). Sustainable nanofiber films based on polylactic acid/modified cellulose nanocrystals containing various types of polyphenols, exhibiting antioxidant activity and high stability. ***Food Chemistry***, 477, 143514.